Physical wavelets and their sources: real physics in complex spacetime

2003 J. Phys. A: Math. Gen. 36 R291

(http://iopscience.iop.org/0305-4470/36/30/201)

INSTITUTE OF PHYSICS PUBLISHING JOURNAL OF PHYSICS A: MATHEMATICAL AND GENERAL

J. Phys. A: Math. Gen. **36** (2003) R291–R338 PII: S0305-4470(03)57541-2

TOPICAL REVIEW

Physical wavelets and their sources: real physics in complex spacetime

Gerald Kaiser

Center for Signals and Waves, 1921 Kings Road, Glen Allen, VA 23059, USA

E-mail: kaiser@wavelets.com

Received 4 March 2003, in final form 1 June 2003
Published 16 July 2003
Online at stacks.iop.org/JPhysA/36/R291

Abstract
A thorough review of acoustic and electromagnetic wavelets is given, including a first account of recent progress in understanding their sources. These *physical wavelets*, introduced in 1994, are families of 'small' solutions of the wave and Maxwell equations generated from a single member by group operations including translations, Lorentz transformations, and scaling. They are parametrized by complex spacetime points $z = x - \mathrm{i}y$, where x gives the centre of their *region of origin* and y gives the *extension and orientation* of this region in spacetime. They are thus *pulsed beams* whose origin, direction and focus are all governed by z and which give, by superposition, 'wavelet representations' of acoustic and electromagnetic waves. Recently this idea has been developed substantially by the rigorous understanding of the source distributions required to launch and absorb the wavelets, defined as *extended delta functions*. The unexpected simplicity and complex structure of the sources in the Fourier domain suggests their potential use in the construction of fast algorithms for the analysis and synthesis of acoustic and electromagnetic waves. The review begins with a brief account of the physical wavelets associated with *massive* (Klein–Gordon and Dirac) fields, which are *relativistic coherent states*.

PACS numbers: 41.85.−p, 03.50.De, 41.20.Jb, 03.65.Pm

M This article features online multimedia enhancements

Contents

1. Overview

Since the introduction of electromagnetic wavelets in [K94], I have been intrigued by two related questions: (a) what are the sources responsible for their emission and absorption, and (b) can these sources be *realized* and used to launch and detect the wavelets? In principle, it should be easy to find the source for a known solution of a linear system. However, these wavelets are *pulsed-beam propagators* that are, in a 'poetic' sense at least, waves generated by a single event in *complex* spacetime as seen by an observer in *real* spacetime. Their sources, therefore, should be (ignoring polarization for simplicity) *extended delta functions* $\tilde{\delta}(x' - z)$, where x' is the real observation point and z the complex source point. Attempts to make mathematical sense of all this have presented a number of challenges that have occupied me for the past several years. I am now pleased to report that the effort has been successful and the results are interesting. The sources for scalar (acoustic) wavelets have been rigorously computed both in spacetime and Fourier space and will be presented here. The spacetime expressions turn out to be singular objects with a wealth of geometric structure and, most interestingly, their Fourier transforms are extremely simple—contrary to all my previous expectations. To understand how these simple expressions generate such rich spacetime structures, I complete the circle by computing the pulsed beams from their Fourier sources. As a welcome by-product, this gives an angular spectrum representation of time-harmonic *complex-source beams*, used extensively in the engineering literature since the 1970s, that generalizes Weyl's well-known representation of the fundamental solution for the Helmholtz equation. The sources for *electromagnetic* wavelets are polarization and magnetization densities obtained by multiplying $\tilde{\delta}(x' - z)$ by electric and magnetic dipole moments or, more generally, convolving them in time with variable dipoles representing a 'driving signal'.

I believe that question (a) above has now been largely addressed, though some important points of interpretation remain, as do no doubt many others. This opens the possibility suggested by question (b). Furthermore, although the wavelets were introduced in classical electrodynamics, I have hoped from the beginning that they may be useful in QED. This is encouraged by the simplicity of their momentum space propagators, which should offer a useful computational tool.

2. Waves, wavelets and complex spacetime

I begin with a brief review of my past efforts to extend classical and quantum theories to complex spacetime and interpret the results physically. By that I mean that the imaginary spacetime coordinates, and any other extras associated with analyticity, are to be understood *directly* in terms of common observable attributes and not merely as a technical device for proving theorems or exotic higher dimensions inaccessible to mortals stuck in the 'real' world like the poor souls in Plato's cave.

I have tried not to impose an *a priori* grand vision but, rather, interpret the imaginary coordinates in each theory by understanding their *effects* within that theory. Consequently, the interpretations vary somewhat from one theory to another. But they all have in common the following theme. *In the extended theory, certain singular points (evaluation maps, source points, etc) become 'inflated' to extended objects*. This transformation is determined by analyticity for each particular theory. In every case, the structure of the objects is shaped by the equations of the theory and their degrees of freedom are specified precisely by the complex spacetime coordinates. The real coordinates give the *centre*, and the imaginary coordinates the *extent and orientation* of the object in space and time.

These ideas are similar in spirit to wavelet analysis, where a function of one variable (time, say) is expressed in terms of an additional variable describing the scale or *resolution* in the first. This analogy goes farther in the treatment of massless rather than massive fields, since the latter have an intrinsic scale and thus cannot be scaled arbitrarily. For relativistic fields with mass, spacetime 'orientation' includes *velocity*, and this makes the complex spacetime an *extended phase space*. The *relativistic coherent-state representations* for massive Klein–Gordon and Dirac fields constructed in [K77, K78] (for single particles) and [K87, K90] (for free quantized fields) interpolate between 'time-frequency' and 'wavelet' descriptions, behaving like the former in the nonrelativistic regime and like the latter in the ultra-relativistic regime. In fact, there is a very close correspondence between the nonrelativistic limit in physics and the *narrow-band approximation* in signal theory; see [K90, K94, K96].

Although the results cited in this section are not new, I believe they have acquired some currency because of substantial progress recently in the understanding of the *sources* associated with *retarded* holomorphic[1] fields. The new results focus on massless fields, but it is likely that similar computations exist for massive fields where the integrals are more difficult.

Sources describe the breakdown of analyticity due to natural singularities and physically necessary branch cuts. What I find especially fascinating is that such branch cuts behave much like 'real' matter. Depending on the theory, they carry charge, mass and spin, and they emit and absorb radiation. In spite of their simple origins, they turn out to have surprising and complex (pardon the expression) properties, the pursuit of which has the feeling of exploring some fundamental forms of matter and not merely mathematical properties of branch cuts. The results of this search have intrigued and inspired me, and I hope to share this excitement with the reader.

Partial reports have appeared in [K00, K01, K01a, K02, K02a, K03], but the detailed computation of complex spacetime point sources and their Fourier transforms, and the angular spectrum representation of complex-source beams, has not appeared previously in print or preprint form.

2.1. Spacetime and Fourier notation

Real spacetime vectors will be written in the form of *complex Euclidean* vectors with real space coordinates and an imaginary time coordinate:

$$x = (\boldsymbol{x}, \mathrm{i}t) \in M = \mathbb{R}^{3,1} \qquad x^2 = r^2 - t^2 \qquad r = |\boldsymbol{x}|. \tag{1}$$

[1] According to most papers, *holomorphic* simply means *analytic*. Possibly, the term is used to emphasize *complex* as opposed to real analyticity—or perhaps just to intimidate the reader!

This is known in physics as '*ict*' (we take $c = 1$) and is often regarded as unphysical because it cannot be used in 'generic' curved spacetimes where the metric tensor cannot be continued analytically in t. (See [MTW73, p 52], *Farewell to* '*ict*'.) Therefore I feel compelled to explain at the outset why I use it nevertheless. The view of physical time as an essentially *imaginary* variable comes from the idea of *complex distance* [K00], rooted in Euclidean spacetime, which is the basis for the recent progress in the analysis of sources. In previous work I followed a more conventional path, starting with known quantities in Minkowski space and extending them analytically when possible. That approach, reviewed later in this section, works best for *free* fields, where the splitting into positive and negative frequency components provides a natural setting for analytic continuation. To understand sources, we must rather look at *propagators*, i.e. waves emitted by a single *point source* $\delta(x)$, since waves emitted by all other sources can then be obtained by convolution. However, propagators are much more complicated than their elliptic counterparts, the *potentials* due to point sources in Euclidean space. In the hyperbolic case, we must choose between retarded and advanced propagators (or hybrid ones, like Feynman's). Each choice is singular not only at the source but also on at least one half of the light cone, and it is not clear whether and how such solutions can be extended to complex spacetime. The Euclidean case, by contrast, is a picture of simplicity. Because the δ-source in $\mathbb{R}^n$ is spherically symmetric, its potential G_n depends only on the distance r. To extend G_n analytically we need only extend r, and this is easily done. The only complication is that the resulting *complex distance* $\tilde{r}(z)$ is double valued in $\mathbb{C}^n$ because of the square root in its definition, and a branch cut must be chosen. For even $n \geqslant 4$, the extended G_n is even in $\tilde{r}$ and so does not depend on the choice of branch, while in all other cases it does.

This suggests an alternative strategy for extending physical fields without excluding the possibility of sources. Since the original signature is irrelevant once spacetime is made complex, why not *begin* in the Euclidean setting, where operators are elliptic and life is simple, and continue analytically to the Minkowskian world? There may be advantages to starting directly with Euclidean concepts, unencumbered by baggage imported from Minkowski space, even if in the end we intend to study propagators. Thus we begin with the extended potential $G_4(z)$ in $\mathbb{C}^4$ and look for extended versions of the retarded and advanced propagators $D^+(x)$ and $D^-(x)$. However, since the concepts of propagation and causality are foreign to the Euclidean world, $G_4(z)$ cannot distinguish between retarded and advanced propagators. In fact, it turns out to be the extension of the *Riemann function*, which is the sourceless difference of the advanced and retarded propagators. To split off the retarded part, a branch must be chosen for the *spatial* complex distance $\tilde{r}_3(\boldsymbol{z})$, where $\boldsymbol{z} = \boldsymbol{x} - \mathrm{i}\boldsymbol{y} \in \mathbb{C}^3$ is the vector from the imaginary source point $\mathrm{i}\boldsymbol{y}$ to the observer at $\boldsymbol{x}$. This gives a splitting into extended propagators $\tilde{D}^+(z)$ and $\tilde{D}^-(z)$ that depend on the branch cut of $\tilde{r}_3$. This branch cut, $\mathcal{D} \subset \mathbb{R}^3$, is a 'blown up' version of the original point source acting as a *disc source* for $\tilde{D}^+(z)$ and $\tilde{D}^-(z)$.[2] Finally, $D^{\pm}(x)$ are recovered as jumps in boundary values across $\mathbb{R}^{3,1}$,

$$D^{\pm}(x) = \lim_{\varepsilon \searrow 0} \{\tilde{D}^{\pm}(x - \mathrm{i}\varepsilon y) - \tilde{D}^{\pm}(x + \mathrm{i}\varepsilon y)\} \tag{2}$$

with y in the future cone of $\mathbb{R}^{3,1}$. This shows that while analytic extension is very simple for Euclidean potentials, it is rather involved for propagators, lending support to the strategy of beginning in the Euclidean setting. But in this approach, physical time must be imaginary, just as 'Euclidean time' must be imaginary when beginning with Minkowskian or Lorentzian spacetime.

At any rate, the dismissal of *ict* in [MTW73] may have been premature. Even in general relativity, analytic continuations in time and space have borne some rich fruit—although

[2] Going through the cut means entering a world where distance becomes negative and $\tilde{D}^{\pm}(z)$ trade places. As $\boldsymbol{z}$ becomes real, the disc contracts to a point and the door is closed!

the physical basis of the procedure is often ill-understood. For example, an exquisitely simple geometric derivation of the Hawking temperature for Schwarzschild black holes is obtained [HI79] by analytically continuing the metric in time, interpreting the 'Euclidean time' coordinate as an angle, and choosing its period to make the horizon a coordinate singularity like the origin in polar coordinates. The reciprocal of the imaginary time period is interpreted in the usual (KMS) way as a temperature, and this turns out to be nothing but the Hawking temperature! I confess that I do not understand this derivation in more than a formal way, but analytic continuation has, in any case, become the main strategy of black-hole thermodynamics, as explained in [Kr03]. The analytic continuation of spatial coordinates also has an honourable history in relativity, having played a major role (and conceptually an equally obscure one) in the discovery of charged spinning black holes by Newman *et al* [N65a]; see also [N73, NW74, K01a, N02]. And then there are the theories of twistors and H-spaces (see [P87, HNPT78, BFP80] and references therein).

Returning to our summary of notation, we denote by M' the 'momentum space' dual to M and write the pairing between the two as a complex Euclidean scalar product,

$$k \cdot x = \boldsymbol{k} \cdot \boldsymbol{x} - \omega t \qquad k = (\boldsymbol{k}, \mathrm{i}\omega) \in M' \qquad x = (\boldsymbol{x}, \mathrm{i}t) \in M. \tag{3}$$

The Fourier transform and its inverse are written as

$$\hat{F}(k) = \int_M \mathrm{d}x\, \mathrm{e}^{-\mathrm{i}k\cdot x} F(x) \tag{4}$$

$$F(x) = \int_{M'} \mathrm{đ}k\, \mathrm{e}^{\mathrm{i}k\cdot x} \hat{F}(k) \tag{5}$$

where we have introduced the notation

$$\mathrm{d}x = \mathrm{d}\boldsymbol{x}\, \mathrm{d}t \qquad \mathrm{đ}k = \frac{\mathrm{d}\boldsymbol{k}\, \mathrm{d}\omega}{(2\pi)^4} \qquad \mathrm{đ} = \mathrm{d}/2\pi \tag{6}$$

which eliminates most factors of 2π in Fourier analysis. Strictly speaking, we should include factors of i in front of the integrals[3] since the time and the frequency are imaginary, but this seems overly pedantic and we choose to leave them out. Instead, we will introduce factors of i in the causal splitting (49), which makes the propagators $D^{\pm}(x)$ in (75) and (77) real.

Note: even though $x = (\boldsymbol{x}, \mathrm{i}t)$ and $k = (\boldsymbol{k}, \mathrm{i}\omega)$, we will write $F(\boldsymbol{x}, t)$ and $\hat{F}(\boldsymbol{k}, \omega)$ instead of $F(\boldsymbol{x}, \mathrm{i}t)$ and $\hat{F}(\boldsymbol{k}, \mathrm{i}\omega)$ to keep the notation simple.

We also need the following cones in M and M':

- The positive and negative frequency light cones

$$C_{\pm} = \{(\boldsymbol{k}, \mathrm{i}\omega) \in M' : \pm\omega = \kappa > 0\} \qquad \text{where} \quad \kappa = |\boldsymbol{k}|. \tag{7}$$

  Note that we exclude the 'DC component' $k = 0$, i.e., nonvanishing constant solutions; a wave must *oscillate* to be a wave. (This will be related to the admissibility condition in wavelet theory.)
- The future and past cones in $\mathbb{R}^{3,1}$,

$$V_{\pm} = \{(\boldsymbol{y}, \mathrm{i}u) \in M : \pm u > a\} \qquad \text{where} \quad a = |\boldsymbol{y}| \tag{8}$$

  which are characterized by the duality relations

$$y \in V_{\pm} \quad \Leftrightarrow \quad k \cdot y < 0 \qquad \forall k \in C_{\pm}. \tag{9}$$

[3] To be precise, one should begin with dual vectors $(\boldsymbol{k}, -\mathrm{i}\omega')$, since the frequency in units of it is $-\mathrm{i}\omega'$, so that $\mathrm{d}x = \mathrm{i}\mathrm{d}\boldsymbol{x}\,\mathrm{d}t$ and $\mathrm{đ}k = -\mathrm{i}\mathrm{đ}\boldsymbol{k}\,\mathrm{đ}\omega'$. The change to $\omega = -\omega'$ (or $k^4 = -k_4$), which makes the phase velocity $+\boldsymbol{k}/\omega$ instead of $-\boldsymbol{k}/\omega$, does not affect $\mathrm{đ}k$ since $\int_{-\infty}^{\infty} \mathrm{đ}\omega' \cdots = \int_{-\infty}^{\infty} \mathrm{đ}\omega \cdots$.

- The solid positive and negative frequency cones

$$V'_{\pm} \equiv \{k = (\boldsymbol{k}, \mathrm{i}\omega) \in M' : \pm\omega \geqslant \kappa > 0\} \tag{10}$$

which are the convex hulls of $C_{\pm}$, characterized by

$$k \in V'_{\pm} \quad \Leftrightarrow \quad k \cdot y < 0 \qquad \forall y \in V_{\pm}. \tag{11}$$

- The double cones

$$C = C_+ \cup C_- \qquad V = V_+ \cup V_- \qquad V' = V'_+ \cup V'_-. \tag{12}$$

Our main complex spacetime domains will be the *forward and backward tubes*

$$\mathcal{T}_{\pm} = \{z = x - \mathrm{i}y : x \in M, y \in V_{\pm}\} \tag{13}$$

and their union, which we call the *causal tube*,

$$\mathcal{T} = \mathcal{T}_+ \cup \mathcal{T}_- = \{z = x - \mathrm{i}y : x \in M, y^2 < 0\}.$$

2.2. The extension of relativistic fields

All *free* relativistic fields extend analytically to $\mathcal{T}$ in a sense to be explained. This can be done directly in spacetime by the *analytic-signal transform* (AST) [K90, KS92, K94][4]

$$\tilde{F}(x - \mathrm{i}y) = \frac{1}{2\pi\mathrm{i}} \int_{-\infty}^{\infty} \frac{\mathrm{d}s}{s - \mathrm{i}u} F(x - sy/u) \qquad y = (\boldsymbol{y}, \mathrm{i}u) \in V. \tag{14}$$

To see how this works, suppose to begin with that F is a general function not necessarily satisfying any differential equation, and substitute the Fourier expression for F:

$$\tilde{F}(x - \mathrm{i}y) = \frac{1}{2\pi\mathrm{i}} \int_{-\infty}^{\infty} \frac{\mathrm{d}s}{s - \mathrm{i}u} \int_{M'} \mathrm{đ}k\, \mathrm{e}^{\mathrm{i}k\cdot x}\, \mathrm{e}^{-\mathrm{i}sk\cdot y/u} \hat{F}(k).$$

Assuming the order of integration can be reversed, compute the integral over s by closing the contour in the upper or lower half-plane depending on the behaviour of the exponential. This gives

$$\int_{-\infty}^{\infty} \frac{\mathrm{d}s}{s - \mathrm{i}u}\, \mathrm{e}^{-\mathrm{i}sk\cdot y/u} = \hat{u}\Theta(-k \cdot y)\, \mathrm{e}^{k\cdot y} \tag{15}$$

where Θ is the Heaviside function and we have introduced a simple notation for the sign function, which will be used frequently:

$$\hat{u} = \operatorname{Sgn} u \quad \text{and} \quad \Theta(\xi) = \begin{cases} 1 & \xi > 0 \\ 0 & \xi < 0. \end{cases} \tag{16}$$

(This is easily remembered since $\hat{u}$ is just a one-dimensional (1D) version of a unit vector $\hat{\boldsymbol{u}}$.) That gives the AST as an extension of the inverse Fourier transform,

$$\tilde{F}(x - \mathrm{i}y) = \hat{u} \int_{M'} \mathrm{đ}k\, \Theta(-k \cdot y)\, \mathrm{e}^{\mathrm{i}k\cdot(x - \mathrm{i}y)} \hat{F}(k) \tag{17}$$

which also tells us that the Fourier transform in x of the AST is

$$\hat{F}(k, y) \equiv \int_M \mathrm{d}x\, \mathrm{e}^{-\mathrm{i}k\cdot x} \tilde{F}(x - \mathrm{i}y) = \hat{u}\Theta(-k \cdot y)\, \mathrm{e}^{k\cdot y} \hat{F}(k). \tag{18}$$

Despite the notation, $\tilde{F}$ is in general not analytic because the Heaviside factor spoils analyticity as y varies. (F may not have an analytic extension.) However, if $\hat{F}(k)$ is supported in V',

[4] The AST defined by (14) differs from that introduced in the above references by a sign to make it consistent with hyperfunction theory. Either one is Lorentz invariant when applied to free fields.

defined in (10), then the Heaviside function in (17) disappears after correlating positive frequencies with the future cone and negative frequencies with the past cone,

$$\Theta(-k\cdot y) = \Theta(\omega u) = \begin{cases} 1 & k \in V'_\pm \quad \text{and} \quad y \in V_\pm \\ 0 & k \in V'_\pm \quad \text{and} \quad y \in V_\mp \end{cases}$$

and we get a third expression for the AST,

$$\tilde{F}(z) = \pm \int_{V'_\pm} đk\, \mathrm{e}^{\mathrm{i}k\cdot z} \hat{F}(k) \qquad z \in \mathcal{T}_\pm. \tag{19}$$

Now

$$k \in V'_\pm \quad y \in V_\pm \Rightarrow k \cdot y \leqslant \kappa(a \mp u) < 0$$

hence the factor $\mathrm{e}^{k\cdot y}$ in the Fourier–Laplace kernel $\mathrm{e}^{\mathrm{i}k\cdot z}$ decays exponentially. If $\hat{F}(k)$ does not *grow* exponentially, the integrals (19) define holomorphic functions in $\mathcal{T}_\pm$. (Note, however, that the exponential decay gets weaker and weaker as y approaches the light cone. This will later give the ability to *focus* pulsed-beam wavelets.)

Of course, it cannot be claimed that $\tilde{F}$ is an extension of F itself since only the positive frequency part is represented in $\mathcal{T}_+$ and only the negative frequency part in $\mathcal{T}_-$. Define the *partial* boundary values

$$\tilde{F}(x \mp \mathrm{i}0) = \lim_{\varepsilon \searrow 0} \tilde{F}(x \mp \mathrm{i}\varepsilon y) \qquad y \in V_+$$

which do not depend on the particular choice of y. Then F is a boundary value of $\tilde{F}$ in the same sense as (2),[5]

$$F(x) = \tilde{F}(x - \mathrm{i}0) - \tilde{F}(x + \mathrm{i}0). \tag{20}$$

Generally, the restrictions of $\tilde{F}(z)$ to the disjoint domains $\mathcal{T}_\pm$ are unrelated holomorphic functions, but if $F(x)$ vanishes in an open region of spacetime, then (20) implies that they are part of a *single* holomorphic function. This is the famous *edge of the wedge* theorem [SW64].

It is instructive to compute the AST of a function depending only on time,

$$\begin{aligned} \tilde{F}(t - \mathrm{i}u) &= \frac{1}{2\pi\mathrm{i}} \int_{-\infty}^{\infty} \frac{\mathrm{d}s}{s - \mathrm{i}u} F(t-s) \qquad u \neq 0 \\ &= \frac{1}{2\pi\mathrm{i}} \int_{-\infty}^{\infty} \frac{\mathrm{d}s}{t - \mathrm{i}u - s} F(s) \\ &= \hat{u} \int_{-\infty}^{\infty} đ\omega\, \Theta(\omega u)\, \mathrm{e}^{-\mathrm{i}\omega(t - \mathrm{i}u)} \hat{F}(\omega) \end{aligned} \tag{21}$$

or

$$\tilde{F}(t - \mathrm{i}u) = \begin{cases} \int_0^\infty đ\omega\, \mathrm{e}^{-\mathrm{i}\omega(t-\mathrm{i}u)} \hat{F}(\omega) & u > 0 \\ -\int_{-\infty}^0 đ\omega\, \mathrm{e}^{-\mathrm{i}\omega(t-\mathrm{i}u)} \hat{F}(\omega) & u < 0. \end{cases} \tag{22}$$

This is a pair of *analytic signals* extending the positive and negative frequency parts to the lower and upper complex half-planes, a useful concept introduced by Gabor [G46] which also explains the name of our transform. (Actually, Gabor worked with real signals, where it suffices to consider only one of the above pair since the other is merely its complex conjugate.)

Equation (21) shows that $\tilde{F}$ is a convolution of F with the *Cauchy kernel*,

$$\tilde{F}(\tau) = \int_{-\infty}^{\infty} \mathrm{d}s\, C(\tau - s) F(s) \qquad \tau = t - \mathrm{i}u \qquad C(\tau) = \frac{1}{2\pi\mathrm{i}\tau} \tag{23}$$

[5] The *sum* gives a spacetime version of the Hilbert transform [K90].

and that the Fourier transform of C is

$$\hat{C}(\omega, u) \equiv \int_{-\infty}^{\infty} \mathrm{d}t\, \mathrm{e}^{\mathrm{i}\omega t} C(t - \mathrm{i}u) = \hat{u}\Theta(\omega u)\, \mathrm{e}^{-\omega u}. \tag{24}$$

The role of the sign $\hat{u}$ in the AST can be understood by assuming that $F(t)$ is compactly supported in an interval I. Then, according to the edge of the wedge theorem, $\tilde{F}(\tau)$ is holomorphic for all $\tau \notin I$ and we may therefore rewrite (21) as a contour integral

$$\tilde{F}(\tau) = \frac{1}{2\pi\mathrm{i}} \int_{-\infty}^{\infty} \frac{\mathrm{d}s}{\tau - s} \{\tilde{F}(s - \mathrm{i}0) - \tilde{F}(s + \mathrm{i}0)\} = \frac{1}{2\pi\mathrm{i}} \int_{\gamma} \frac{\mathrm{d}s}{\tau - s} \tilde{F}(s) \tag{25}$$

where γ is a closed contour surrounding I, running in the *positive* direction at $s - \mathrm{i}0$ and in the *negative* direction at $s + \mathrm{i}0$. Equation (25) is Cauchy's formula for the values of an analytic function *outside* γ if the contour can be deformed through infinity in the Riemann sphere. This interpretation would not exist without the sign in the definition of the AST.

Equation (25) shows that the sign $\hat{u}$ in (21) gives a positive orientation to the boundary of the lower-half complex time plane (i.e., the time axis as seen from below) and a negative orientation to the boundary of the upper-half complex time plane (the time axis as seen from above), which is obviously correct. This interpretation carries over directly to the spacetime AST. In a reference frame where $y = (\mathbf{0}, u)$, (14) reduces essentially to (21):

$$\tilde{F}(\boldsymbol{x}, \tau) = \frac{1}{2\pi\mathrm{i}} \int_{-\infty}^{\infty} \frac{\mathrm{d}s}{\tau - s} F(\boldsymbol{x}, s) \qquad \tau = t - \mathrm{i}u.$$

In what follows, it will be helpful to keep in mind the following correspondence between the four-dimensional (4D) geometry of spacetime and the 1D geometry of time:

$$\begin{aligned} V'_{\pm}, C_{\pm} &\longleftrightarrow \{\omega : \pm\omega > 0\} \\ V_{\pm} &\longleftrightarrow \{u : \pm u > 0\} \\ \mathcal{T}_{\pm} &\longleftrightarrow \{t - \mathrm{i}u : \pm u > 0\}. \end{aligned}$$

2.3. Massive fields and relativistic coherent states

Free particles and fields of mass $m > 0$ satisfy the Klein–Gordon equation

$$\Box F(x) \equiv \left(\Delta - \partial_t^2\right) F(x) = m^2 F(x). \tag{26}$$

(In the case of spinor or tensor fields, all components satisfy (26). We consider scalars for simplicity. Dirac particles and fields are treated in [K87, K90].) In Fourier space, this means

$$\begin{aligned} &(k^2 + m^2)\hat{F}(k) = 0 \\ &\qquad \Rightarrow \hat{F}(k) = 2\pi\delta(m^2 + k^2) f(k) = 2\pi\delta(E^2 - \omega^2) f(k), \qquad E = \sqrt{m^2 + \kappa^2} \\ &\qquad\qquad = \frac{\pi}{E}\{\delta(E - \omega) f(\boldsymbol{k}, E) + \delta(E + \omega) f(\boldsymbol{k}, -E)\} \end{aligned}$$

for some function f defined on the *double mass shell*

$$\Omega_{\pm} = \{k \in M' : \pm\omega = E\} \qquad \Omega = \Omega_+ \cup \Omega_-.$$

Therefore

$$F(x) = \int_{\Omega_+} \mathrm{d}\tilde{k}\, \mathrm{e}^{\mathrm{i}k\cdot x} f(k) + \int_{\Omega_-} \mathrm{d}\tilde{k}\, \mathrm{e}^{\mathrm{i}k\cdot x} f(k) = \int_{\Omega} \mathrm{d}\tilde{k}\, \mathrm{e}^{\mathrm{i}k\cdot x} f(k)$$

where

$$\mathrm{d}\tilde{k} = \frac{\bar{\mathrm{d}}\boldsymbol{k}}{2E} = \frac{\mathrm{d}\boldsymbol{k}}{16\pi^3 E} \tag{27}$$

is the Lorentz-invariant relativistic measure on $\Omega_\pm$ [IZ80]. Applying the AST gives

$$\begin{aligned}\tilde{F}(z) &= \hat{u}\int_\Omega \mathrm{d}\tilde{k}\,\Theta(-k\cdot y)\,\mathrm{e}^{\mathrm{i}k\cdot z} f(k)\\ &= \pm\int_{\Omega_\pm} \mathrm{d}\tilde{k}\,\mathrm{e}^{\mathrm{i}k\cdot z} f(k) \qquad z = x - \mathrm{i}y \in \mathcal{T}_\pm.\end{aligned}$$

This has been used to build a coherent-state representation for massive particles (where $f(k)$ is a 'c-number' function vanishing on Ω_- to give a positive-energy solution) and fields (where $f(\boldsymbol{k}, E)$ and $f(\boldsymbol{k}, -E)$ are creation and annihilation operators). These representations have a physical interpretation relating y to the *expected energy–momentum* of the coherent states. I am not going to repeat this construction here as it is readily available [K77, K78, K87, K90], but merely indicate how the above interpretation comes about.

Fix $y \in V_+$ and consider the exponential $\mathrm{e}^{k\cdot y}$ as a function of $k \in \Omega_+$. The Lorentzian scalar product satisfies the reverse Schwartz inequality

$$k\cdot y \leqslant -m\lambda \qquad \text{where} \quad \lambda = \sqrt{-y^2} = \sqrt{u^2 - a^2} > 0$$

which becomes an equality if and only if k is parallel to y:

$$\begin{aligned}&k\cdot y = -m\lambda \quad \Leftrightarrow \quad k = (m/\lambda)y \equiv k_y\\ &\qquad\therefore \quad \mathrm{e}^{k\cdot y} \leqslant \mathrm{e}^{-m\lambda} \qquad \text{and} \qquad \mathrm{e}^{k\cdot y} = \mathrm{e}^{-m\lambda} \quad \Leftrightarrow \quad k = k_y.\end{aligned} \tag{28}$$

Therefore $\mathrm{e}^{k\cdot y}$ acts as a *ray filter* in momentum space, favouring those plane waves propagating approximately in the direction of y. The larger we take λ, the narrower the filter and the more collimated the ray bundle passed by it. The coherent states are defined in momentum space by

$$e_z(k) = \mathrm{e}^{-\mathrm{i}k\cdot z^*} \qquad z^* = x + \mathrm{i}y \tag{29}$$

so that they act as *evaluation maps* on the Hilbert space $\tilde{\mathcal{H}}$ of holomorphic solutions with inner product defined in $L^2(\mathrm{d}\tilde{k})$:

$$\tilde{F}(z) = \langle e_z | f\rangle \qquad \langle \tilde{F}_1 | \tilde{F}_2\rangle \equiv \langle f_1 | f_2\rangle. \tag{30}$$

This makes $\tilde{\mathcal{H}}$ a reproducing kernel Hilbert space, and that kernel is

$$K(z', z^*) \equiv \langle e_{z'} | e_z\rangle = \int_{\Omega_+} \mathrm{d}\tilde{k}\,\mathrm{e}^{\mathrm{i}k\cdot(z'-z^*)} = -\mathrm{i}\Delta^+(m; z' - z^*) \tag{31}$$

where Δ^+ is the *Wightman 2-point function for the scalar field of mass m*.

To obtain a resolution of unity, choose any oriented three-dimensional (3D) submanifold S in M as a prospective configuration space and the six-dimensional (6D) submanifold

$$\sigma_\lambda = \{x - \mathrm{i}y \in \mathcal{T}_+ : x \in S,\, y^2 = -\lambda^2\} \qquad \lambda > 0$$

as the associated classical phase space, with $\lambda > 0$ arbitrary. A symplectic form and covariant measure on σ_λ are chosen as follows. Define the invariant 2-form and 6-form

$$\alpha = \mathrm{d}x_\mu \wedge \mathrm{d}y^\mu \qquad \alpha^3 = \alpha\wedge\alpha\wedge\alpha.$$

Then the following are proved:

- The restriction of α to σ_λ is a symplectic form if and only if S is *nowhere timelike*, i.e. it must be locally spacelike or lightlike. In other words, σ_λ *is a reasonable phase space if and only if S is a reasonable configuration space*, so the symplectic geometry is compatible with the spacetime geometry.

- If S satisfies the above condition, then α^3 defines a positive measure $\mathrm{d}\mu_\lambda$ on σ_λ and we have a resolution of unity

$$\int_{\sigma_\lambda} \mathrm{d}\mu_\lambda(z)|e_z\rangle\langle e_z| = I \qquad \mathrm{d}\mu_\lambda = C(\lambda, m)\alpha^3 \tag{32}$$

  where $C(\lambda, m)$ is an invariant and I is the identity operator on $L^2(\mathrm{d}\tilde{k})$.
- The physical interpretation of σ_λ as a phase space is confirmed explicitly in the case when S is the hyperplane $\{t = \text{constant}\}$ by the expected positions and momenta in the state e_z,

$$\begin{array}{lll} \langle P_\mu\rangle_{e_z} = a y_\mu & y_\mu = -\mathrm{Im}\, z_\mu & \mu = 0, 1, 2, 3 \\ \langle X_j(t)\rangle_{e_z} = x_j & x = (\boldsymbol{x}, \mathrm{i}t) & j = 1, 2, 3 \end{array} \tag{33}$$

  where $a(\lambda, m)$ is an invariant and X_j are the Newton–Wigner operators in the Heisenberg picture at time t. (For general S, the position operators obtained by quantization on σ_λ do not commute; see [K76].)
- The parameter $1/\lambda$ measures the uncertainty or *resolution* in the momentum of coherent states parametrized by $z \in \sigma_\lambda$, in accordance with the above discussion of ray filters.
- Unlike the usual spacetime representation, *the coherent-state representation admits a conserved, covariant probability current density*, given by

$$j_\mu(z) = -\frac{\partial|\tilde{F}(z)|^2}{\partial y^\mu} = \mathrm{i}\,\tilde{F}(z)^* \frac{\partial\tilde{F}(z)}{\partial x^\mu} - \mathrm{i}\frac{\partial\tilde{F}(z)^*}{\partial x^\mu}\tilde{F}(z). \tag{34}$$

- In the nonrelativistic limit one obtains a coherent-state representation of the centrally extended Galilean group with Gaussian measure in momentum,

$$\mathrm{d}\mu_\lambda^{\mathrm{NR}} = C\,\mathrm{e}^{-m\boldsymbol{y}^2/u}\mathrm{d}\boldsymbol{x}\,\mathrm{d}\boldsymbol{y} \qquad \boldsymbol{y} = \frac{u}{m}\langle\boldsymbol{P}\rangle. \tag{35}$$

The weight function is imposed on the relativistic (hence *uniform*) measure $\mathrm{d}\mu_\lambda$ in compensation for the deformation of the mass shell Ω_+ to a 3-plane at infinity (the nonrelativistic momentum space). Upon applying a 'holomorphic gauge transformation' [KM80] to the nonrelativistic wavefunctions (solutions of Schrödinger's equation), the representation becomes identical to the Bargmann–Segal representation of the Weyl–Heisenberg group:

$$\tilde{F}_{\mathrm{NR}} \to \mathrm{e}^{m\boldsymbol{z}^2/4u}\tilde{F}_{\mathrm{NR}} \Rightarrow \mathrm{d}\mu_\lambda^{\mathrm{NR}} \to C\,\mathrm{e}^{-m|\boldsymbol{z}|^2/2u}\mathrm{d}\boldsymbol{x}\,\mathrm{d}\boldsymbol{y}. \tag{36}$$

2.4. Massless fields and wavelets

In the limit $m \to 0$, the 'reconstruction constant' $C(\lambda, m)$ in (32) diverges and the coherent-state representation is no longer square-integrable due to the disappearance of the 'mass gap' $\kappa \geqslant m > 0$. At the same time, the symmetry group grows from the Poincaré group to the conformal group $\mathcal{C}$. In its realization as $SU(2, 2), \mathcal{C}$ acts on $\mathcal{T}_\pm$ by matrix-valued Möbius transformations. Thus it is reasonable to look for resolutions of unity adapted to the new symmetries. This took me several years to realize, and only when studying wavelet theory (while helping organize Daubchies' 1990 *Ten Lectures* conference [D92]) did I understand that *scaling* needed to be brought into the picture. Since massless fields are important in classical as well as quantum physics, I decided to begin with classical fields, the prime examples of which are acoustic and electromagnetic fields. This led to the construction of acoustic and electromagnetic wavelets [K92, K94, K94a]. From a foundational as well as applied point of view, I believe the electromagnetic wavelets hold far more promise and the 'acoustic' ones serve mainly to simplify the analysis by stripping away all complications related to polarization. I now briefly review the construction of acoustic wavelets, leaving the electromagnetic ones to the end of the paper where they and their sources will be constructed from the scalar acoustic sources.

Solutions of the scalar wave equation are given by

$$\Box F(x) = 0 \Rightarrow F(x) = \int_C \mathrm{d}\tilde{k}\, \mathrm{e}^{\mathrm{i}k\cdot x} f(k) \tag{37}$$

where $\mathrm{d}\tilde{k} = \text{đ}\boldsymbol{k}/2\kappa$ is the massless version of (27) on the double light cone C (12). Applying the AST gives the extension to $z \in \mathcal{T}_\pm$,

$$\tilde{F}(z) = \hat{u} \int_C \mathrm{d}\tilde{k}\, \Theta(-k\cdot y)\, \mathrm{e}^{\mathrm{i}k\cdot z} f(k) = \pm \int_{C_\pm} \mathrm{d}\tilde{k}\, \mathrm{e}^{\mathrm{i}k\cdot z} f(k). \tag{38}$$

In the massive case, we chose the coherent states to be the complex conjugates of $\mathrm{e}^{\mathrm{i}k\cdot z}$. However, this cannot be done now because $\mathrm{e}^{\mathrm{i}k\cdot z}$ does not vanish near $\omega = 0$ and this will spoil the resolution of unity. (In wavelet terms, $\mathrm{e}^{\mathrm{i}k\cdot z}$ is not *admissible*.) We get around this difficulty by changing the inner product of solutions to

$$\langle F_1|F_2\rangle \equiv \langle f_1|f_2\rangle = \int_C \frac{\mathrm{d}\tilde{k}}{\kappa^\nu} f_1(k)^* f_2(k) \qquad \nu \geqslant 0. \tag{39}$$

For $\nu = 0$ this is the Lorentz-invariant inner product, but it will turn out that we need $\nu > 1$ to obtain admissible wavelets. Next, write the extension (38) in the form of an inner product

$$\tilde{F}(z) = \hat{u} \int_C \frac{\mathrm{d}\tilde{k}}{\kappa^\nu} \kappa^\nu \Theta(-k\cdot y)\, \mathrm{e}^{\mathrm{i}k\cdot z} f(k) = \langle \psi_z|f\rangle \tag{40}$$

where

$$\psi_z(k) = \hat{u}\kappa^\nu \Theta(-k\cdot y)\, \mathrm{e}^{-\mathrm{i}k\cdot z^*} \tag{41}$$

are to be the 'acoustic wavelets' in Fourier space, representing spacetime solutions

$$\Psi_z(x') = \hat{u} \int_C \mathrm{d}\tilde{k}\, \kappa^\nu \Theta(-k\cdot y)\, \mathrm{e}^{\mathrm{i}k\cdot(x'-x+\mathrm{i}y)} \equiv \Psi(x' - z^*). \tag{42}$$

From the invariance of $\mathrm{d}\tilde{k}$ under $k \to -k$ it follows that

$$\Psi(-z) = -\Psi(z) \tag{43}$$

hence it suffices to compute Ψ in $\mathcal{T}_+$. For any fixed $y \in V_+$, the function $\Psi(x - \mathrm{i}y)$ may be called a 'mother wavelet' from which all others are obtained by complex translations. Note that *imaginary translations* replace scaling: the deeper we go into $\mathcal{T}_+$, the more blurred our fields become.

As in the massive case, where a great deal of freedom existed to choose a phase space σ due to the abundance of coherent states, there is now a lot of freedom in choosing a family of Ψ_z to build a resolution of unity. Perhaps the simplest choice for a *continuous* frame is by analogy with 1D wavelets, which are parametrized by position and scale. 'Position' is now $\boldsymbol{x}$, and we take 'scale' to be u, since it dominates the other scale parameters $\boldsymbol{y}$. Thus we fix any time t, say $t = 0$, and set $\boldsymbol{y} = \boldsymbol{0}$ (this will give *spherical* wavelets). Our parameter space is then

$$E = \{z = (\boldsymbol{x}, u) : \boldsymbol{x} \in \mathbb{R}^3, u \neq 0\} \tag{44}$$

which is a *Euclidean spacetime* consisting of real space and imaginary time coordinates, with the Euclidean time u acting as a scale in $\mathbb{R}^{3,1}$. A quick dimensional analysis shows that to compensate for the weight κ^ν in Fourier space, we need a measure

$$\mathrm{d}\mu_\nu(z) = C_\nu\, \mathrm{d}\boldsymbol{x} |u|^{\nu-2}\, \mathrm{d}u,$$

with C_ν adjusted to give a resolution of the identity I_ν in $L^2(\mathrm{d}\tilde{k}/\kappa^\nu)$. This turns out to be correct, with

$$\int_E \mathrm{d}\mu_\nu(z)|\Psi_z\rangle\langle\Psi_z| = I_\nu \qquad C_\nu = 2^\nu/\,\Gamma(\nu-1). \tag{45}$$

Thus we must take $\nu > 1$ to get 'admissible' wavelet representations, and (45) then gives solutions of the wave equation as superpositions of spherical wavelets centred at $\boldsymbol{x}$ with a pulse duration of order u. These wavelets are sourceless, *converging* onto $\boldsymbol{x}$ when $t < 0$ and *diverging* from $\boldsymbol{x}$ when $t > 0$, and their radius at the *waist* $t = 0$ is, like the pulse duration, of order u. As promised, u controls all scales.

Converging spherical wavelets are unnatural under ordinary conditions[6]. We want to eliminate the converging (advanced) part and retain only the diverging (retarded) part. The resulting wavelets will have *sources*, but the splitting cannot be done by brute force (e.g. multiplying by the Heaviside function $\Theta(t)$) since that will spoil the analyticity and amount to introducing sources with infinite support at $t = 0$. A natural separation into advanced and retarded wavelets was found in [K94, chapter 11] while computing $\Psi(z)$. We review this because it foreshadows the recent developments.

Assuming ν is a nonnegative integer, we have for $z \in \mathcal{T}_+$

$$\Psi(z) = \int_{C_+} \mathrm{d}\tilde{k}\,\kappa^\nu\,\mathrm{e}^{\mathrm{i}k\cdot z} = (-\partial_u)^\nu G(z) \qquad G(z) = \int_{C_+} \mathrm{d}\tilde{k}\,\mathrm{e}^{\mathrm{i}k\cdot z} = \frac{1}{4\pi^2 z^2} \tag{46}$$

where $G(z)$, the original inadmissible kernel with $\nu = 0$, is most easily computed by using the Lorentz invariance of the integral. Now

$$z^2 = (\boldsymbol{x} - \mathrm{i}\boldsymbol{y})^2 - (t - \mathrm{i}u)^2 = -(t - \mathrm{i}u - \tilde{r})(t - \mathrm{i}u + \tilde{r}) \tag{47}$$

where

$$\tilde{r}(\boldsymbol{x} - \mathrm{i}\boldsymbol{y}) = \sqrt{(\boldsymbol{x} - \mathrm{i}\boldsymbol{y})^2} \qquad \mathrm{Re}\,\tilde{r} \geqslant 0 \tag{48}$$

is the *complex distance* from the source point $\mathrm{i}\boldsymbol{y}$ to the observation point $\boldsymbol{x}$, which will be studied in detail. Thus $G(z)$ can be expanded in partial fractions

$$G(z) = \mathrm{i}\tilde{D}^-(z) - \mathrm{i}\tilde{D}^+(z) \qquad \tilde{D}^\pm(z) = \frac{1}{8\mathrm{i}\pi^2\tilde{r}}\cdot\frac{1}{t - \mathrm{i}u \mp \tilde{r}} = \frac{1}{8\pi^2\tilde{r}}\cdot\frac{1}{u + \mathrm{i}(t \mp \tilde{r})}$$

and (46) gives

$$\Psi(z) = \mathrm{i}\Psi^-(z) - \mathrm{i}\Psi^+(z) \qquad \Psi^\pm(z) = \frac{1}{8\mathrm{i}\pi^2\tilde{r}}\cdot\frac{\Gamma(\nu+1)}{(u + \mathrm{i}(t \mp \tilde{r}))^{\nu+1}}. \tag{50}$$

These expression remain valid if ν is not an integer, provided an appropriate branch cut is chosen. $\Psi(z)$ splits naturally into retarded and advanced parts without spoiling analyticity *everywhere*, as would a brute-force splitting. Instead, the two parts inherit only the singularities of the complex distance function. For given $\boldsymbol{y} \neq \boldsymbol{0}$,

- they diverge on the *branch circle* $\mathcal{S}$ of radius $|\boldsymbol{y}|$ in the plane $\boldsymbol{y}^\perp$, where $\tilde{r} = 0$;
- they are discontinuous across the *branch disc* $\mathcal{D}$ (56) spanning $\mathcal{S}$;
- Ψ^- and Ψ^+ are *pulsed beams* converging to $\mathcal{D}$ at $t < 0$ and diverging from $\mathcal{D}$ at $t > 0$;
- Ψ^- and Ψ^+ have a common source supported in $\mathcal{D}$, so that Ψ is sourceless.

[6] There are exceptions, including the recent method of *time-reversed acoustics* [F97] where sound is recorded by an array of microphones which are then played in reverse, sending the waves back.

We have called $\tilde{r}$ the 'distance' from an imaginary source point $\mathrm{i}\boldsymbol{y}$ to a real observation point $\boldsymbol{x}$. At this stage, such language must be viewed as 'poetry' since the idea of a point source at $\mathrm{i}\boldsymbol{y}$ has not been defined and it is not even clear what it means. In physics, a complex distance function identical to $\tilde{r}$ was the basis for the construction of spinning, charged black holes; see [N65a, N73]. In engineering, 'complex-source pulsed beams' similar to the above[7] have been applied extensively since the 1980s, and their time-harmonic components, known as 'complex-source beams,' have been used similarly since the 1970s; see [HF01] for a comprehensive review. But until recently, no serious study seems to have been undertaken to make mathematical sense of the idea of a 'complex point source', whether time harmonic or pulsed, and therefore of how such beams may be realized. (See [HLK00] for an earlier attempt.) Perhaps this is because their singular and convoluted near-field structure appears to make the requisite analysis difficult if not impossible. We will see that the sources are not only tractable in spacetime but, most significantly, even simple and computationally effective in Fourier space.

Although the requirement $\nu > 1$ precludes a Lorentz-invariant wavelet representation for acoustic waves, it does admit one for electromagnetic waves, where the invariant measure on the light cone has $\nu = 2$. Note that

$$\frac{\mathrm{d}\tilde{k}}{\kappa^2} = \frac{\text{đ}\boldsymbol{k}}{2\kappa^3} \tag{51}$$

is *scaling invariant* as well as Lorentz invariant. In fact, the associated Hilbert space of solutions of Maxwell's equations carries a unitary representation of the full conformal group $\mathcal{C}$, as proved by Gross [Gr64]. The electromagnetic wavelet representation is likewise covariant under $\mathcal{C}$ [K94, chapter 9], and this opens up some interesting applications. I will not discuss the details here since more recent developments are discussed later.

3. Point sources in complex space

We now begin implementing the 'Euclidean strategy' of setting up base camp in the Euclidean world from which to tackle the hyperbolic world by

- analytically extending the fundamental solutions of Laplace's equation,
- computing the extended δ-sources, and
- extracting Minkowskian propagators and sources from these extensions.

Because we will need the fundamental solutions in $\mathbb{R}^3$ as well as $\mathbb{R}^4$, we work in this section with $\mathbb{R}^n$ for $n \geqslant 3$. The fundamental solution [T96] G_n for Laplace's equation in $\mathbb{R}^n$ is

$$\Delta_n G_n(\boldsymbol{x}) = -\delta_n(\boldsymbol{x}) \qquad G_n(\boldsymbol{x}) = \frac{1}{\omega_n}\frac{r^{2-n}}{n-2} \qquad n \geqslant 3 \tag{52}$$

where $\omega_n = 2\pi^{n/2}/\,\Gamma(n/2)$ is the area of the unit sphere in $\mathbb{R}^n$ and

$$r(\boldsymbol{x}) = \sqrt{\boldsymbol{x}^2}$$

is the Euclidean distance[8]. To extend G_n analytically, we need only extend r. Define the *complex distance* from $\mathrm{i}\boldsymbol{y}$ (source point) to $\boldsymbol{x}$ (observation point) as

$$\tilde{r}(\boldsymbol{x} - \mathrm{i}\boldsymbol{y}) = \sqrt{(\boldsymbol{x} - \mathrm{i}\boldsymbol{y})^2} = \sqrt{r^2 - a^2 - 2\mathrm{i}\boldsymbol{x}\cdot\boldsymbol{y}}. \tag{53}$$

[7] I was unaware of this work when developing acoustic and electromagnetic wavelets, and thank Udi Heyman for pointing it out.

[8] The potential in $\mathbb{R}^2$ is $G_2 = (2\pi)^{-1}\ln r$. Although our method works here as well, this case is somewhat special and will be treated elsewhere [K0x].

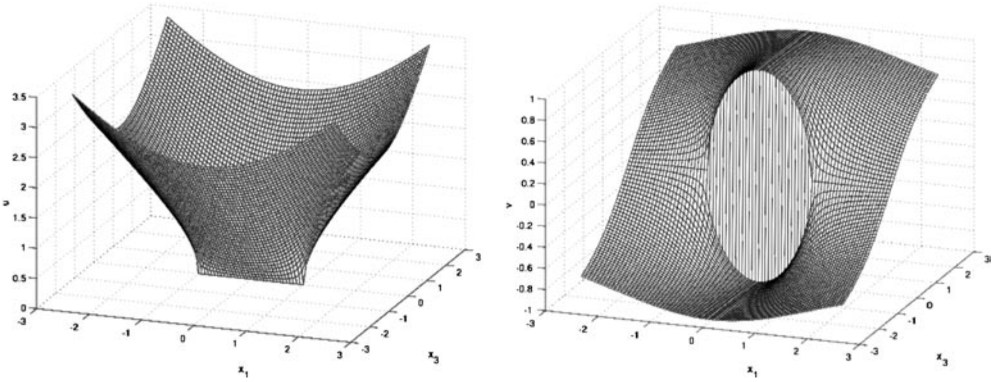

Figure 1. Plots of Re $\tilde{r}$ (left) and Im $\tilde{r}$ (right) with $n = 2$ and $\boldsymbol{y} = (0, 1)$. The branch cut $\mathcal{D}(\boldsymbol{y})$ is now the interval $[-1, 1]$ along the x_1-axis. The graph of Re $\tilde{r}(\boldsymbol{x})$ is a pinched cone, and the jump in Im $\tilde{r}(\boldsymbol{x})$ across $D(\boldsymbol{y})$ is $2\sqrt{1 - x_1^2}$, hence the cut is circular. Note from (61) that far from the cut, Re $\tilde{r} \approx r$ and Im $\tilde{r} \approx -\cos\theta$ (since $a = 1$ here).

Fixing $\boldsymbol{y} \neq \mathbf{0}$, the branch points form an $(n-2)$-sphere in the hyperplane $\boldsymbol{y}^{\perp}$ of $\mathbb{R}^n$,

$$\mathcal{S}(\boldsymbol{y}) = \{\boldsymbol{x} \in \mathbb{R}^n : r = a, \boldsymbol{x} \cdot \boldsymbol{y} = 0\}. \tag{54}$$

We will use the cylindrical coordinates[9] $(\rho, \boldsymbol{\sigma}, \xi)$ given by

$$\xi = \hat{\boldsymbol{y}} \cdot \boldsymbol{x} \qquad \rho = \sqrt{r^2 - \xi^2} \qquad \boldsymbol{x} = \rho\boldsymbol{\sigma} + \xi\hat{\boldsymbol{y}} \tag{55}$$

where $\hat{\boldsymbol{y}} = \boldsymbol{y}/a$ and $\boldsymbol{\sigma}$ is a unit vector orthogonal to $\boldsymbol{y}$. The intersection of $\mathcal{S}(\boldsymbol{y})$ with the half-plane through $\pm\boldsymbol{y}$ and $\boldsymbol{\sigma}$ is the point $(a, \boldsymbol{\sigma}, 0)$. If $\boldsymbol{x}$ follows a simple loop in the half-plane surrounding this point (a *link* around the circle), then $\tilde{r}$ changes sign. To make $\tilde{r}$ single valued, we must prevent the completion of such loops by choosing a *branch cut* consisting of a hypersurface with $\mathcal{S}$ as its boundary. The branch cut must be chosen so that $\tilde{r}$ reduces to the usual distance in $\mathbb{R}^n$, i.e.,

$$\boldsymbol{y} \to \mathbf{0} \Rightarrow \tilde{r}(\boldsymbol{x} - \mathrm{i}\boldsymbol{y}) \to +r(\boldsymbol{x}).$$

The simplest such cut is obtained by requiring

$$\operatorname{Re} \tilde{r} \geqslant 0$$

which gives the *disc* spanning $\mathcal{S}(\boldsymbol{y})$,

$$\mathcal{D}(\boldsymbol{y}) = \{\boldsymbol{x} : r \leqslant a, \boldsymbol{x} \cdot \boldsymbol{y} = 0\} \qquad \partial\mathcal{D} = \mathcal{S}. \tag{56}$$

The most general branch cut is a *membrane* obtained from $\mathcal{D}$ by an arbitrary continuous deformation leaving its boundary invariant.

Note: by 'branch cut' we really mean a *slice* of the branch cut of $\tilde{r}(\boldsymbol{z})$ at constant $\boldsymbol{y}$, since the source is taken as fixed.

Fixing $\boldsymbol{y} \neq \mathbf{0}$, write

$$\tilde{r} \equiv \sqrt{(\boldsymbol{x} - \mathrm{i}\boldsymbol{y})^2} = p(\boldsymbol{x}) - \mathrm{i}q(\boldsymbol{x}) \tag{57}$$

with the $\boldsymbol{y}$-dependence understood. Then $p(\boldsymbol{x}) \geqslant 0$ in $\mathbb{R}^n$, $\mathcal{D}$ is characterized by $p = 0$, and $\mathcal{S}$ by $p = q = 0$. See figure 1 for the graphs of $p(x)$ and $q(x)$.

[9] To help visualize the geometry, the reader may think of the case $n = 3$, where $\mathcal{S}(\boldsymbol{y})$ is the circle forming the equator of the sphere whose north pole is $\boldsymbol{y}$ and the unit vector $\boldsymbol{\sigma}$ is represented by the azimuthal angle ϕ in the plane $\boldsymbol{y}^{\perp}$.

Squaring (57) and equating real and imaginary parts gives

$$r^2 - a^2 = p^2 - q^2 \qquad \boldsymbol{x}\cdot\boldsymbol{y} = pq. \tag{58}$$

The cylindrical coordinates (55) are thus given by

$$\begin{aligned} a\xi &= pq \\ a^2\rho^2 &= a^2r^2 - p^2q^2 = a^2(p^2 - q^2 + a^2) - p^2q^2 \\ &= (p^2 + a^2)(a^2 - q^2). \end{aligned} \tag{59}$$

In particular, note that $|q| \leqslant a = |\boldsymbol{y}|$, i.e., *the imaginary part of* $\tilde{r}(\boldsymbol{z})$ *is bounded by the modulus of the imaginary part of* $\boldsymbol{z}$.

It follows immediately from (59) that the *level surfaces* of $p(\boldsymbol{x})$ and $q(\boldsymbol{x})$ are

$$\begin{aligned} E_p &\equiv \{\text{constant } p > 0\} = \left\{\boldsymbol{x} : \frac{\rho^2}{p^2 + a^2} + \frac{\xi^2}{p^2} = 1\right\} \\ H_q^{\pm} &\equiv \{\text{constant } 0 < \pm q < a\} = \left\{\boldsymbol{x} : \frac{\rho^2}{a^2 - q^2} - \frac{\xi^2}{q^2} = 1, \pm\xi > 0\right\}. \end{aligned} \tag{60}$$

The E_p are a family of *confocal oblate spheroids* filling the complement of $\mathcal{D}$ in $\mathbb{R}^n$ having $\mathcal{S}$ as their common focal set, and the $H_q^{\pm}$ are the orthogonal family of upper and lower semi-hyperboloids, also $\mathcal{S}$-confocal and joining in $\mathcal{D}$. As $p \to 0$, E_p converges to a *double cover* of $\mathcal{D}$, a fact that will be important in our computations. Similarly, as $q \to 0$, $H_q^{\pm}$ converge to the upper and lower covers of the *complement* of $\mathcal{D}$ in the hyperplane $\xi = 0$. Finally, as $q \to \pm a$, the semi-hyperboloids collapse to the half-lines

$$H_a^{\pm} = \{q = \pm a\} = \{\pm\lambda\boldsymbol{y} : \lambda > 0\}.$$

For the pulsed beams, the E_p (with $n = 3$) will be *wave fronts*, the $H_q^{\pm}$ give the orthogonal surfaces of *radiation flow*, and $H_a^{\pm}$ will be the forward and backward *beam axes*. Use will also be made of the *far-zone approximation*. By (58),

$$r \gg a \Rightarrow p \approx r \quad q \approx a\cos\theta \tag{61}$$

hence far from the disc E_p becomes the sphere $r = p$ and $H_q^{\pm}$ become the cones $\cos\theta = q/a$.

The complex distance thus provides a natural set of coordinates in $\mathbb{R}^n$, called *oblate spheroidal* (OS) *coordinates*, given by

$$(p, q, \boldsymbol{\sigma}) : p \geqslant 0 \qquad -a \leqslant q \leqslant a \quad \boldsymbol{\sigma} \in \mathcal{S}(\hat{\boldsymbol{y}}).$$

We now *define the point source at* i$\boldsymbol{y}$ by

$$\tilde{\delta}_n(\boldsymbol{x} - \mathrm{i}\boldsymbol{y}) = -\Delta_n G_n(\boldsymbol{x} - \mathrm{i}\boldsymbol{y}) \qquad G_n(\boldsymbol{z}) \equiv \frac{1}{\omega_n}\frac{\tilde{r}^{2-n}}{n-2} \tag{62}$$

where Δ_n is the (distributional) Laplacian in $\boldsymbol{x}$. It can be shown [K00] that for any $\boldsymbol{y}$, $\tilde{\delta}_n(\boldsymbol{x}-\mathrm{i}\boldsymbol{y})$ is a *compactly supported distribution* in $\boldsymbol{x} \in \mathbb{R}^n$ in the sense of Schwartz. Although the proof is somewhat involved, the supports are easily found. For *even* $n \geqslant 4$, $G_n(\boldsymbol{z})$ is analytic wherever $\boldsymbol{z}^2 \neq 0$, in which case $\Delta_n G_n(\boldsymbol{z}) = 0$. Hence[10]

$$\operatorname{supp}_{\boldsymbol{x}} \tilde{\delta}_n(\boldsymbol{x} - \mathrm{i}\boldsymbol{y}) = \mathcal{S}(\boldsymbol{y}) \quad \text{for even} \quad n \geqslant 4. \tag{63}$$

But for *odd* n, G_n inherits a branch cut from $\tilde{r}$, where differentiating across the discontinuity contributes to the support of $\tilde{\delta}_n$. Thus

$$\operatorname{supp}_{\boldsymbol{x}} \tilde{\delta}_n(\boldsymbol{x} - \mathrm{i}\boldsymbol{y}) = \mathcal{D}(\boldsymbol{y}) \quad \text{for odd} \quad n \geqslant 3. \tag{64}$$

[10] In the Minkowski space $\mathbb{R}^{n-1,1}$, $\boldsymbol{y}$ becomes the time axis, $\mathcal{S}$ a slice of the light cone $r = |t|$, $\mathcal{D}$ a slice of the future cone $r \leqslant |t|$, and (63) and (64) translate to *Huygens' principle* for even $n \geqslant 4$ and lack thereof for odd $n \geqslant 3$; see [K00].

(The same holds for $n = 2$ since $2\pi G_2(\boldsymbol{z}) = \ln \tilde{r}$ has a branch cut on the interval $\mathcal{D}$.) The distribution $\tilde{\delta}_3(\boldsymbol{z})$ will be computed later along with its time-dependent version for pulsed beams.

To illustrate the above, we work out the case $n = 1$ which, although trivial, will be seen to be indicative. Recalling our notation $\hat{x}$ for the sign of x, we have for $z = x - \mathrm{i}y \in \mathbb{C}$

$$\tilde{r} = \sqrt{(x - \mathrm{i}y)^2} = \hat{x}(x - \mathrm{i}y) = |x| - \mathrm{i}\hat{x}y \qquad x \neq 0.$$

(Note that this is *not* simply the distance in $\mathbb{C}$ between $\mathrm{i}y$ and x, which would be $\sqrt{|x - \mathrm{i}y|^2}$ and not $\sqrt{(x - \mathrm{i}y)^2}$.) Since the 'unit sphere' in $\mathbb{R}$ consists of $x = \pm 1$, its 'area' is $\omega_1 = 2$, and (52) gives the correct solution in $\mathbb{R}$:

$$G_1(x) = -\frac{|x|}{2} \Rightarrow \partial_x^2 G_1 = -\delta_1(x).$$

Therefore

$$G_1(x - \mathrm{i}y) = -\frac{|x| - \mathrm{i}\hat{x}y}{2} \qquad \partial_x G_1(x - \mathrm{i}y) = -\frac{\hat{x}}{2} + \mathrm{i}y\delta_1(x)$$

hence

$$\tilde{\delta}_1(x - \mathrm{i}y) = -\partial_x^2 G_1(x - \mathrm{i}y) = \delta_1(x) - \mathrm{i}y\delta_1'(x) \tag{65}$$

with Fourier transform

$$\widehat{\tilde{\delta}}_1(k, y) \equiv \int_{-\infty}^{\infty} \mathrm{d}x\, \mathrm{e}^{-\mathrm{i}kx} \tilde{\delta}_1(x - \mathrm{i}y) = 1 + ky. \tag{66}$$

4. Point sources in complex spacetime

Following our 'Euclidean strategy', we bring time into the picture by complexifying Euclidean spacetime:

$$x_E = (\boldsymbol{x}, u) \in \mathbb{R}^4 \qquad y_E = (\boldsymbol{y}, -t) \in \mathbb{R}^4$$
$$z = x_E - \mathrm{i}y_E = (\boldsymbol{x} - \mathrm{i}\boldsymbol{y}, u + \mathrm{i}t) \in \mathbb{C}^4.$$

This can be rewritten as a complex *Minkowski* vector

$$z = x - \mathrm{i}y = (\boldsymbol{z}, \mathrm{i}\tau) \qquad \boldsymbol{z} = \boldsymbol{x} - \mathrm{i}\boldsymbol{y} \qquad \tau = t - \mathrm{i}u \qquad z^2 = \boldsymbol{z}^2 - \tau^2$$

where

$$x = (\boldsymbol{x}, \mathrm{i}t) \qquad y = (\boldsymbol{y}, \mathrm{i}u) \in \mathbb{R}^{3,1}$$

are regarded as *real* Minkowski vectors with pseudonorms

$$x^2 = \boldsymbol{x}^2 - t^2 \qquad y^2 = \boldsymbol{y}^2 - u^2.$$

Now consider the fundamental solution for the Laplacian in $\mathbb{R}^4$ and its holomorphic extension,

$$\begin{aligned} &G_4(x_E) = \frac{1}{4\pi^2 x_E^2} \qquad G_4(z) = \frac{1}{4\pi^2 z^2} \\ &\Delta_4 G_4(\boldsymbol{x}, u) = \left(\Delta_{\boldsymbol{x}} + \partial_u^2\right) G_4(\boldsymbol{x}, u) = -\delta_4(\boldsymbol{x}, u). \end{aligned} \tag{67}$$

We have already seen $G(z) = G_4(z)$ in (46), but there it had the above form only in $\mathcal{T}_+$, being antisymmetric because of the sign factor $\hat{u}$ in (42). This 'twist' was the result of applying the AST to a spacetime field and is another example of the pitfalls of starting from the Lorentzian world. To be precise, $\hat{u}$ gives the orientation of $\mathcal{T}_-$ *relative to the way* $\mathbb{R}^{3,1}$ *is embedded in* $\mathbb{C}^4$ (recall the one-dimensional case (25)), thus it has no role in the Euclidean world. In fact, we can now see that the restrictions to $\mathcal{T}_\pm$ of the extended relativistic field $\Psi(z)$ in (46) are part of a single holomorphic function, just as $\hat{u}G(z)$ are both part of $G_4(z)$.

Before defining point sources in complex spacetime, or *complex event sources*, we must understand how *real* point sources in $\mathbb{R}^{3,1}$ fit into this picture. *Naively*, it might be hoped that the substitution $u \to \mathrm{i}t$ into (67) gives a propagator for the wave equation,

$$\Box\, G_4(\boldsymbol{x}, \mathrm{i}t) \equiv \left(\Delta_{\boldsymbol{x}} - \partial_t^2\right) G_4(\boldsymbol{x}, \mathrm{i}t) \overset{??}{\sim} -\delta_{3,1}(\boldsymbol{x}, t). \tag{68}$$

We will see that this fails for the following reasons:

- G_4 is singular on the light cone $x^2 = 0$ and must be defined as a *distribution* in $\mathbb{R}^{3,1}$ by a limiting process.
- When properly defined in $\mathbb{R}^{3,1}$, it turns out to be *sourceless*.
- Propagators are related to *causality*, which depends on the existence of the light cone and hence makes sense in $\mathbb{R}^{3,1}$ but not in $\mathbb{R}^4$. Thus $G_4(z)$, which comes from $\mathbb{R}^4$, cannot itself be a propagator.

To find the extended propagators, we repeat the construction initiated in (47),

$$z^2 = \boldsymbol{z}^2 - \tau^2 = \tilde{r}^2 - \tau^2 = -(\tau - \tilde{r})(\tau + \tilde{r}) \tag{69}$$

which gives the causal–anticausal splitting already encountered in (50),

$$G_4(z) = \mathrm{i}\tilde{D}^-(z) - \mathrm{i}\tilde{D}^+(z) \qquad \tilde{D}^\pm(z) = \frac{1}{8\mathrm{i}\pi^2 \tilde{r}(\tau \mp \tilde{r})}. \tag{70}$$

Since formal differentiation gives

$$\Box\, \tilde{D}^\pm(z) = 0$$

$\tilde{D}^\pm$ can have sources only at $\boldsymbol{x} \in \mathcal{D}$ or $\tilde{r} = \pm\tau$. We will show that $\tilde{D}^\pm(z)$ are the proper extensions of the advanced and retarded propagators in $\mathbb{R}^{3,1}$. Note that choosing the 'unphysical' branch of $\tilde{r}$ simply reverses the sense of causality:

$$\tilde{r} \to -\tilde{r} \Rightarrow \tilde{D}^\pm(z) \to -\tilde{D}^\mp(z). \tag{71}$$

Thus it will suffice to study the properties of $\tilde{D}^+(z)$. Its time behaviour is governed by the *retarded Cauchy kernel,*

$$C(\tau - \tilde{r}) = \frac{1}{2\pi\mathrm{i}(\tau - \tilde{r})} = \frac{1}{2\pi} \cdot \frac{1}{(u - q) + \mathrm{i}(t - p)}$$

which gives the *time-domain radiation pattern*. This shows that the ellipsoids E_p are wave fronts, i.e., *surfaces of constant retardation* for $\tilde{D}^+$. An observer fixed at $\boldsymbol{x}$ will see a pulse peaking at time $t = p(\boldsymbol{x})$, with *duration*

$$T(\boldsymbol{x}) = |u - q(\boldsymbol{x})|.$$

The *peak magnitude*

$$|C(\tau - \tilde{r})|_{t=p} = \frac{1}{2\pi|u - q|}$$

is constant along the hyperboloids $H_q^\pm$. Thus, apart from the attenuation factor $1/\tilde{r}$, the peak value of $|\tilde{D}^+(z)|$ remains constant along the hyperboloids. This shows that *the radiation flows along* H_q^+ *if* $0 < q \leqslant a$ *and* H_q^- *if* $-a \leqslant q < 0$. In the far zone, $C(\tau - \tilde{r})$ has peak magnitude

$$\mathcal{R}(\theta) \equiv |C(\tau - \tilde{r})|_{t=r} = \frac{1}{2\pi} \frac{1}{|u - a\cos\theta|} \qquad r \gg a \tag{72}$$

which shows that there are three qualitatively different cases depending on the *causal* character of the imaginary source point:

(1) If y is *timelike* ($y^2 < 0$), then $|u| > a$ and $\tilde{D}^+$ is a smooth *pulse* outside the source region $\mathcal{D}$. Furthermore, the peak radiation pattern $\mathcal{R}(\theta)$ is an *ellipse* with *eccentricity* $a/|u|$ *and the source at one of the foci*. If y is in the future cone ($u > a$), then the semimajor axis of the ellipse points in the direction $\boldsymbol{y}$, so that the *exploding* wave $\tilde{D}^+(z)$ is emitted along $\boldsymbol{y}$. It will be shown that $G_4 = \mathrm{i}\tilde{D}^- - \mathrm{i}\tilde{D}^+$ is sourceless, so $\tilde{D}^-(z)$ is an *imploding* wave that is simultaneously absorbed along $-\boldsymbol{y}$.

If y is in the past cone ($u < -a$), then $\tilde{D}^-(z)$ is absorbed along $\boldsymbol{y}$ while $\tilde{D}^+(z)$ is emitted along $-\boldsymbol{y}$. As $y^2 \to 0^-$, the ellipses become more and more eccentric and the pulsed beams become sharper and sharper. Note that they have no *sidelobes*[11], hence could be useful in applications such as radar tracking and directed communications [K96, K97, K01].

(2) If y is *future lightlike* ($u = a$), then $\tilde{D}^+$ is singular on the *ray* along $\boldsymbol{y}$ at $t = r$. If y is *past lightlike* ($u = -a$), $\tilde{D}^+$ is singular along $-\boldsymbol{y}$ at $t = r$. In either case, the peak radiation pattern $\mathcal{R}(\theta)$ is *parabolic*.

(3) If y is *spacelike* ($y^2 > 0$), then $|u| < a$ and $\tilde{D}^+$ is singular at $t = r$ on the cone $\cos\theta = u/a$, with a *hyperbolic* radiation pattern.

Only case 1 gives reasonable pulsed beams with a chance to be realized with finite energy, although cases 2 and 3 should also be of interest since $G_4(z)$ is analytic for *all* $z^2 \neq 0$. We therefore assume from now on that $y \in V_\pm$, so that z belongs to the *causal tube*,

$$z \in \mathcal{T} = \mathcal{T}_+ \cup \mathcal{T}_- \tag{73}$$

already introduced in (13) starting from Minkowski space. Figure 2 shows the time evolution of $\tilde{D}^+(x - \mathrm{i}y)$ for various choices of $y \in V_+$ in the far zone, and figure 3 shows its evolution in the near zone for a particular choice of y.

We are now ready to learn how $\tilde{D}^\pm(z)$ are related to the wave propagators in $\mathbb{R}^{3,1}$. It suffices to focus on $\tilde{D}^+(z)$. Fix $y \in V_+$ and define the partial boundary values

$$\tilde{D}^+(x \pm \mathrm{i}0) = \lim_{\varepsilon \searrow 0} \tilde{D}^+(x \pm \mathrm{i}\varepsilon y). \tag{74}$$

The limits in (74) do not depend on the choice of $y \in V_+$, hence we may choose $y = (\mathbf{0}, \mathrm{i}u)$ with $u > 0$ so that

$$\tilde{D}^+(z) = \tilde{D}^+(\boldsymbol{x}, \tau) = \frac{1}{8\mathrm{i}\pi^2 r} \cdot \frac{1}{\tau - r} \qquad \tau = t - \mathrm{i}u$$

and the Plemelj jump conditions [T96] give the distributional relations

$$\tilde{D}^+(x \mp \mathrm{i}0) = \frac{1}{8\mathrm{i}\pi^2 r} \lim_{\varepsilon \searrow 0} \frac{1}{t - r \mp \mathrm{i}\varepsilon u} = \frac{1}{8\mathrm{i}\pi^2 r} \mathcal{P} \frac{1}{t - r} \pm \frac{\delta(t - r)}{8\pi r}$$

where $\mathcal{P}$ is the Cauchy principal value. We require *Huygens' principle* [BC87] to be valid in $\mathbb{R}^{3,1}$, hence the principal-value terms must be eliminated and the only combination acceptable as a retarded propagator is

$$D^+(x) \equiv \tilde{D}^+(x - \mathrm{i}0) - \tilde{D}^+(x + \mathrm{i}0) = \frac{\delta(t - r)}{4\pi r}. \tag{75}$$

This combination of boundary values, already encountered earlier, will be called the *Minkowskian limit*. It does indeed give a fundamental solution of the wave equation:

$$\Box D^+(x) = -\delta_3(\boldsymbol{x})\delta(t) = -\delta_{3,1}(x). \tag{76}$$

[11] Sidelobes are angular patterns resulting from interference between waves coming from opposite ends of the source. They can cause problems in radar and communications.

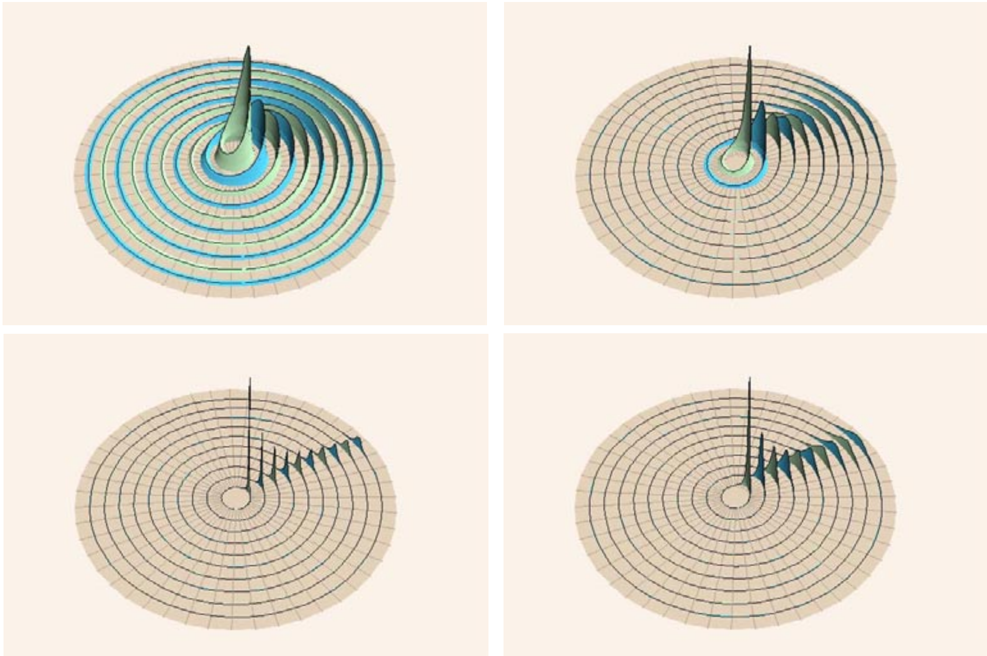

Figure 2. Time-lapse plots of $|\tilde{D}^{+}(x - iy)|$ in the far zone, showing the evolution of a *single pulse* with propagation vector $y = (0, 0, 1, iu)$. We have taken the slice $x_2 = 0$, so that the source disc becomes the interval $[-1, 1]$ on the x_1-axis and the pulse propagates in the x_3 direction of the x_1–x_3 plane. Clockwise from upper left: $u = 1.5, 1.1, 1.01, 1.001$. As $u \to 1$, y approaches the light cone and the pulsed beam becomes more and more focused.

M An MP4 movie of this figure is available from stacks.iop.org/JPhysA/36/R291

The substitution $r \to -r$ as in (71) now gives

$$D^{-}(x) \equiv \tilde{D}^{-}(x - i0) - \tilde{D}^{-}(x + i0) = \frac{\delta(t + r)}{4\pi r} \qquad \Box D^{-}(x) = -\delta_{3,1}(x). \tag{77}$$

Equation (76) is the desired hyperbolic counterpart of (67). Its derivation confirms the points made about the failed attempt (68):

- The distributional limit (75) played a key role in reproducing Huygens' principle.
- By (70), the Minkowskian limit of $iG_4(z)$ is

$$\begin{aligned} R(x) &\equiv iG_4(x - i0) - iG_4(x + i0) = D^{+}(x) - D^{-}(x) \\ &= \frac{\delta(t - r)}{4\pi r} - \frac{\delta(t + r)}{4\pi r}. \end{aligned} \tag{78}$$

This is the *Riemann function* [T96], which solves the following initial-value problem of the *sourceless* wave equation:

$$\Box R(x) = 0 \qquad R(\boldsymbol{x}, 0) = 0 \qquad \partial_t R(\boldsymbol{x}, 0) = \delta_3(\boldsymbol{x}). \tag{79}$$

$iG_4(z)$ can therefore be considered the *extended* Riemann function. It is also identical with Synge's *elementary wavefunction* [S65].

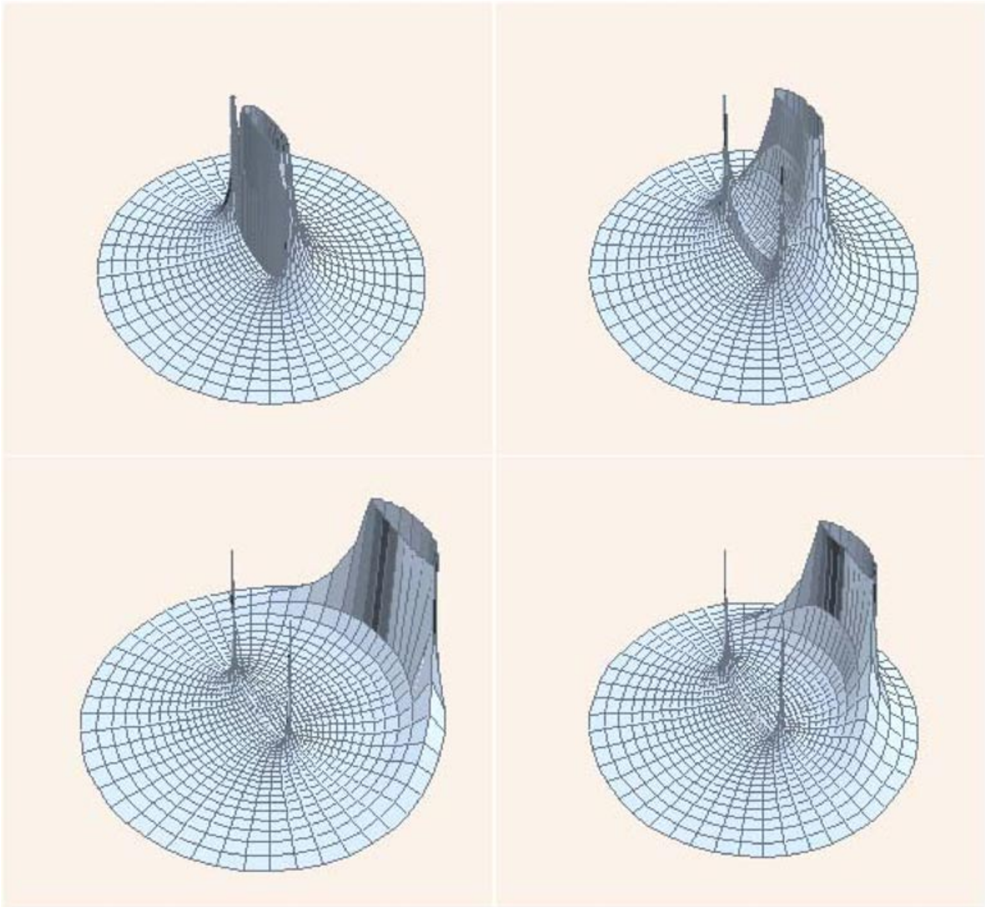

Figure 3. Near-zone graphs of $|\tilde{D}^{+}(x - \mathrm{i}y)|^{2}$ with $y = (0, 0, 1, 1.01\mathrm{i})$ immediately after launch, evolving in the x_1–x_3 plane with $x_2 = 0$ as in figure 2. Clockwise from upper left: $t = 0.1, 1, 2, 3$. The ellipsoidal wave fronts and hyperbolic flow lines are clearly visible. The top of the peak is cut off to show the behaviour near the base. The two spikes represent the branch circle, whose slice with $x_2 = 0$ consists of the points $(\pm 1, 0, 0)$.

M An MP4 movie of this figure is available from stacks.iop.org/JPhysA/36/R291

- Causality has no meaning for $G_4(z)$ and appears only when a branch cut is chosen for $\tilde{r}$, as equations (70) and (71) confirm.

The limits (75) and (78) are typical of *hyperfunction theory* [K88, I92], where distributions are represented as signed combinations of boundary values of functions holomorphic in 'local' wedgelike domains surrounding the support. In general, there is no preferred set of such domains and it is necessary to use sheaf cohomology, which makes the theory rather abstract. In our case, however, the two domains $\mathcal{T}_{\pm}$ suffice due to the natural cone structure of relativistic fields.

Following (76), we now define the *point source at* iy as

$$\tilde{\delta}_{3,1}(x - \mathrm{i}y) = -\Box_x \tilde{D}^{\pm}(x - \mathrm{i}y) \qquad y^2 < 0. \tag{80}$$

We list some of its basic properties:

- The left-hand side of (80) is independent of the sign on the right-hand side. Recall that $\square\, G_4(z) = 0$ wherever G_4 is holomorphic. For $z = x - \mathrm{i}y \in \mathcal{T}$,
$$z^2 = 0 \Rightarrow x^2 = y^2 < 0 \quad \text{and} \quad x \cdot y = 0$$
but $x \cdot y$ cannot vanish since both vectors are timelike. Hence $G_4(z)$ is holomorphic in $\mathcal{T}$ and
$$\square\, \tilde{D}^{+}(z) - \square\, \tilde{D}^{-}(z) = \square\, \mathrm{i}G_4(z) = 0.$$
- The Minkowskian limit of $\tilde{\delta}_{3,1}(z)$ is $\delta_{3,1}(x)$:
$$\begin{aligned}\tilde{\delta}_{3,1}(x - \mathrm{i}0) - \tilde{\delta}_{3,1}(x + \mathrm{i}0) &= -\square\, \tilde{D}^{\pm}(x - \mathrm{i}0) + \square\, \tilde{D}^{\pm}(x + \mathrm{i}0)\\ &= -\square\, D^{\pm}(x) = \delta_{3,1}(x).\end{aligned} \tag{81}$$
- $\tilde{\delta}_{3,1}(x - \mathrm{i}y)$ is supported in the world tube swept out in $\mathbb{R}^{3,1}$ by $\mathcal{D}(\boldsymbol{y})$ at rest:
$$\operatorname{supp} \tilde{\delta}_{3,1}(x - \mathrm{i}y) = \{(\boldsymbol{x}, \mathrm{i}t) : \boldsymbol{x} \in \mathcal{D}(\boldsymbol{y})\} \equiv \tilde{\mathcal{D}}(\boldsymbol{y}) \qquad \forall y \in V_{\pm}.$$

This follows since $\square\, \tilde{D}^{+} = 0$ outside the singularities and
$$-\mathrm{Im}(\tau - \tilde{r}) = u - q \neq 0 \qquad \forall z \in \mathcal{T} \tag{82}$$
(because $q^2 \leqslant a^2 < u^2$), so the only singularities come from the $1/\tilde{r}$ factor.

Note that while the Minkowskian limits $D^{\pm}(x)$ and $\delta_{3,1}(x)$ are Lorentz invariant, the extended propagators $\tilde{D}^{\pm}(z)$ and their sources $\tilde{\delta}_{3,1}(z)$ are *frame dependent*, the preferred frame being the rest frame of $\mathcal{D}$. This can be traced back to the fact that we have obtained the factorization (69) and associated splitting (70) by choosing a branch cut for $\tilde{r}(\boldsymbol{z})$ in a particular Lorentz frame. Of course, since $G_4(z)$ is Lorentz invariant, we may choose to do the splitting in any other frame.

5. Driven complex sources

Suppose we 'drive' a point source fixed at $\mathrm{i}y$ with a real time signal $g_0(t)$. The resulting retarded wave is the convolution
$$\begin{aligned}W(\boldsymbol{z}, \tau) &= \int_{-\infty}^{\infty} \mathrm{d}t'\, \tilde{D}^{+}(\boldsymbol{z}, \tau - t') g_0(t')\\ &= \frac{1}{8\mathrm{i}\pi^2 \tilde{r}} \int_{-\infty}^{\infty} \frac{g_0(t')\, \mathrm{d}t'}{\tau - t' - \tilde{r}}\\ &= \frac{g(\tau - \tilde{r})}{4\pi \tilde{r}} = g(\tau - \tilde{r}) G_3(\boldsymbol{z})\end{aligned} \tag{83}$$
where $G_3(\boldsymbol{z})$ is the *holomorphic Coulomb potential* [N73, K01a] and
$$g(\tau) \equiv \frac{1}{2\pi \mathrm{i}} \int_{-\infty}^{\infty} \frac{g_0(t')\, \mathrm{d}t'}{\tau - t'} \tag{84}$$
is the analytic-signal transform (AST) (21) of g_0. The source distribution for the associated field $W(z)$ is defined as
$$S(z) = -\square_x\, W(z). \tag{85}$$
Since g is analytic off the real axis and $\mathrm{Im}(\tau - \tilde{r}) \neq 0$ in $\mathcal{T}$ (82), it follows that $W(z)$, like $\tilde{D}^{\pm}(z)$, is analytic outside the world tube $\tilde{\mathcal{D}}$ swept out by $\mathcal{D}(\boldsymbol{y})$ at rest. Moreover, formal differentiation gives
$$\square\, W(z) = 0$$
therefore $S(x - \mathrm{i}y)$ is also supported in $x \in \tilde{\mathcal{D}}$.

Examples. We give three driving signals that will be needed later, with their ASTs and radiated waves (83):

$$g_0(t) = \delta(t) \qquad g(\tau) = \frac{1}{2\pi \mathrm{i}\tau} = C(\tau) \qquad W = \tilde{D}^{+}(z) \tag{86}$$

$$g_0(t) \equiv 1 \qquad g(t - \mathrm{i}u) = \hat{u}/2 \qquad W = (\hat{u}/2)G_3(\boldsymbol{z}) \tag{87}$$

$$g_0(t) = \mathrm{e}^{-\mathrm{i}\omega t} \qquad g(\tau) = \hat{C}(\omega, u)\,\mathrm{e}^{-\mathrm{i}\omega t} \qquad W(z) = g(\tau)B_\omega(\boldsymbol{z}) \tag{88}$$

where $\hat{C}$ is the Fourier transform of the Cauchy kernel (24)

$$\hat{C}(\omega, u) = \hat{u}\Theta(\omega u)\,\mathrm{e}^{-\omega u} \tag{89}$$

and

$$B_\omega(\boldsymbol{z}) = \frac{\mathrm{e}^{\mathrm{i}\omega\tilde{r}}}{4\pi\tilde{r}} \tag{90}$$

is the *time-harmonic complex-source beam*, applied widely in engineering [HF01]. In the last equality of (88) we used

$$|q| \leqslant a \Rightarrow \mathrm{Sgn}(u - q) = \mathrm{Sgn}\, u \Rightarrow \Theta(\omega(u - q)) = \Theta(\omega u). \tag{91}$$

Note that to make (87) a special case of (86) with $\omega = 0$, we must define $\Theta(0) = 1/2$.

The far-zone approximation (61) to (88) shows that W is indeed a beam in the direction of $\hat{u}\boldsymbol{y}$ which becomes more and more focused as y approaches the light cone:

$$r \gg a \Rightarrow W(z) \approx \hat{u}\Theta(\omega u)\,\mathrm{e}^{-\omega(u - a\cos\theta)}\frac{\mathrm{e}^{-\mathrm{i}\omega(t-r)}}{4\pi r}. \tag{92}$$

This is not surprising, since (88) is a Fourier component of the pulsed beam (86). The beam W is exponentially stronger for $\hat{q} = \hat{u}$ than for $\hat{q} = -\hat{u}$, so the beams are *directed* along $\boldsymbol{y}$ if $z \in \mathcal{T}_+$ and along $-\boldsymbol{y}$ if $z \in \mathcal{T}_-$, as already seen in the time domain. Equation (92) shows that *the imaginary retardation $u \to u - q$ serves to focus the beam.*

Just as the spatial displacement of a point source from $\boldsymbol{x} = \boldsymbol{0}$ to $\mathrm{i}\boldsymbol{y}$ expands it to a disc, the temporal displacement of the impulse from $t = 0$ to $\mathrm{i}u$ gives it duration, as seen in (86). We may interpret the parameter $|u|$ as a *response time* for the source at $\mathrm{i}y$. A large response time suppresses rapid variations in the driving signal. This is modelled[12] by the factor $\Theta(\omega u)\,\mathrm{e}^{-\omega u}$, which acts as a *filter* to smooth the signal. The larger the source, the longer the response time since the excitation can travel to different parts of the source before emitting a wave. Thus, a rough but intuitive way of understanding the timelike character of y is to note that the time needed for a signal to travel from the centre to the rim of the disc is a (recall that we take $c = 1$), so the condition for emitting a coherent wave is $|u| > a$.

With the interpretation of u as a 'response time,' all four components of y have a direct significance in terms of the *source* itself, without reference to the radiated beam.

[12] Admittedly, this model leaves something to be desired since g decays slowly even if g_0 has compact support. In particular, it is not strictly causal since the vanishing of $g_0(t)$ for $t < 0$ does not imply the same for $g(t - \mathrm{i}u)$; in fact, the latter cannot vanish on *any* interval because it is analytic. One way to improve the model is to represent the response by derivatives of $g(\tau)$, as in (50). This suppresses the low frequencies and amounts to putting g_0 through a 'band-pass filter' of the form $\omega^\alpha\Theta(\omega u)\,\mathrm{e}^{-\omega u}$ centred around $\omega = \alpha/u$.

6. Main results on sources

In this section, we present our main results on the source distribution for beams $W(z)$ of the general type (83), which will be proved in the appendix. The choices (86)–(88) for g_0 yield the sources for pulsed, static and time-harmonic beams generated by complex point sources. Furthermore, choosing a plane wave for the test function will yield the spacetime Fourier transforms of the sources and their beams, giving valuable insight into their propagation properties and making them a promising computational tool.

For clarity, the results are stated as theorems. However, I have included some discussion to help make them digestible for readers without training in the art of arid mathematical discourse. A more extensive discussion of the results and their interpretation is given in the next section.

To compute $S(z)$ as a distribution, we must deal with its singularities. This will be done by *shielding* $\mathcal{D}$ with an ellipsoid $E_{\varepsilon a}$ and taking the limit $\varepsilon \to 0$ once the computations are complete. Thus let $\varepsilon > 0$ and

$$W_\varepsilon(z) = \Theta(p - \varepsilon a) W(z) = \begin{cases} W(z) & \text{if } \boldsymbol{x} \text{ is outside } E_{\varepsilon a} \\ 0 & \text{if } \boldsymbol{x} \text{ is inside } E_{\varepsilon a}. \end{cases}$$

The singularities on $\mathcal{D}$, consisting of the discontinuity in the interior of the disc and infinities on the boundary $\mathcal{S} = \partial\mathcal{D}$, have been replaced by a *uniformly finite* jump discontinuity across $E_{\varepsilon a}$. The *regularized source*, defined by

$$S_\varepsilon(z) \equiv -\Box\, W_\varepsilon(z)$$

is therefore supported on the world tube swept out by $E_{\varepsilon a}$ at rest,

$$\tilde{E}_{\varepsilon a} = \{x = (\boldsymbol{x}, \mathrm{i}t) : \boldsymbol{x} \in E_{\varepsilon a}\}.$$

The 'bare' source S will then be defined by

$$S(z) = \lim_{\varepsilon \searrow 0} S_\varepsilon(z) \tag{93}$$

where the limit is taken in the distributional (weak) sense by 'smearing' over test functions.

Note: The definition (93) is necessary on *conceptual* as well as technical grounds for the following subtle reason. We have chosen a branch of the complex distance $\tilde{r}$ to reduce to the usual positive distance as $\boldsymbol{y} \to \boldsymbol{0}$, but nowhere have we actually *enforced* this in our equations—until now! The definition (93) clearly communicates our choice to the equations.

Theorem 1 (Shielded complex source)**.** *Let* $\alpha = \varepsilon a - \mathrm{i}a$ *and* $\alpha^* = \varepsilon a + \mathrm{i}a$ *denote the* north and south poles *of* $E_{\varepsilon a}$*. Define*

$$\mathring{f}(\tilde{r}) = \mathring{f}(p, q) = \frac{1}{2\pi}\int_0^{2\pi} f(p, q, \phi)\, \mathrm{d}\phi \tag{94}$$

$$2\mathring{f}_{\tilde{r}}(\tilde{r}) = 2\partial_{\tilde{r}}\mathring{f} = \partial_p \mathring{f} + \mathrm{i}\partial_q \mathring{f} = \mathring{f}_p + \mathrm{i}\mathring{f}_q. \tag{95}$$

*(*This is merely convenient notation and does not assume that $\mathring{f}$ is analytic in $\tilde{r} = p - \mathrm{i}q$.*) Then, for given timelike* y, $S_\varepsilon(x - \mathrm{i}y)$ *is a distribution in* $x \in \mathbb{R}^{3,1}$ *supported in* $\tilde{E}_{\varepsilon a}$ *which is regular in t (*no smearing necessary*) and acts on a spatial test function* $f(\boldsymbol{x})$ *in the following equivalent ways:*

$$\langle S_\varepsilon, f\rangle = \frac{\alpha^*\alpha}{2a}\int_{-a}^{a} \mathrm{d}q \left\{ \frac{g\mathring{f}_p}{\tilde{r}} + \frac{g'\mathring{f}}{\tilde{r}} + \frac{g\mathring{f}}{\tilde{r}^2} \right\} \tag{96}$$

$$\langle S_\varepsilon, f\rangle = \frac{\alpha^*\alpha}{a}\int_{-a}^{a} \mathrm{d}q \left\{ \frac{g\mathring{f}_{\tilde r}}{\tilde r} \right\} + \frac{\alpha^*\alpha}{2a}\left[\frac{g\mathring{f}}{\mathrm{i}\tilde r} \right]_{\tilde r=\alpha^*}^{\tilde r=\alpha} \tag{97}$$

$$\langle S_\varepsilon, f\rangle = \frac{\alpha^*\alpha}{2a}\int_{-a}^{a} \mathrm{d}q \left\{ \frac{g\mathring{f}_p}{\tilde r} + \frac{g'\mathring{f} - g_0'\mathring{f}_0}{\tilde r} + \frac{g\mathring{f} - g_0\mathring{f}_0 - \mathrm{i}qg_0'\mathring{f}_0}{\tilde r^2} \right\} + g_0\mathring{f}_0 + \varepsilon a g_0'\mathring{f}_0 \tag{98}$$

where $p = \varepsilon a$ *throughout and the subscript* 0 *denotes values at* $q = 0$*:*

$$g_0 = g(\tau - \varepsilon a) \qquad g_0' = g'(\tau - \varepsilon a)$$
$$\mathring{f}_0 = \mathring{f}(\varepsilon a) = \textit{mean of } f \textit{ on the } \text{equator} \textit{ of } E_{\varepsilon a}.$$

The first and second forms, but not the third, can be expressed locally*, i.e. without smearing by test functions:*

$$S_\varepsilon(z) = \frac{\delta(p-\varepsilon a)}{4\pi}\left|\frac{\alpha}{\tilde r}\right|^2 \left\{ \frac{g}{\tilde r}\partial_p + \frac{g'}{\tilde r} + \frac{g}{\tilde r^2} \right\} \tag{99}$$

$$S_\varepsilon(z) = W(z)\left\{ \delta(p-\varepsilon a)\left|\frac{\alpha}{\tilde r}\right|^2 (\partial_p + \mathrm{i}\partial_q) - \mathrm{i}\delta(\tilde r - \alpha) + \mathrm{i}\delta(\tilde r - \alpha^*) \right\} \tag{100}$$

where

$$\delta(\tilde r - \alpha) = \delta(p-\varepsilon a)\delta(q-a) \qquad \delta(\tilde r - \alpha^*) = \delta(p-\varepsilon a)\delta(q+a)$$

are point sources *at the north and south poles of* $E_{\varepsilon a}$*. The term with the normal derivative* ∂_p *is interpreted as a* double layer*, and that with the tangential derivative* ∂_q *as a* surface flow *on* $E_{\varepsilon a}$ *from the south pole* α^* *to the north pole* α*. In (100), the entire distribution is modulated in space and time by the pulsed beam* $W(z) = g(\tau - \tilde r)/4\pi\tilde r$*, which amplifies forward waves* ($q > 0$) *and dampens backward waves* ($q < 0$)*.* $S_\varepsilon(z)$ *must be applied as a differential operator to a test function, then integrated.*

Remark 1. As expected, (96) and (99) show that S_ε is a smooth *surface distribution* on $E_{\varepsilon a}$. Equation (97) is then obtained by integrating by parts in q using $g' = -\mathrm{i}g_q$, which follows from the analyticity of $g(\tau - \tilde r)$. The point sources at the poles are the resulting boundary terms, hence they are *removable singularities*. As long as $\varepsilon > 0$, (96) and (99) are the most natural representations of the source. However, the second and third integrals in (96) diverge as $\varepsilon \to 0$. They must be *regularized* by subtracting and adding 'counter terms' in the numerator before taking the limit. The *added* counter terms are integrated separately, leading to (98), where all integrals remain finite as $\varepsilon \to 0$. This is a special case of the method developed in [K00] to compute the complex point sources in $\mathbb{R}^n$.

Remark 2. Because of the subtractions associated with the regularization, (98) cannot be expressed locally. Local representations are especially important for examining the possibility of *realizing* the sources, i.e., building instruments that can emit (and, by reciprocity, *detect*) the pulsed beams. For this purpose, (96) and (97) seem preferable to (98), giving (99) and (100). Requiring *disc* sources instead of ellipsoidal ones will further eliminate (99), leaving only the local source (100) as $\varepsilon \to 0$.

Theorem 2 (unshielded complex source)**.** *Let* $\tilde g(\tau, q)$ *be the average of* $g(\tau - \tilde r)$ *across the branch cut* $\mathcal{D}$*,*

$$\tilde g(\tau, q) = \tfrac{1}{2}\{g(\tau + \mathrm{i}q) + g(\tau - \mathrm{i}q)\} \qquad \tilde g_q(\tau, q) = \partial_q \tilde g(\tau, q). \tag{101}$$

For given timelike y, $S(x - \mathrm{i}y)$ *is a distribution in* $x \in \mathbb{R}^{3,1}$ *that is regular in* t *and acts on a spatial test function* $f(\boldsymbol{x})$ *in either of the following equivalent ways:*

$$\langle S, f\rangle = \mathrm{i}a \int_0^a \mathrm{d}q\, \tilde{g} \left\{ \frac{\mathring{f}_p + \mathrm{i}\mathring{f}_q}{q} \right\} + \tilde{g}(\tau, a) f(\mathbf{0}) \tag{102}$$

$$\langle S, f\rangle = a \int_0^a \mathrm{d}q \left\{ \frac{\mathrm{i}\tilde{g}\mathring{f}_p + \tilde{g}_q \mathring{f}}{q} - \frac{\tilde{g}\mathring{f} - g(\tau)\mathring{f}(0)}{q^2} \right\} + g(\tau)\mathring{f}(0) \tag{103}$$

where $p = 0$ *throughout. The integrals converge because the continuity of* $f(\boldsymbol{x})$ *across* $\mathcal{D}$ *and its differentiability on* $\mathcal{D}$ *imply that the partial derivatives of* $\mathring{f}$ *on* $\mathcal{D}$ *are* $\mathcal{O}(q)$*:*

$$p = 0 \Rightarrow \mathring{f}_p = \frac{q}{a}\mathring{f}_\xi \qquad \mathring{f}_q = -\frac{q}{\rho}\mathring{f}_\rho \tag{104}$$

where $\mathring{f}_\rho = \partial_\rho \mathring{f}$, $\mathring{f}_\xi = \partial_\xi \mathring{f}$. *In cylindrical coordinates,* $q = \sqrt{a^2 - \rho^2}$ *and (102) becomes*

$$\langle S, f\rangle = \int_0^a \mathrm{d}\rho\, \tilde{g} \left\{ \frac{a\mathring{f}_\rho + \mathrm{i}\rho\mathring{f}_\xi}{\sqrt{a^2 - \rho^2}} \right\} + \tilde{g}(\tau, a) f(\mathbf{0}) \tag{105}$$

where $\xi = 0$ *in the integrant. The forms (102) and (105), but not (103), can be expressed* locally *as*

$$S(z) = \tilde{g}(\tau, q)\delta(\xi)\frac{\Theta(a - \rho)}{2\pi\sqrt{a^2 - \rho^2}}\left(\frac{a}{\rho}\partial_\rho + \mathrm{i}\partial_\xi\right) + \tilde{g}(\tau, a)\delta_3(\boldsymbol{x}). \tag{106}$$

The ∂_ρ *term may be interpreted as a radial* flow *or* shear *on* $\mathcal{D}$*, being the sum of the flow terms* ∂_q *(100) in the upper and lower discs as* $\varepsilon \to 0$*, and the* ∂_ξ *term may be similarly interpreted as a* double layer *on* $\mathcal{D}$*, being the sum of the double layer terms* ∂_p*. The entire distribution is modulated in space and time by* $\tilde{g}(\tau, q)$*, providing directivity along* $\hat{u}\boldsymbol{y}$*.*

Remark 1. The point source in (106) results from the merger of the 'removable' singularities at the north and south poles in (100). However, although it can be eliminated *formally* in (102) and (105) by integrating by parts in q and ρ, respectively, this now gives rise to divergent terms. Note that $\mathring{f}(0)$ in (103) is the mean of $f(\boldsymbol{x})$ on the branch circle $\mathcal{S} = \partial\mathcal{B}$. Thus, we can avoid the point source in (106) by using (103), which contains nonlocal effects on the rim $\mathcal{S}$ (in the form of the last term) and on the interior of $\mathcal{D}$ (in the form of the subtraction in the second term). We may therefore say that *the point source in* (106) *actually represents a combination of nonlocal effects distributed on the source disc*. However, if one is interested in *launching* pulsed-beam wavelets, then local sources seem necessary and the form (106) seems most promising for this purpose.

Remark 2. An even more intriguing possibility is that some naturally occurring phenomena can be associated with the emission and absorption of radiation by complex source points. Extensions of the present construction to Maxwell's equations exist, as explained below; see also [K02].

Corollary 1 (event sources, static and time-harmonic point sources)**.** *Letting* $g_0(t) = \delta(t)$ *as in (86) gives* $g(\tau) = 1/2\pi\mathrm{i}\tau$ *and*

$$\tilde{g}(\tau, q) = \frac{\tau}{2\pi\mathrm{i}(\tau^2 + a^2 - \rho^2)} = -\frac{\tau}{2\pi\mathrm{i}z^2} \qquad z \in \tilde{\mathcal{D}}.$$

Therefore the imaginary event source *at* iy *is*

$$\tilde{\delta}_{3,1}(x - \mathrm{i}y) = \frac{\mathrm{i}\tau}{2\pi z^2}\left\{\delta(\xi)\frac{\Theta(a-\rho)}{2\pi\sqrt{a^2-\rho^2}}\left(\frac{a}{\rho}\partial_\rho + \mathrm{i}\partial_\xi\right) + \delta_3(\boldsymbol{x})\right\}. \tag{107}$$

Letting $g_0(t) \equiv 1$ *as in (87) gives the* static point source *at* i$\boldsymbol{y}$*:*

$$\tilde{\delta}_3(\boldsymbol{x} - \mathrm{i}\boldsymbol{y}) = \delta(\xi)\frac{\Theta(a-\rho)}{2\pi\sqrt{a^2-\rho^2}}\left(\frac{a}{\rho}\partial_\rho + \mathrm{i}\partial_\xi\right) + \delta_3(\boldsymbol{x}). \tag{108}$$

Letting $g_0(t) = \mathrm{e}^{-\mathrm{i}\omega t}$ *as in (88) gives the analytic driving signal for the time-harmonic point source at* i$\boldsymbol{y}$*:*

$$\tilde{g}(\tau, q) = \hat{u}\Theta(\omega u)\,\mathrm{e}^{-\mathrm{i}\omega\tau}\cosh(\omega q). \tag{109}$$

Valuable information is gained by computing the Fourier transforms of the pulsed beams and their sources. Although this seems daunting at first because of the convoluted near-field spatial dependence of the beams through $\tilde{r}$ and its oblate spheroidal coordinates, the result is surprisingly simple.

Recall our notation for Minkowski space M and its dual Fourier space M'. Given a spatial direction $\hat{\boldsymbol{y}}$, we use the cylindrical coordinates (55) in M and M'

$$\begin{array}{lll} x = (\boldsymbol{\rho}, \xi, \mathrm{i}t) & k = (\boldsymbol{h}, l, \mathrm{i}\omega), & \boldsymbol{\rho}\cdot\hat{\boldsymbol{y}} = \boldsymbol{h}\cdot\hat{\boldsymbol{y}} = 0 \\ \xi = \hat{\boldsymbol{y}}\cdot\boldsymbol{x} & \rho = |\boldsymbol{\rho}| = \sqrt{r^2-\xi^2} & r = |\boldsymbol{x}| \\ l = \hat{\boldsymbol{y}}\cdot\boldsymbol{k} & h = |\boldsymbol{h}| = \sqrt{\kappa^2 - l^2} & \kappa = |\boldsymbol{k}| \end{array} \tag{110}$$

so that l and h are the *longitudinal and transverse wave numbers* with respect to $\hat{\boldsymbol{y}}$ and the pairing between M' and M is

$$k \cdot x = \boldsymbol{k}\cdot\boldsymbol{x} - \omega t = \boldsymbol{h}\cdot\boldsymbol{\rho} + l\xi - \omega t = h\rho\cos\phi + l\xi - \omega t. \tag{111}$$

Theorem 3 (Fourier transform of shielded source)**.** *Given* $y = (\boldsymbol{y}, u) \in V$ *with* $|\boldsymbol{y}| = a > 0$ *and* $\varepsilon > 0$*, define the complex wave vector*

$$\begin{array}{lll} k_\varepsilon = (\boldsymbol{h}_\varepsilon, l_\varepsilon, \mathrm{i}\omega_\varepsilon) & \eta \equiv \varepsilon - \mathrm{i} = \alpha/a & \\ \boldsymbol{h}_\varepsilon = |\eta|\boldsymbol{h} & l_\varepsilon = l - \mathrm{i}\varepsilon\omega & \omega_\varepsilon = \omega - \mathrm{i}\varepsilon l \end{array} \tag{112}$$

which satisfies

$$k_\varepsilon^2 = |\eta|^2 k^2 = k^2 + \varepsilon^2 k^2 \tag{113}$$

so that $k \mapsto k_\varepsilon$ *preserves the light cone. Then the Fourier transform (18) with respect to* x *of the shielded source,*

$$\hat{S}_\varepsilon(k, y) \equiv \int_M \mathrm{d}x\, S_\varepsilon(x - \mathrm{i}y)\,\mathrm{e}^{-\mathrm{i}k\cdot x}$$

is given by

$$\hat{S}_\varepsilon(k, y) = \hat{g}(\omega, u)\,\mathrm{e}^{\mathrm{i}\varepsilon\omega a}\,\Omega(k_\varepsilon, \boldsymbol{y}) \qquad \Omega(k_\varepsilon, \boldsymbol{y}) = \cos(\mu_\varepsilon a) + \frac{l_\varepsilon}{\mu_\varepsilon}\sin(\mu_\varepsilon a) \tag{114}$$

where

$$\hat{g}(\omega, u) = \hat{C}(\omega, u)\hat{g}_0(\omega) = \hat{u}\Theta(\omega u)\,\mathrm{e}^{-\omega u}\,\hat{g}_0(\omega) \tag{115}$$

and

$$\mu_\varepsilon = \sqrt{h_\varepsilon^2 - \omega_\varepsilon^2} = \sqrt{k_\varepsilon^2 - l_\varepsilon^2}. \tag{116}$$

The transformation $k \mapsto k_\varepsilon$ *is the product of a* scaling $k \mapsto |\eta|k$ *and a* real rotation *in the* l–$\mathrm{i}\omega$ *plane, or* imaginary Lorentz transformation *in the* l–ω *plane, given by*

$$l \mapsto \frac{l - \varepsilon \mathrm{i}\omega}{\sqrt{1+\varepsilon^2}} \qquad \mathrm{i}\omega \mapsto \frac{\mathrm{i}\omega + \varepsilon l}{\sqrt{1+\varepsilon^2}}.$$

The function Ω*, which is even in* μ *and thus independent of the branch of the square root, is a* focusing filter *that simplifies on the light cone as follows,*

$$k^2 = 0 \quad \Leftrightarrow \quad l_\varepsilon = \pm \mathrm{i}\mu_\varepsilon \quad \Leftrightarrow \quad \mathrm{e}^{\mathrm{i}\varepsilon\omega a}\Omega(k_\varepsilon, \boldsymbol{y}) = \mathrm{e}^{\mathrm{i}\varepsilon\omega a}\,\mathrm{e}^{\pm \mathrm{i}\mu_\varepsilon a} = \mathrm{e}^{la} = \mathrm{e}^{\boldsymbol{k}\cdot\boldsymbol{y}}. \tag{117}$$

Ω *thus amplifies forward propagating waves* $(l > 0)$ *and dampens backward waves* $(l < 0)$.

Corollary 2 (Fourier transforms of bare sources)**.** *The Fourier transform of the bare source* $S(x - \mathrm{i}y)$ *is*

$$\hat{S}(k, y) = \hat{g}(\omega, u)\Omega(k, \boldsymbol{y}) = \hat{g}(\omega, u)\left\{\cos(\mu a) + \frac{l}{\mu}\sin(\mu a)\right\} \tag{118}$$

where

$$\mu = \sqrt{h^2 - \omega^2} = \sqrt{k^2 - l^2}$$

can be real or imaginary. The Fourier transform of the event source *at* $\mathrm{i}y$ *is*

$$\widehat{\tilde{\delta}}_{3,1}(k, y) = \hat{C}(\omega, u)\Omega(k, \boldsymbol{y}) \qquad \hat{C}(\omega, u) = \hat{u}\Theta(\omega u)\,\mathrm{e}^{-\omega u} \tag{119}$$

and that of the static point source at $\mathrm{i}\boldsymbol{y}$ *is*

$$\widehat{\tilde{\delta}}_3(\boldsymbol{k}, \boldsymbol{y}) = \cos(ha) + \frac{l}{h}\sin(ha). \tag{120}$$

Surprisingly, complex sources are much simpler in Fourier space than in space or in spacetime! This suggests that effective computations can be performed with them and their radiated beams using ‘fast’ numerical methods such as the FFT. For example, spacetime convolutions of complex sources with arbitrary densities can be performed with ease by multiplying the Fourier transforms. Thus, although physical wavelets do not seem to have a natural *multiresolution analysis* structure based on scaling relations (see [K94]), this does not necessarily prevent them from giving rise to fast transforms.

The simplicity of the above expressions may be a ‘miracle,’ but it cannot be an accident. Its possible origin and some consequences are discussed in the next section.

Expression (120) is actually valid for $\widehat{\tilde{\delta}}_n(\boldsymbol{k}, \boldsymbol{y})$ with *any* value of $n \geqslant 1$, as will be proved elsewhere [K0x]. In particular, note that it holds in the trivial case $n = 1$ (66), where $a = y, l = k$ and $h = 0$.

7. Interpretation and discussion of results

Let us attempt to understand some of the expressions given in the last section. Our discussion is necessarily somewhat speculative, undertaken with the desire to add qualitative value to the raw mathematical equations.

7.1. The bare source $S(z)$

Looking at equation (106),

$$S(z) = \tilde{g}(\tau, q)\left\{\delta(\xi)\frac{\Theta(a-\rho)}{2\pi\sqrt{a^2-\rho^2}}\left(\frac{a}{\rho}\partial_\rho + \mathrm{i}\partial_\xi\right) + \delta_3(\boldsymbol{x})\right\} \tag{121}$$

we note that

$$G_{2,1}(x_1, x_2, a) \equiv \frac{\Theta(a-\rho)}{2\pi\sqrt{a^2-\rho^2}}$$

is the *retarded propagator for the wave equation in two space dimensions, with $a = |\boldsymbol{y}|$ playing the role of time* [T96]:

$$\left(\Delta_2 - \partial_a^2\right)G_{2,1} = -\delta(x_1)\delta(x_2)\delta(a).$$

The origin of this analogy is not difficult to find. By complexifying the distance function

$$r(\boldsymbol{x}) \to \tilde{r}(\boldsymbol{x} - \mathrm{i}\boldsymbol{y}) = \sqrt{r^2 - a^2 - 2\mathrm{i}\boldsymbol{x}\cdot\boldsymbol{y}}$$

we have implicitly introduced a as 'time' measured along the axis defined by the unit vector $\hat{\boldsymbol{y}}$, in exactly the same way as complexifying the Euclidean time u opened up the light cone and gave rise to the physical time t. In a coordinate system where $\hat{\boldsymbol{y}} = (0, 0, 1)$, the branch cut $\mathcal{D}(\boldsymbol{y})$ is simply a slice of the 'future cone'

$$V_+(\hat{\boldsymbol{y}}) = \left\{(x_1, x_2, \mathrm{i}s) : \rho \equiv \sqrt{x_1^2 + x_2^2} < s\right\} \subset \mathbb{R}^{2,1}$$

at $s = a$, with ρ as the distance function in the orthogonal 'space' $\mathbb{R}^2$. The Heaviside function $\Theta(a-\rho)$ thus merely enforces 'causality,' and the factor $\sqrt{a^2-\rho^2}$ in the denominator reflects the absence of Huygens' principle in $\mathbb{R}^{2,1}$, where an 'observer' at (x_1, x_2) will 'hear' nothing for $s < \rho$, then a 'sonic boom' at $s = \rho$ with a decaying tail for $s > \rho$.

Does this give any insight into the nature of $S(z)$? It suggests looking at a as an *evolution parameter*. Think of 'morphing' from a point source to a disc source by gradually changing a, then (121) shows how the source flows while evolving.

7.2. The shielded source (100)

$$S_\varepsilon(z) = W(z)\left\{\delta(p - \varepsilon a)\left|\frac{\alpha}{\tilde{r}}\right|^2(\partial_p + \mathrm{i}\partial_q) - \mathrm{i}\delta(\tilde{r} - \alpha) + \mathrm{i}\delta(\tilde{r} - \alpha^*)\right\}. \tag{122}$$

This expression is extremely simple, reflecting the regularity achieved by replacing the singular disc $\mathcal{D}$ with the oblate spheroid $E_{\varepsilon a}$. The first two terms are a pair of real point sources at the north and south poles of $E_{\varepsilon a}$,

$$\alpha = \varepsilon a - \mathrm{i}a = \eta a \qquad \alpha^* = \eta^* a.$$

As already mentioned, the terms with the normal derivative ∂_p and the tangential derivative ∂_q may be interpreted as a double layer and a flow on $E_{\varepsilon a}$. Further insight is gained from the Fourier transform (114),

$$\hat{S}_\varepsilon(k, y) = \hat{g}(\omega, u)\,\mathrm{e}^{\mathrm{i}\varepsilon a}\,\Omega(k_\varepsilon, \boldsymbol{y}) \qquad \Omega(k, \boldsymbol{y}) = \cos(\mu a) + \frac{l}{\mu}\sin(\mu a). \tag{123}$$

In the proof of (123) in the appendix, we saved the final details for this discussion because they shed light on the nature of the source, and also because they contain some spectacular cancellations and reveal an amazing hidden structure, namely the complex mapping $k \to k_\varepsilon$

of Fourier space associated with the replacement of the disc source $\mathcal{D}$ by the *Huygens source* S_ε that generates the identical field outside $E_{\varepsilon a}$ by emitting 'secondary wavelets'.

By (A.11), (A.12) and (A.13),

$$\begin{aligned}
&\Omega_\varepsilon(k, \boldsymbol{y}) = I_0 - I_1 + \mathrm{i}\varepsilon I_2 + \eta^*\eta I_3 \\
&I_0 = \cosh(\omega_\varepsilon a) - \mathrm{i}\varepsilon \sinh(\omega_\varepsilon a) \qquad (124)\\
&I_1 = \cosh(\omega_\varepsilon a) - \cos(\mu_\varepsilon a)
\end{aligned}$$

$$\left.\begin{aligned}
&I_2 = \sinh(\omega_\varepsilon a) - (\omega_\varepsilon/\mu_\varepsilon)\sin(\mu_\varepsilon a) \\
&I_3 = (l/\mu_\varepsilon)\sin(\mu_\varepsilon a).
\end{aligned}\right. \qquad (125)$$

The derivation shows that I_0 is due to point sources at α and α^* and the other terms are due to the combined double layer and flow. Specifically, I_1 and I_2 come from the ρ-derivative and I_3 comes from the ξ-derivative. The first terms of I_1 and I_2 *entirely cancel the point-source term* I_0, resulting in

$$\Omega_\varepsilon(k, \boldsymbol{y}) = \cos(\mu_\varepsilon a) - \mathrm{i}\varepsilon(\omega_\varepsilon/\mu_\varepsilon)\sin(\mu_\varepsilon a) + (\varepsilon^2 + 1)(l/\mu_\varepsilon)\sin(\mu_\varepsilon a).$$

This cancellation is related to the fact that the point sources in I_0 resulted from an integration by parts, which in turn was needed to get a local expression for $S(z)$ (see the note below (A.8)). But

$$(\varepsilon^2 + 1)l - \mathrm{i}\varepsilon\omega_\varepsilon = (\varepsilon^2 + 1)l - \mathrm{i}\varepsilon(\omega - \mathrm{i}\varepsilon l) = l - \mathrm{i}\varepsilon\omega = l_\varepsilon$$

which gives the final form (123).

The cancellations and simplifications taking place to yield this simple result appear to be 'miraculous.' This could be merely good fortune or, more likely, an indication that the Fourier sources, and possibly also the unexpected complex mapping $k \to k_\varepsilon$, are more 'fundamental' than the spacetime beams we started with and should therefore be thoroughly understood.

On the practical side, simplicity in the Fourier domain usually means enhanced analytical power and the existence of efficient implementations by 'fast' algorithms. The above Fourier sources offer a promising new tool, modelling processes of *directed emission and absorption* that could be useful in quantum as well as classical physics.

As an example of working with the Fourier sources, we now compute the pulsed beam $W(z)$ from its source.

8. Weyl representations for complex-source beams

How does the simple Fourier source $\hat{S}(k, y)$ radiate a pulsed beam as complex as $W(z)$? To learn the answer, we now compute W from $\hat{S}(k, y)$. This will lead us back to our starting point and thus validate our expressions for the sources and their Fourier transforms. In the process, we prove a generalization to *beams* of Weyl's representation of the fundamental solution of the Helmholtz equation.

From equations (83), (85) and (118), recall our path from W to $\hat{S}$:

$$\begin{aligned}
&W(\boldsymbol{z}, \tau) = \frac{g(\tau - \tilde{r})}{4\pi\tilde{r}} \\
&S(x - \mathrm{i}y) = -\Box_x W(x - \mathrm{i}y) \\
&\hat{S}(k, y) \equiv \int_M \mathrm{d}x\, \mathrm{e}^{-\mathrm{i}k\cdot x} S(x - \mathrm{i}y) = \hat{g}(\omega, u)\Omega(k, \boldsymbol{y})
\end{aligned} \qquad (126)$$

where

$$\Omega(k, \boldsymbol{y}) = \cos(\mu a) + \frac{l}{\mu}\sin(\mu a)$$

and g is the AST of a driving signal $g_0(t)$ obtained by convolution (21) with the Cauchy kernel $C(\tau)$, so that

$$\hat{g}(\omega, u) = \hat{C}(\omega, u)\hat{g}_0(\omega) \qquad \hat{C}(\omega, u) = \hat{u}\Theta(\omega u)\,\mathrm{e}^{-\omega u}.$$

Formally, (126) implies

$$W(x - \mathrm{i}y) = \int_{M'} đk\,\mathrm{e}^{\mathrm{i}k\cdot x}\,\frac{\hat{S}(k, y)}{k^2} \tag{127}$$

but the right-hand side must be defined since k^2 vanishes on the light cone. In spacetime terms, this corresponds to the fact that 'initial values' must be specified in order to solve (126) for W. More precisely, since we are dealing with $-\infty < t < \infty$, we need the behaviour of W as $t \to \pm\infty$, which describes the *causal* relation between the source and the solution. This amounts to a choice of contour in Fourier space that avoids the light cone singularities, so that the solution can be computed by residues.

The temporal Fourier transform of W is

$$\frac{1}{4\pi\tilde{r}}\int_{-\infty}^{\infty} \mathrm{d}t\,\mathrm{e}^{\mathrm{i}\omega t} g(t - \mathrm{i}u - \tilde{r}) = \hat{g}(\omega, u)B_\omega(\boldsymbol{z})$$

where

$$B_\omega(\boldsymbol{z}) = \frac{\mathrm{e}^{\mathrm{i}\omega\tilde{r}}}{4\pi\tilde{r}} \tag{128}$$

is the time-harmonic complex-source beam (90), and translating the integration contour by $t \to t + \tilde{r}$, or $t \to t - \mathrm{i}q$, is justified because g is analytic off the real axis and $|q| \leqslant |a| < |u|$. Therefore, we need to establish that the function

$$\begin{aligned} U(\boldsymbol{z}, \omega) &\equiv \int_{\mathbb{R}^3} đ\boldsymbol{k}\,\mathrm{e}^{i\boldsymbol{k}\cdot\boldsymbol{x}} \cdot \frac{\Omega(k, \boldsymbol{y})}{k^2} \\ &= \int h\,đh\,đ\phi\,đl\,\mathrm{e}^{\mathrm{i}h\rho\cos\phi}\,\mathrm{e}^{\mathrm{i}l\xi} \cdot \frac{\Omega(k, \boldsymbol{y})}{\mu^2 + l^2} \\ &= \int_0^\infty h\,đh\,J_0(h\rho)\int_{-\infty}^{\infty} đl\,\mathrm{e}^{\mathrm{i}l\xi} \cdot \frac{\Omega(k, \boldsymbol{y})}{\mu^2 + l^2} \end{aligned} \tag{129}$$

is identical with $B_\omega(\boldsymbol{z})$, provided the integration contour is chosen to give the known behaviour of W. Note that

$$\begin{aligned} \Omega(k, \boldsymbol{y}) &= \frac{1}{\mu}\{\mu\cos(\mu a) + l\sin(\mu a)\} \\ &= \frac{1}{2\mu}\{(\mu - \mathrm{i}l)\,\mathrm{e}^{\mathrm{i}\mu a} + (\mu + \mathrm{i}l)\,\mathrm{e}^{-\mathrm{i}\mu a}\} \end{aligned}$$

giving

$$\frac{\Omega(k, \boldsymbol{y})}{k^2} = \frac{\mathrm{e}^{\mathrm{i}\mu a}}{2\mu(\mu + \mathrm{i}l)} + \frac{\mathrm{e}^{-\mathrm{i}\mu a}}{2\mu(\mu - \mathrm{i}l)}. \tag{130}$$

This key identity will reveal how the 'focusing filter' Ω amplifies forward waves and suppresses backward waves. Inserted into (129), it gives

$$U(\boldsymbol{z}, \omega) = \int_0^\infty \frac{h\,đh}{2\mu} J_0(h\rho)\int_{-\infty}^{\infty} đl\,\mathrm{e}^{\mathrm{i}l\xi}\left\{\frac{\mathrm{e}^{\mathrm{i}\mu a}}{\mu + \mathrm{i}l} + \frac{\mathrm{e}^{-\mathrm{i}\mu a}}{\mu - \mathrm{i}l}\right\}. \tag{131}$$

The choice of contour thus amounts to picking a branch of $\mu = \sqrt{h^2 - \omega^2}$. Since the denominators $\mu \pm \mathrm{i}l$ will give residues at $l = \pm\mathrm{i}\mu$, the plane waves $\mathrm{e}^{\mathrm{i}l\xi}$ will be *propagating* when $h^2 < \omega^2$ and *evanescent* when $h^2 > \omega^2$. Define the branch

$$\mu = \begin{cases} -\mathrm{i}\sqrt{\omega^2 - h^2} & h^2 \leqslant \omega^2 \\ \sqrt{h^2 - \omega^2} & h^2 \geqslant \omega^2 \end{cases}$$

and note that all its values can be shifted to the right half-plane by the infinitesimal translation $\mu \to \mu + 0$. If we use this branch in (131), then by closing the integration contour in the upper or lower complex half-plane, depending on the behaviour of $\mathrm{e}^{\mathrm{i}l\xi}$, and using Cauchy's theorem, we obtain

$$\mathrm{e}^{\mathrm{i}\mu a} \int_{-\infty}^{\infty} đl \frac{\mathrm{e}^{\mathrm{i}l\xi}}{\mu + \mathrm{i}l} = \Theta(\xi)\, \mathrm{e}^{\mathrm{i}\mu a}\, \mathrm{e}^{-\mu\xi} = \Theta(\xi)\, \mathrm{e}^{-\mu\zeta} \qquad \zeta = \xi - \mathrm{i}a$$
$$\mathrm{e}^{-\mathrm{i}\mu a} \int_{-\infty}^{\infty} đl \frac{\mathrm{e}^{\mathrm{i}l\xi}}{\mu - \mathrm{i}l} = \Theta(-\xi)\, \mathrm{e}^{-\mathrm{i}\mu a}\, \mathrm{e}^{\mu\xi} = \Theta(-\xi)\, \mathrm{e}^{\mu\zeta}.$$

This gives U as the even part of a function U^+ defined by

$$U(\boldsymbol{z}, \omega) = U^+(\boldsymbol{z}, \omega) + U^+(-\boldsymbol{z}, \omega) \qquad \boldsymbol{z} = (\boldsymbol{\rho}, \zeta)$$
$$U^+(\boldsymbol{z}, \omega) = \Theta(\xi) \int_0^{\infty} \frac{h\, đh}{2\mu} J_0(h\rho)\, \mathrm{e}^{-\mu\zeta}. \tag{132}$$

Thus, using the branch μ results in all waves propagating in the $+\boldsymbol{y}$ direction ($\xi > 0$) being amplified by $\mathrm{e}^{\mathrm{i}\mu a} = \mathrm{e}^{\sqrt{\omega^2 - h^2} a}$ and all those propagating in the $-\boldsymbol{y}$ direction ($\xi < 0$) being suppressed by its reciprocal. The evanescent waves decay in both directions, as they should. Note that $U(\boldsymbol{z}, \omega)$ is even in $\boldsymbol{z}$, but not in $\boldsymbol{x}$ alone. That is, while it has a preferred direction in *real* space, it does not have one in *complex* space. This is obvious since a pulsed beam in the $-\boldsymbol{y}$ direction will have the same behaviour in $-\boldsymbol{x}$ as the original one has in $\boldsymbol{x}$.

Now recall from the discussion below (72) that the retarded pulsed beams propagate in the direction of $\hat{u}\boldsymbol{y}$, i.e., along $\boldsymbol{y}$ if $u > 0$ and along $-\boldsymbol{y}$ if $u < 0$. But the factor $\Theta(\omega u)$ in the Fourier transform of the Cauchy kernel forces the signs of u and ω to be identical on the support of $\hat{W}$. Therefore we need the growing exponential $\mathrm{e}^{\mathrm{i}\mu a}$ associated with the $+\xi$ direction if $\omega > 0$ and the $-\xi$ direction if $\omega < 0$, and the decaying exponential $\mathrm{e}^{-\mathrm{i}\mu a}$ associated with the $-\xi$ direction if $\omega > 0$ and the $+\xi$ direction if $\omega < 0$.

This shows that (132) gives the correct value for $\omega > 0$ but the wrong one for $\omega < 0$. The correct branch of μ for $\omega < 0$ can be obtained by noting that $\tilde{r}(\boldsymbol{z}^*) = \tilde{r}(\boldsymbol{z})^*$, hence

$$B_\omega(\boldsymbol{z}^*)^* = \frac{\mathrm{e}^{-\mathrm{i}\omega\tilde{r}}}{4\pi\tilde{r}} = B_{-\omega}(\boldsymbol{z}).$$

Therefore we define U for negative frequencies by

$$U(\boldsymbol{z}, -\omega) = U(\boldsymbol{z}^*, \omega)^* = U^-(\boldsymbol{z}, \omega) + U^-(-\boldsymbol{z}, \omega)$$
$$U^-(\boldsymbol{z}, \omega) \equiv U^+(\boldsymbol{z}^*, \omega)^* = \Theta(\xi) \int_0^{\infty} \frac{h\, đh}{2\mu^*} J_0(h\rho)\, \mathrm{e}^{-\mu^*\zeta},$$

where μ^* is the branch

$$\mu^* = \begin{cases} \mathrm{i}\sqrt{\omega^2 - h^2} & h^2 \leqslant \omega^2 \\ \sqrt{h^2 - \omega^2} & h^2 \geqslant \omega^2. \end{cases}$$

With this, proving (129) reduces to the following.

Theorem 4 (generalized Weyl formula)**.** *The time-harmonic complex-source beam $B_\omega(\boldsymbol{z})$ has the following* angular spectrum *representation,*

$$\frac{\mathrm{e}^{\mathrm{i}\omega\tilde{r}}}{4\pi\tilde{r}} = \begin{cases} U^+(\boldsymbol{z}, \omega) & \omega > 0 \quad \xi > 0 \quad \text{(large right component)} \\ U^+(-\boldsymbol{z}, \omega) & \omega > 0 \quad \xi < 0 \quad \text{(small left component)} \\ U^+(\boldsymbol{z}^*, \omega)^* & \omega < 0 \quad \xi > 0 \quad \text{(small right component)} \\ U^+(-\boldsymbol{z}^*, \omega)^* & \omega < 0 \quad \xi < 0 \quad \text{(large left component)} \end{cases} \tag{133}$$

where, for $\boldsymbol{z} = (\boldsymbol{\rho}, \zeta) = (\boldsymbol{\rho}, \xi - \mathrm{i}a)$, $\omega > 0$ *and* $\xi > 0$,

$$U^{+}(\boldsymbol{z}, \omega) = \int_{\mathbb{R}^2} \frac{\text{đ}\boldsymbol{h}}{2\mu}\, \mathrm{e}^{\mathrm{i}\boldsymbol{h}\cdot\boldsymbol{\rho}-\mu\zeta} = U^{+}_{\mathrm{prop}}(\boldsymbol{z}, \omega) + U^{+}_{\mathrm{evan}}(\boldsymbol{z}, \omega) \tag{134}$$

with the propagating and evanescent parts given by

$$U^{+}_{\mathrm{prop}}(\boldsymbol{z}, \omega) = \mathrm{i}\int_0^{\omega} \frac{h\, \text{đ}h}{2\sqrt{\omega^2 - h^2}} J_0(h\rho)\, \mathrm{e}^{\mathrm{i}\zeta\sqrt{\omega^2-h^2}} \tag{135}$$

$$U^{+}_{\mathrm{evan}}(\boldsymbol{z}, \omega) = \int_{\omega}^{\infty} \frac{h\, \text{đ}h}{2\sqrt{h^2 - \omega^2}} J_0(h\rho)\, \mathrm{e}^{-\zeta\sqrt{h^2-\omega^2}}. \tag{136}$$

The components $U^{+}(\boldsymbol{z}, \omega)$ *and* $U^{+}(-\boldsymbol{z}, \omega)$ *in (133) are analytic continuations of one another across the plane* $\xi = 0$*, with equal boundary values on that plane for* $\rho > a$*. The jump discontinuity, due to the branch cut* $\mathcal{D}$*, is imaginary and given by*

$$\begin{aligned} J(\boldsymbol{\rho}, \omega) &\equiv \lim_{\varepsilon \searrow 0} \{B_{\omega}(\boldsymbol{\rho}, \varepsilon - \mathrm{i}a) - B_{\omega}(\boldsymbol{\rho}, -\varepsilon - \mathrm{i}a)\} \\ &= \mathrm{i}\frac{\Theta(a - \rho)}{2\pi\sqrt{a^2 - \rho^2}} \cosh(\omega\sqrt{a^2 - \rho^2}) \end{aligned} \tag{137}$$

with angular spectral decomposition

$$J(\boldsymbol{\rho}, \omega) = \mathrm{i}\int_{\mathbb{R}^2} \text{đ}\boldsymbol{h}\, \mathrm{e}^{\mathrm{i}\boldsymbol{h}\cdot\boldsymbol{\rho}} \frac{\sin(\mu a)}{\mu} = \mathrm{i}\int_0^{\infty} h\, \text{đ}h\, J_0(h\rho) \frac{\sin(\mu a)}{\mu}. \tag{138}$$

Remarks.

- In the limit $a \to 0$, (133) becomes Weyl's angular-spectrum decomposition of the fundamental solution of Helmholtz's equation (see [MW95], pp 120–5, where $m = \mathrm{i}\mu$)

$$\frac{\mathrm{e}^{\mathrm{i}\omega r}}{4\pi r} = \int_{\mathbb{R}^2} \frac{\text{đ}\boldsymbol{h}}{2\mu}\, \mathrm{e}^{\mathrm{i}\boldsymbol{h}\cdot\boldsymbol{\rho}-\mu|\xi|} \qquad r = \sqrt{\rho^2 + \xi^2} \qquad \omega > 0.$$

- Since $\tilde{r}$ depends only on the squares of the components of $\boldsymbol{z}$, it suffices to reverse only the component $\zeta = \xi - \mathrm{i}a$ in the $\hat{\boldsymbol{y}}$ direction. However, the beams are cylindrically symmetric about the $\hat{\boldsymbol{y}}$-axis, therefore

$$B_{\omega}(\boldsymbol{\rho}, -\zeta) = B_{\omega}(-\boldsymbol{\rho}, -\zeta) = B_{\omega}(-\boldsymbol{z})$$

  and reversing ζ is equivalent to reversing $\boldsymbol{z}$.

Proof. Equation (133) is a direct consequence of formula (26) on page 9 of [E54]. With

$$x = h \qquad b = \omega \qquad y = \rho \qquad \alpha = \zeta = \xi - \mathrm{i}a \qquad \xi > 0$$
$$\sqrt{y^2 + \alpha^2} = \sqrt{\rho^2 + \zeta^2} = \tilde{r}$$

it states that the function

$$f(h) = \begin{cases} \pm\mathrm{i}\sqrt{h/(\omega^2 - h^2)}\, \mathrm{e}^{\pm\mathrm{i}\zeta\sqrt{\omega^2-h^2}} & 0 < h < \omega \\ \sqrt{h/(h^2 - \omega^2)}\, \mathrm{e}^{-\zeta\sqrt{h^2-\omega^2}} & \omega < h < \infty \end{cases}$$

has *Hankel transform*

$$\int_0^{\infty} \mathrm{d}h\, f(h) J_0(h\rho)\sqrt{h\rho} = \frac{\sqrt{\rho}\, \mathrm{e}^{\pm\mathrm{i}\omega\tilde{r}}}{\tilde{r}} \tag{139}$$

which gives (133) for positive ω and ξ. The other cases follow from the symmetries discussed above. That $U^+(\boldsymbol{\rho}, -\xi + \mathrm{i}a, \omega)$ is the analytic continuation of $U^+(\boldsymbol{\rho}, \xi - \mathrm{i}a, \omega)$ to $\xi < 0$ follows from the known analyticity of $B_\omega(\boldsymbol{z})$ outside the branch cut $\mathcal{D}$. Recall that

$$\xi \to \pm 0 \Rightarrow \tilde{r} = \sqrt{\rho^2 + (\xi - \mathrm{i}a)^2} \to \begin{cases} \mp\mathrm{i}\sqrt{a^2 - \rho^2} & 0 \leqslant \rho \leqslant a \\ \sqrt{\rho^2 - a^2} & \rho \geqslant a \end{cases}$$

hence

$$\begin{aligned} B_\omega(\boldsymbol{\rho}, \xi - \mathrm{i}a) &\to \pm\mathrm{i}\frac{\mathrm{e}^{\pm\omega\sqrt{a^2-\rho^2}}}{4\pi\sqrt{a^2 - \rho^2}} \qquad 0 \leqslant \rho \leqslant a \\ &\to \frac{\mathrm{e}^{\mathrm{i}\omega\sqrt{\rho^2-a^2}}}{4\pi\sqrt{\rho^2 - a^2}} \qquad \rho \geqslant a \end{aligned}$$

and the jump across $\xi = 0$ is indeed given by (137). By (134), the boundary values of the propagating and evanescent parts are

$$\lim_{\varepsilon \searrow 0} U^+_{\text{prop}}(\boldsymbol{\rho}, \varepsilon - \mathrm{i}a, \omega) = \mathrm{i}\int_0^\omega \frac{h\, \text{đ}h}{2\sqrt{\omega^2 - h^2}} J_0(h\rho)\, \mathrm{e}^{a\sqrt{\omega^2-h^2}} = \mathrm{i}A$$

$$\lim_{\varepsilon \searrow 0} U^+_{\text{prop}}(\boldsymbol{\rho}, \mathrm{i}a - \varepsilon, \omega) = \mathrm{i}\int_0^\omega \frac{h\, \text{đ}h}{2\sqrt{\omega^2 - h^2}} J_0(h\rho)\, \mathrm{e}^{-a\sqrt{\omega^2-h^2}} = \mathrm{i}A'$$

$$\lim_{\varepsilon \searrow 0} U^+_{\text{evan}}(\boldsymbol{\rho}, \varepsilon - \mathrm{i}a, \omega) = \int_\omega^\infty \frac{h\, \text{đ}h}{2\sqrt{h^2 - \omega^2}} J_0(h\rho)\, \mathrm{e}^{\mathrm{i}a\sqrt{h^2-\omega^2}} = B + \mathrm{i}C$$

$$\lim_{\varepsilon \searrow 0} U^+_{\text{evan}}(\boldsymbol{\rho}, \mathrm{i}a - \varepsilon, \omega) = \int_\omega^\infty \frac{h\text{đ}h}{2\sqrt{h^2 - \omega^2}} J_0(h\rho)\, \mathrm{e}^{-\mathrm{i}a\sqrt{h^2-\omega^2}} = B - \mathrm{i}C$$

with A, A', B and C real. Hence the real part of B_ω is continuous and the jump across $\xi = 0$ is

$$\begin{aligned} J(\rho, \omega) &= \mathrm{i}A - \mathrm{i}A' + 2\mathrm{i}C \\ &= \mathrm{i}\int_0^\omega \frac{h\text{đ}h}{\sqrt{\omega^2 - h^2}} J_0(h\rho) \sinh\left(a\sqrt{\omega^2 - h^2}\right) \\ &\quad + \mathrm{i}\int_\omega^\infty \frac{h\text{đ}h}{\sqrt{h^2 - \omega^2}} J_0(h\rho) \sin\left(a\sqrt{h^2 - \omega^2}\right) \\ &= \mathrm{i}\int_0^\infty \frac{h\, \text{đ}h}{\mu} J_0(h\rho) \sin(\mu a). \end{aligned}$$

□

Now that we have the correct contour, we also know the Fourier transform of the pulsed beam. By (130),

$$\hat{W}(k, y) = \frac{\hat{g}(\omega, u)\Omega(k, \boldsymbol{y})}{\mu^2 + l^2} = \frac{\hat{g}(\omega, u)}{2\mu} \left\{ \frac{\mathrm{e}^{\mathrm{i}\mu a}}{\mu + 0 + \mathrm{i}l} + \frac{\mathrm{e}^{-\mathrm{i}\mu a}}{\mu + 0 - \mathrm{i}l} \right\} \qquad \omega > 0. \tag{140}$$

9. Electromagnetic wavelets revisited

The complex scalar sources will now be used to construct complex vector-valued point sources for electromagnetic wavelets. The most direct formulation is in terms of *Hertz potentials*, which are reviewed briefly.

Although Hertz potentials have a long history in electrodynamics, they have been sadly ignored in most modern textbooks. Many books that do mention them have only a short section on the subject, usually under various specialized assumptions, and so it is difficult to see their generality because each text gives only a partial picture. It is not widely known, for example, that the electric and magnetic 'Hertz vectors' (which are often introduced alone, with their partner gauged away) transform as a skew-symmetric tensor under the Lorentz group, are compatible with external currents, do not require the Lorenz[13] condition, and have a very large gauge group containing that of the 4-vector potential.

A comprehensive theory of Hertz potentials and their gauge freedom was developed beautifully by Nisbet [N55, N57] and reformulated in spacetime tensor form by McCrea [M57]. (See also Kannenberg [Kan87].) Nisbet's formualtion becomes even more compelling when translated to the language of differential forms. In this setting, it was used to define and compute electromagnetic wavelets in terms of polarization sources [K02]. Sourceless EM wavelets were originally constructed in Fourier space [K94]. But their explicit spacetime form and its splitting into retarded and advanced parts were unknown until recently. I summarize the main results below. Please refer to [K02] for details. Hertz potentials form a skew-symmetric tensor (i.e., a 2-form in $\mathbb{R}^{3,1}$) like the electromagnetic field itself. They are given in a reference frame by the *electric and magnetic Hertz vectors* $\boldsymbol{Z}_e, \boldsymbol{Z}_m$, which will be used here in the *selfdual* combination

$$\boldsymbol{Z}(x) = \boldsymbol{Z}_m(x) - \mathrm{i}\boldsymbol{Z}_e(x). \tag{141}$$

These vectors are generated by electric and magnetic polarization densities $\boldsymbol{P}_e, \boldsymbol{P}_m$, again represented in the selfdual form

$$\boldsymbol{P}(x) = \boldsymbol{P}_m(x) - \mathrm{i}\boldsymbol{P}_e(x). \tag{142}$$

($\boldsymbol{P}_m$ is called the *magnetization* and usually denoted by $\boldsymbol{M}$.) The two fields are connected by the wave equation

$$\Box\boldsymbol{Z}(x) = -\boldsymbol{P}(x) \qquad \Box = \Delta - \partial_t^2. \tag{143}$$

The electromagnetic field will be presented in the *anti*-selfdual combination

$$\boldsymbol{F}(x) = \boldsymbol{D}(x) + \mathrm{i}\boldsymbol{B}(x) \tag{144}$$

called the *Riemann–Silberstein wavefunction* by Bialynicki-Birula because of its connection with the wavefunction of the photon [B96]. Maxwell's equations become

$$\mathrm{i}\partial_t\boldsymbol{F} = \nabla\times\boldsymbol{F} - \mathrm{i}\nabla\times\boldsymbol{P} - \mathrm{i}\boldsymbol{J} \qquad \nabla\cdot\boldsymbol{F} = \rho \tag{145}$$

where we have taken into account the constitutive relations (in SI units with $c = 1$)

$$\boldsymbol{D} = \boldsymbol{E} + \boldsymbol{P}_e \qquad \boldsymbol{B} = \boldsymbol{H} + \boldsymbol{P}_m. \tag{146}$$

We will need only polarization sources, and therefore assume that the external charge-current density vanishes: $\boldsymbol{J} = \mathbf{0}$ and $\rho = 0$. Then $\boldsymbol{F}$ is generated by $\boldsymbol{Z}$ according to [BW75, p 80]

$$\boldsymbol{F}(x) = \mathrm{i}\mathcal{L}\boldsymbol{Z}(x) \tag{147}$$

where $\mathcal{L}$ is the operator

$$\mathcal{L}\boldsymbol{Z} = \nabla\times(\nabla\times\boldsymbol{Z}) + \mathrm{i}\partial_t\nabla\times\boldsymbol{Z}. \tag{148}$$

External charge-current densities can be included in (143) via *stream potentials* [N55].

As in the scalar case, we first construct sourceless EM wavelets. These will split into advanced and retarded parts, which are then the vectorial counterparts of the scalar pulsed-beam wavelets. Thus begin with $\boldsymbol{P} = \mathbf{0}$, so that

$$\Box\boldsymbol{Z}(x) = \mathbf{0} \Rightarrow \boldsymbol{Z}(x) = \int_C \mathrm{d}\tilde{k}\, \mathrm{e}^{\mathrm{i}k\cdot x}\boldsymbol{\zeta}(k). \tag{149}$$

[13] Apparently due to L V Lorenz and not H A Lorentz; see [PR84, B99].

Since $k \cdot x = \boldsymbol{k} \cdot \boldsymbol{x} - \omega t$, (147) gives

$$\boldsymbol{F}(x) = \mathrm{i} \int_C \mathrm{d}\tilde{k}\, \mathrm{e}^{\mathrm{i}k\cdot x} \{-\boldsymbol{k} \times (\boldsymbol{k} \times \boldsymbol{\zeta}) + \mathrm{i}\omega \boldsymbol{k} \times \boldsymbol{\zeta}\}. \tag{150}$$

To check that this indeed solves Maxwell's equations, note that (145) reduces to

$$\mathrm{i}\partial_t \boldsymbol{F} = \nabla \times \boldsymbol{F} \Rightarrow \omega \boldsymbol{f} = \mathrm{i}\boldsymbol{k} \times \boldsymbol{f} \qquad \text{or} \qquad \mathbb{S}(k)\boldsymbol{f}(k) = \boldsymbol{f}(k) \tag{151}$$

where $\mathbb{S}(k) : \mathbb{C}^3 \to \mathbb{C}^3$ is the 3×3 matrix function on C defined by

$$\mathbb{S}(k)\boldsymbol{v} = \mathrm{i}\boldsymbol{n} \times \boldsymbol{v} \qquad \boldsymbol{n}(k) \equiv \boldsymbol{k}/\omega \qquad \boldsymbol{n}^2 = 1 \tag{152}$$

which is Hermitian and satisfies

$$\mathbb{S}^2 \boldsymbol{v} = \boldsymbol{v} - \boldsymbol{n}(\boldsymbol{n} \cdot \boldsymbol{v}) \qquad \mathbb{S}^3 = \mathbb{S}. \tag{153}$$

Equation (150) therefore reads

$$\boldsymbol{F}(x) = 2\mathrm{i} \int_C \mathrm{d}\tilde{k}\, \mathrm{e}^{\mathrm{i}k\cdot x} \omega^2 \mathbb{P}(k) \boldsymbol{\zeta}(k) \qquad \text{where} \quad \mathbb{P}(k) = \frac{1}{2}\left(\mathbb{S}^2 + \mathbb{S}\right). \tag{154}$$

By (153) $\mathbb{S}(k)$ has the nondegenerate spectrum $\{1, 0, -1\}$, and (151) requires $\boldsymbol{f}$ to have eigenvalue 1.[14] But

$$\mathbb{P}^2 = \mathbb{P} \quad \text{and} \quad \mathbb{S}\mathbb{P} = \mathbb{P} \tag{155}$$

so $\mathbb{P}(k)$ is precisely the orthogonal projection to the eigenspace with eigenvalue 1. This shows how Hertz potentials solve the free Maxwell equations in Fourier space.

By (154), $\boldsymbol{F}$ has coefficient function

$$\boldsymbol{f}(k) = 2\mathrm{i}\omega^2 \mathbb{P}(k)\boldsymbol{\zeta}(k) = \mathbb{P}(k)\boldsymbol{f}(k). \tag{156}$$

Next, extend $\boldsymbol{Z}(x)$ and $\boldsymbol{F}(x)$ to $\mathcal{T}$ with the analytic-signal transform (AST),

$$\tilde{\boldsymbol{Z}}(z) = \hat{u} \int_C \mathrm{d}\tilde{k}\, \Theta(\omega u)\, \mathrm{e}^{\mathrm{i}k\cdot z} \boldsymbol{\zeta}(k) \tag{157}$$

$$\tilde{\boldsymbol{F}}(z) = \hat{u} \int_C \mathrm{d}\tilde{k}\, \Theta(\omega u)\, \mathrm{e}^{\mathrm{i}k\cdot z} \mathbb{P}(k)\boldsymbol{f}(k) = \mathrm{i}\mathcal{L}_x \tilde{\boldsymbol{Z}}(z). \tag{158}$$

The positive and negative frequency parts of $\boldsymbol{f}$ also have positive and negative *helicities* [K94], so the restrictions of $\tilde{\boldsymbol{F}}(z)$ to $\mathcal{T}_+$ and $\mathcal{T}_-$ are positive and negative helicity solutions.

To construct the wavelets we need a Hilbert space of solutions. The inner product in Fourier space is uniquely determined (up to a constant factor) by Lorentz invariance as

$$\langle \boldsymbol{F}_1 | \boldsymbol{F}_2 \rangle = \int_C \frac{\mathrm{d}\tilde{k}}{\omega^2} \boldsymbol{f}_1(k)^* \boldsymbol{f}_2(k) = 4 \int_C \mathrm{d}\tilde{k}\, \omega^2 \boldsymbol{\zeta}_1^* \mathbb{P} \boldsymbol{\zeta}_2.$$

Denote the Hilbert space of all solutions with finite norm by

$$\mathcal{H} = \{\boldsymbol{F} : \|\boldsymbol{F}\|^2 = \langle \boldsymbol{F} | \boldsymbol{F} \rangle < \infty\}. \tag{159}$$

The wavelets will be *dyadics*, and to streamline the notation, we rewrite the inner product by thinking of $|\boldsymbol{F}_1\rangle$ as an (infinite-dimensional) *column vector* and $\langle \boldsymbol{F}_1|$ as its adjoint *row vector* with respect to the above inner product:

$$\langle \boldsymbol{F}_1 | = \boldsymbol{F}_1^* : \mathcal{H} \to \mathbb{C} \qquad |\boldsymbol{F}_2\rangle = \boldsymbol{F}_2 : \mathbb{C} \to \mathcal{H} \qquad \langle \boldsymbol{F}_1 | \boldsymbol{F}_2 \rangle = \boldsymbol{F}_1^* \boldsymbol{F}_2 \tag{160}$$

where $\boldsymbol{F}_2 : \mathbb{C} \to \mathcal{H}$ is the map of scalar multiplication $c \mapsto c\boldsymbol{F}_2$. This notation extends Dirac's bra–ket formalism because $\boldsymbol{F}_1$ and $\boldsymbol{F}_2$ can now be replaced by other linear mappings

[14] $\mathbb{S}\boldsymbol{f} = \boldsymbol{f}$ means $\boldsymbol{F}$ is anti-selfdual; $\mathbb{S}\boldsymbol{f} = -\boldsymbol{f}$ means $\boldsymbol{F}$ is selfdual; $\mathbb{S}\boldsymbol{f} = \boldsymbol{0}$ is longitudinal, $\boldsymbol{F} = \boldsymbol{0}$.

into $\mathcal{H}$. That will enable us to write orthogonality and completeness relations for Hilbert spaces of vector fields (or even operators) with the same ease as in the scalar case[15].

Note that the measure $\mathrm{d}\tilde{k}/\omega^2 = \mathrm{đ}\boldsymbol{k}/2|\boldsymbol{k}|^3$ is invariant under scaling. In fact, an equivalent inner product has been shown by Gross [Gr64] to be invariant under the *conformal group* of Minkowski space, $\mathcal{C} \approx O(4, 2) \approx SU(2, 2)$. Therefore the Hilbert space of anti-selfdual solutions carries a unitary representation of $\mathcal{C}$.

Returning to (158), define the matrix-valued ('dyadic') function on C,

$$\widehat{\mathbb{W}}_z(k) = \hat{u}\Theta(\omega u)\,\mathrm{e}^{-\mathrm{i}k\cdot z^*}\omega^2\mathbb{P}(k) \tag{161}$$

represented in spacetime by

$$\mathbb{W}_z(x') = \hat{u}\int_C \mathrm{d}\tilde{k}\,\Theta(\omega u)\,\mathrm{e}^{\mathrm{i}k\cdot(x'-z^*)}\omega^2\mathbb{P}(k). \tag{162}$$

This is the matrix-valued solution of Maxwell's equations (i.e. every column is a solution) designed so that its vector-valued inner product with any solution $\boldsymbol{F} \in \mathcal{H}$ is $\tilde{\boldsymbol{F}}(z)$:

$$\mathbb{W}_z^*\boldsymbol{F} \equiv \int_C \frac{\mathrm{d}\tilde{k}}{\omega^2}\,\widehat{\mathbb{W}}_z(k)^*\boldsymbol{f}(k) = \tilde{\boldsymbol{F}}(z). \tag{163}$$

This is a vector form of the *evaluation maps* (30) used to define the scalar relativistic coherent states e_z, written in star notation as $e_z^* f = \tilde{f}(z)$. The $\mathbb{W}_z$ are the sourceless electromagnetic wavelets. They span a *reproducing kernel Hilbert space* with a matrix kernel

$$\begin{aligned}\mathbb{K}(z', z^*) \equiv \mathbb{W}_{z'}^*\mathbb{W}_z &= \int_C \frac{\mathrm{d}\tilde{k}}{\omega^2}\,\Theta(\omega u')\Theta(\omega u)\,\mathrm{e}^{\mathrm{i}k\cdot(z'-z^*)}\omega^4\mathbb{P}(k)\\ &\equiv \Theta(u'u)\mathbb{W}(z'-z^*) \qquad z', z \in \mathcal{T}\end{aligned} \tag{164}$$

where the factor $\Theta(u'u)$ enforces the orthogonality of wavelets parametrized by the forward and backward tubes and the holomorphic matrix function

$$\mathbb{W}(z) = \int_C \mathrm{d}\tilde{k}\,\Theta(\omega u)\,\mathrm{e}^{\mathrm{i}k\cdot z}\omega^2\mathbb{P}(k) = \int_{C_\pm} \mathrm{d}\tilde{k}\,\mathrm{e}^{\mathrm{i}k\cdot z}\omega^2\mathbb{P}(k) \qquad z \in \mathcal{T}_\pm \tag{165}$$

generates the entire wavelet family (162) by

$$\mathbb{W}_z(x') = \hat{u}\mathbb{W}(x' - z^*). \tag{166}$$

We now compute $\mathbb{W}(z)$ explicitly. Applying it to a vector $\boldsymbol{p} \in \mathbb{C}^3$ gives, by the same reasoning as in (150) and (154),

$$2\mathbb{W}(z)\boldsymbol{p} = 2\int_{C_\pm} \mathrm{d}\tilde{k}\,\mathrm{e}^{\mathrm{i}k\cdot z}\omega^2\mathbb{P}(k)\boldsymbol{p} = \mathcal{L}[G_4(z)\boldsymbol{p}] \qquad z \in \mathcal{T}_\pm \tag{167}$$

where, according to (46) and (67),

$$G_4(z) = \int_C \mathrm{d}\tilde{k}\,\Theta(\omega u)\,\mathrm{e}^{\mathrm{i}k\cdot z} = \frac{1}{4\pi^2 z^2} \qquad z \in \mathcal{T} \tag{168}$$

is the extension (67) of the Euclidean potential $G_4(x_E)$. As $\boldsymbol{p}$ is arbitrary, (167) determines $\mathbb{W}(z)$. Thus we have made contact with the scalar theory. We already have a good understanding of $G_4(z)$ and its relation to causality. By (70), we have a splitting

$$G_4(z)\boldsymbol{p} = \mathrm{i}\tilde{D}^-(z)\boldsymbol{p} - \mathrm{i}\tilde{D}^+(z)\boldsymbol{p} \qquad \tilde{D}^\pm(z) = \frac{1}{8\mathrm{i}\pi^2\tilde{r}(\tau \mp \tilde{r})}. \tag{169}$$

[15] Called *star notation* in [K94], this method has a number of other advantages over the conventional Dirac formalism. By dropping the baggage of bras and kets, it simplifies the typesetting and appearance of equations. Seasoned bra–ket practitioners may complain that they can no longer label eigenvectors merely by their eigenvalues (i.e., $A|a\rangle = a|a\rangle$), but this confusing practice may be one reason why mathematicians have never adopted this otherwise very useful notation! For example, if $|x\rangle$ and $|p\rangle$ denote position and momentum eigenstates, then what is $|3\rangle$?

Thus (167) and (169) induce a causal splitting of $\mathbb{W}(z)$,

$$\mathbb{W}(z) = \mathbb{W}^-(z) - \mathbb{W}^+(z) \qquad \text{where} \quad 2\mathbb{W}^\pm(z)\boldsymbol{p} \equiv \mathrm{i}\mathcal{L}_x[\tilde{D}^\pm(z)\boldsymbol{p}]. \tag{170}$$

It is natural to define retarded and advanced *pulsed-beam Hertzian dipole potentials*

$$\tilde{\boldsymbol{Z}}_{\boldsymbol{p}}^\pm(z) = \tilde{D}^\pm(z)\boldsymbol{p} \tag{171}$$

whose polarization sources are

$$\tilde{\boldsymbol{P}}_{\boldsymbol{p}}(z) = -\Box\,\tilde{\boldsymbol{Z}}_{\boldsymbol{p}}^\pm(z) = -\boldsymbol{p}\,\Box\,\tilde{D}^\pm(z) = \boldsymbol{p}\tilde{\delta}_{3,1}(z).$$

In the Minkowskian limit, $\boldsymbol{p}$ is therefore interpreted as a combination of magnetic and electric dipole moments:

$$\boldsymbol{P}_{\boldsymbol{p}}(x) = \boldsymbol{p}\delta_{3,1}(x) \qquad \boldsymbol{p} = \boldsymbol{p}_m - \mathrm{i}\boldsymbol{p}_e. \tag{172}$$

$\tilde{\boldsymbol{Z}}_{\boldsymbol{p}}^\pm(x - \mathrm{i}y)$ are interpreted as the *retarded and advanced Hertz potentials of a dipole disturbance occurring 'at'* $\mathrm{i}y$ *and observed at* x. By (147), the associated pulsed-beam fields are

$$\tilde{\boldsymbol{F}}_{\boldsymbol{p}}^\pm(z) = \mathrm{i}\mathcal{L}\tilde{\boldsymbol{Z}}_{\boldsymbol{p}}^\pm(z) = 2\mathbb{W}^\pm(z)\boldsymbol{p} \tag{173}$$

so $\mathbb{W}^\pm(z)$ are retarded and advanced *electromagnetic pulsed-beam propagators* generating the dipole field of $\boldsymbol{p}$ by dyadic action. Clearly, this can be extended to convolutions with arbitrary dipole distributions, in particular, a time-dependent *driving signal* $\boldsymbol{p}(t)$ as in the scalar case.

Since $\tilde{D}^\pm(z)$ is holomorphic in $\mathcal{T}$ outside the world tube $\tilde{\mathcal{D}}$ swept out by the source disc $\mathcal{D}$, so are $\tilde{\boldsymbol{Z}}_{\boldsymbol{p}}^\pm$, $\tilde{\boldsymbol{F}}_{\boldsymbol{p}}^\pm$ and $\mathbb{W}^\pm$. The dipoles are spread over the source disc $\mathcal{D}$ and modulated in space and time, as specified by the distribution $\tilde{\delta}_{3,1}$ in (107). Note that since $\tilde{\delta}_{3,1}$ is complex, the electric and magnetic dipoles become thoroughly mixed while being 'translated' from the origin to $\mathrm{i}y$ and the mixing is space and time dependent. For example, the Fourier component of $\tilde{\delta}_{3,1}(z)$ with frequency ω gives polarization

$$\boldsymbol{p}(t) = \mathrm{e}^{-\mathrm{i}\omega t}\boldsymbol{p} = (\boldsymbol{p}_m\cos\omega t - \boldsymbol{p}_e\sin\omega t) - \mathrm{i}(\boldsymbol{p}_e\cos\omega t + \boldsymbol{p}_m\sin\omega t). \tag{174}$$

If $\boldsymbol{p}_e$ and $\boldsymbol{p}_m$ are orthogonal with equal magnitudes (i.e., $\boldsymbol{p}^2 = 0$), this becomes a circular polarization. Furthermore, the complex spatial dependence of $\tilde{\delta}_{3,1}$ makes the polarization source $\tilde{\boldsymbol{P}}_{\boldsymbol{p}}(z)$ vary in a nontrivial way over $\mathcal{D}$.

The dyadic propagators $\mathbb{W}^\pm$ are exchanged by spacetime reversal (PT) in the same way as $\tilde{D}^\pm$,

$$\tilde{D}^\pm(-z) = -\tilde{D}^\mp(z) \Rightarrow \mathbb{W}^\pm(-z) = -\mathbb{W}^\mp(z)$$

as follows from (170) since the operator $\mathcal{L}$ is even under PT.

The Fourier transform in x of $\mathbb{W}^\pm(x - \mathrm{i}y)$ can be computed from that of the scalar sources. For $\omega > 0$, (171) and (140) with $\hat{g}(\omega, u) = \hat{C}(\omega, u)$ give

$$\hat{\tilde{\boldsymbol{Z}}}_{\boldsymbol{p}}^+(k, y) = \frac{\hat{C}(\omega, u)}{2\mu}\left\{\frac{\mathrm{e}^{\mathrm{i}\mu a}}{\mu + 0 + \mathrm{i}l} + \frac{\mathrm{e}^{-\mathrm{i}\mu a}}{\mu + 0 - \mathrm{i}l}\right\}\boldsymbol{p}. \tag{175}$$

The retarded EM wavelets with $\omega > 0$ are now obtained in Fourier space by taking the transform of (173) and remembering that $\mathbb{S} + \mathbb{S}^2 \neq 2\mathbb{P}$ since we are not on-shell:

$$2\widehat{\mathbb{W}}^+(k, y)\boldsymbol{p} = \mathrm{i}\{-\boldsymbol{k}\times(\boldsymbol{k}\times\boldsymbol{p}) + \mathrm{i}\omega\boldsymbol{k}\times\boldsymbol{p}\}\hat{\tilde{Z}}_p^+(k, y). \tag{176}$$

Remarks.

- *All quantities are real* in spite of the fact that we are dealing with holomorphic functions in complex spacetime! For example,

$$\boldsymbol{D}_{\boldsymbol{p}}^{\pm}(x - \mathrm{i}y) = \mathrm{Re}\,\boldsymbol{F}_{\boldsymbol{p}}^{\pm}(x - \mathrm{i}y) \qquad \boldsymbol{B}_{\boldsymbol{p}}^{\pm}(x - \mathrm{i}y) = \mathrm{Im}\,\boldsymbol{F}_{\boldsymbol{p}}^{\pm}(x - \mathrm{i}y) \tag{177}$$

  define a real electromagnetic field in Minkowski space, for any given imaginary source point $\mathrm{i}y$. This is an example of the motto *real physics in complex spacetime*.
- The analyticity, rooted in the cone structure of relativistic wave equations as explained in the introduction, serves to organize the equations by pairing dual or 'harmonically conjugate' fields. In the case of Maxwell fields, the duality is between magnetic and electric entities. This pairing survives even the introduction of sources in that *local sources introduce only local singularities*. That makes it possible to study the singular sources in terms of the boundary values of the fields, as we have done.
- Note that just as analyticity pairs electric and magnetic *dependent* variables, it paired positions and momenta as *independent* variables in the relativistic coherent-state representations of massive fields.
- It is easily shown that

$$\mathbb{P}(k)^* = \mathbb{P}(k) \Rightarrow \mathbb{W}(z)^* = \mathbb{W}(z^*) \Rightarrow \mathbb{W}_z(x')^* = \mathbb{W}_{z^*}(x') \tag{178}$$

  therefore we need only consider $z \in \mathcal{T}_+$.
- Note that

$$G_4(z) = s^{-2} G_4(z/s) \qquad s \neq 0. \tag{179}$$

  If s is independent of x (but possibly depends on y), then

$$\mathbb{W}(z) = s^{-4}\mathbb{W}(z/s). \tag{180}$$

  Taking s to be the *resolution parameter* discussed below (33),

$$s = \sqrt{-y^2} \equiv \lambda > 0 \tag{181}$$

  (167) and (166) show that

$$\mathbb{W}_z(x') = \pm\lambda^{-4}\mathbb{W}\left(\frac{x' - z^*}{\lambda}\right) = \pm\lambda^{-4}\mathbb{W}\left(\frac{x' - x}{\lambda} - \mathrm{i}\hat{y}\right) \qquad z \in \mathcal{T}_\pm \tag{182}$$

  where

$$\hat{y} = \frac{y}{\lambda} \in V_\pm \qquad \hat{y}^2 = -1.$$

  Thus all the wavelets are obtained from $\mathbb{W}(x - \mathrm{i}y)$ with y on the hyperboloid $y^2 = -1$. Using Lorentz invariance, y can be further restricted to $y = (\mathbf{0}, \pm\mathrm{i})$, which may be further reduced to $y = (\mathbf{0}, \mathrm{i})$ by (178). In this way, the entire family of sourceless EM wavelets is obtained from a single 'mother' matrix function of x alone. Furthermore, the columns and rows of $\mathbb{W}$ are constrained by (161) since $\mathbb{P}$ is the projection matrix to a one-dimensional subspace.
- On the other hand, because the splitting $G_4 = \mathrm{i}\tilde{D}^+ - \mathrm{i}\tilde{D}^-$ depends on the inertial frame where the branch cut is taken (the rest frame of $\mathcal{D}$), we cannot apply Lorentz covariance to the pulsed beams $\mathbb{W}_z^{\pm}(x')$. But $\tilde{D}^{\pm}(z)$ are still *positive-homogeneous*,

$$\tilde{D}^{\pm}(z) = s^{-2}\tilde{D}^{\pm}(z/s) \qquad s > 0 \tag{183}$$

  therefore (182) still holds for $\mathbb{W}_z^{\pm}$. All these wavelets can therefore be obtained from those on the hyperboloid $y^2 = -1$ in $\mathcal{T}_+$, or $u = \sqrt{a^2 + 1}$, representing all states of focus up to scale.

- There exist many equivalent *resolutions of unity in* $\mathcal{H}$ [K94], obtained by integrating over various parameter sets $\mathcal{P} \subset \mathcal{T}$ with appropriate measures $\mathrm{d}\mu_{\mathcal{P}}$:

$$\int_{\mathcal{P}} \mathrm{d}\mu_{\mathcal{P}}(z)\mathbb{W}_z\mathbb{W}_z^* = I_{\mathcal{H}}. \tag{184}$$

  This is a 'completeness relation' dual to the '(non)-orthogonality' relation (164). One natural subset for a resolution is the *Euclidean spacetime* as in (44), where all the wavelets are spherical and are parametrized by their centre $\boldsymbol{x}$ and scale u.
- Each resolution gives a representation of EM fields as superpositions of wavelets,

$$\boldsymbol{F}(x') = \int_{\mathcal{P}} \mathrm{d}\mu_{\mathcal{P}}(z)\mathbb{W}_z(x')\mathbb{W}_z^*\boldsymbol{F} = \int_{\mathcal{P}} \mathrm{d}\mu_{\mathcal{P}}(z)\mathbb{W}_z(x')\tilde{\boldsymbol{F}}(z) \tag{185}$$

  with the AST $\tilde{\boldsymbol{F}}(z)$ restricted to $\mathcal{P}$ as the 'wavelet transform'.
- Applying a conformal transformation to any resolution of unity gives another one. Since $\mathcal{C} \approx SU(2,2)$ acts on $\mathcal{T}$ by matrix-valued Möbius transformations, the wavelets transform covariantly and the new parameter space is simply the transform of $\mathcal{P}$ equipped with the transformed measure.
- The resolutions of unity considered in [K94] were all continuous, but they can be discretized to give *dual pairs of EM wavelet frames*. As shown in [K94], the Fourier transform often plays an important role in the construction of such dual frames.
- Applying the AST to (185) gives

$$\tilde{\boldsymbol{F}}(z') = \int_{\mathcal{P}} \mathrm{d}\mu_{\mathcal{P}}(z)\mathbb{W}_{z'}^*\mathbb{W}_z\tilde{\boldsymbol{F}}(z) = \int_{\mathcal{P}} \mathrm{d}\mu_{\mathcal{P}}(z)\,\mathbb{K}(z', z^*)\tilde{\boldsymbol{F}}(z) \tag{186}$$

  which explains the term 'reproducing kernel'.
- Combining (170) and (185) gives

$$\boldsymbol{F}(x') = \boldsymbol{F}^-(x') - \boldsymbol{F}^+(x') \qquad \boldsymbol{F}^\pm(x') = \int_{\mathcal{P}} \mathrm{d}\mu_{\mathcal{P}}(z)\mathbb{W}_z^\pm(x')\tilde{\boldsymbol{F}}(z) \tag{187}$$

  which is a resolution of the sourceless field $\boldsymbol{F}$ into retarded and advanced fields generated by complex sources distributed over $\mathcal{P}$ (or by discs $\mathcal{D}_z$ parametrized by $z \in \mathcal{P}$).

A great many (most!) aspects of EM wavelets, both theoretical and practical, remain unexplored. As previously mentioned, an exciting possibility is that the pulsed-beam wavelets may be realized by simulating their sources. I hope to report on the continuation of this research in the near future.

10. Conclusions

Examples of analytic continuation to complex time and space abound in physics, although the terminology of 'Wick rotations' is, in my opinion, often used too casually—at times in a purely formal way with not even a *basis* for mathematical justification. (In some papers and books I have actually found it impossible to tell from the context whether the author was working in a Euclidean or Lorentzian signature.) But even when justified, the extensions are usually viewed as 'mathematical methods' without any particular physical significance. Here is the list of examples known to me:

- In the correspondence between quantum field theory and statistical mechanics, the imaginary time (more precisely, its period) is related to the reciprocal temperature. But this is regarded as an *analogy* between the two theories, albeit a precise and very useful one.

- In Wightman field theory, n-point functions are extended to tube domains in their difference variables and powerful methods of complex analysis are used to prove theorems about the fields in *real* spacetime, such as *PCT* and the spin-statistics connection [SW64]. There is no attempt to interpret the complex coordinates $z = x - iy$, although the interpretation of $y \in V_+$ as (proportional to) the expected energy–momentum in relativistic coherent states, proved for free fields in [K77, K78, K87], extends to general fields [K90, section 5.3].
- In constructive quantum field theory [GJ87], models of interacting quantum fields are constructed from free fields as follows. The initial Wightman functions are used to construct a Gaussian random (stochastic) field in the Euclidean region. This is then modified by rigorous (Feynman–Kac) path integral methods, which introduce correlations. The modified Euclidean field is no longer Gaussian but still satisfies the necessary (Osterwalder–Schrader) axioms ensuring that its n-point functions can be continued back to Minkowski space, where they yield the interacting field by Wightman's reconstruction theorem. Again there is no attempt to interpret the intermediate complex spacetime because the quantized field exists only in Minkowski space while the random field exists only in the Euclidean region. In between, there are only the analytic Wightman functions.
- There have been various efforts to represent spacetime as a *Shilov boundary* of a complex domain (see [G01] and references therein), but I am not aware of any claiming to do physics directly *inside* these domains.
- Complex spacetime plays a direct role in the general-relativistic theories of H-spaces (Heavens) with their connection to twistor theory [P75, P76, HNPT78, NPT78, BFP80], but again no direct interpretation is generally given to the complex coordinates[16].
- One of the earliest and most influential advocates of complex spacetime in general relativity has been Ivor Robinson, although the evidence appears mainly in the papers and recollections of his colleagues and collaborators due to his famous reluctance to publish in the early days. Penrose [P87, p 357] recalls first hearing about selfdual Maxwell tensors from Ivor in 1954. Around 1963, Robinson's ideas on twisting, shear-free congruences of null rays (now known as *Robinson congruences*) played a seminal role in the development of twistor theory [P87, p 350]; see also [T02]. These were obtained by applying a complex translation to a *non-twisting* congruence consisting of null rays meeting a given lightlike or timelike world line. This procedure removes the singularity along the world line and simultaneously introduces a *twist* into the congruence. The Robinson congruence motivated Trautman [T62] to propose a method for generating new solutions of special-relativistic field equations from known analytic solutions by applying complex Poincaré or conformal transformations. Applied to Maxwell or linearized Einstein fields, this gives curling solutions from non-curling ones.
- Similar ideas motivated the Kerr–Newman solution [N65a] of the Einstein–Maxwell equations, which is now the universal model for spinning, charged black holes. It was discovered by performing a somewhat mysterious complex coordinate transformation on the spherically symmetric solution with mass and charge (Reissner–Nordström). In the charge-free case, this procedure yields a much simplified derivation of the Kerr solution from the Schwarzschild solution [N65] which is, roughly, a general-relativistic analogue of extending the Newtonian potential from $\mathbb{R}^3$ to $\mathbb{C}^3$, i.e.,

$$G_3(\boldsymbol{x}) = \frac{1}{4\pi r} \to G_3(\boldsymbol{z}) = \frac{1}{4\pi \tilde{r}} \qquad \boldsymbol{z} = \boldsymbol{x} - i\boldsymbol{y}$$

and restricting the latter to the slice of $\mathbb{C}^3$ with constant $\boldsymbol{y} \neq \boldsymbol{0}$.

[16] E T Newman, private communication.

The connection between complex translations and spin becomes considerably clearer in *flat* spacetime, where Newman and Winicour [NW74] have established the following remarkable results. Consider an isolated classical relativistic system in Minkowski space. In any given reference frame, the total angular momentum splits into orbital and spin components ($\boldsymbol{L}$, $\boldsymbol{S}$), and its selfdual form is represented by the complex 3-vector

$$\boldsymbol{M} = \boldsymbol{L} + \mathrm{i}\boldsymbol{S}.$$

Similarly, the total dipole tensor splits into electric and magnetic dipole moments ($\boldsymbol{p}_e, \boldsymbol{p}_m$), represented in selfdual form by

$$\boldsymbol{p} = \boldsymbol{p}_e + \mathrm{i}\boldsymbol{p}_m$$

(this differs from (172) by an insignificant factor of i). If the system has positive total 'mass' M (i.e., $M^2 \equiv P_0^2/c^4 - \boldsymbol{P}^2/c^2 > 0$, where P_μ is the total energy–momentum) and nonzero total charge Q, then $\boldsymbol{L}$ is made to vanish by translating to the centre of mass and $\boldsymbol{p}_e$ is made to vanish by translating to the centre of charge. However, Newman and Winicour proved that this is only half the story.

(1) With a further *imaginary* translation by $\mathrm{i}\boldsymbol{S}/Mc$, the spin is made to vanish. Therefore *spin may be identified with an imaginary centre of mass.*

(2) With an imaginary translation by $\mathrm{i}\boldsymbol{p}_m/Q$, the magnetic moment is made to vanish. Therefore *magnetic moment may be identified with an imaginary centre of charge.*

The necessary and sufficient conditions for the existence of a complex reference frame in which the total angular momentum and dipole tensors both vanish are therefore as follows:

(a) The centres of mass and charge must coincide, so that $\boldsymbol{L}$ and $\boldsymbol{p}_e$ can be transformed away by a single real translation.

(b) The system must have the *Dirac gyromagnetic ratio*

$$\boldsymbol{p}_m = (Q/Mc)\boldsymbol{S}$$

so that the spin and magnetic moment can be transformed away by a single imaginary translation. The Dirac ratio is therefore the 'imaginary' counterpart to a common centre of mass and charge!

As already mentioned, this idea was inspired by the Kerr–Newman solution, which has long been known to have the Dirac ratio [C68]. Recently, an old debate was re-ignited as to whether this ratio, which is double that for a nonrelativistic system, necessarily depended on the nonlinear character of the equations. Newman settled the question by showing that the Dirac ratio was obtained as well for the *linearized* solution [N02].

In [K01a], I computed the charge–current distribution for the (real, static) electromagnetic field defined, as in [N73], by the holomorphic Coulomb potential:

$$\boldsymbol{E}(\boldsymbol{x} - \mathrm{i}\boldsymbol{y}) - \mathrm{i}\boldsymbol{H}(\boldsymbol{x} - \mathrm{i}\boldsymbol{y}) \equiv -\nabla \frac{Q}{4\pi \tilde{r}} = Q\frac{\boldsymbol{x} - \mathrm{i}\boldsymbol{y}}{\tilde{r}^3}. \tag{188}$$

The associated charge–current distribution turns out to be that of a *rigidly spinning charged disc of radius a* (the branch cut $\mathcal{D}$) and angular velocity

$$\boldsymbol{\omega} = c\boldsymbol{y}/a^2$$

precisely the value for which the rim moves at the speed of light. This is consistent with the fact that (188) represents the electromagnetic part of the linearized Kerr–Newman black hole.

Acknowledgments

I thank Iwo Bialynicki–Birula, Ehud Heyman, Ted Newman, Ivor Robinson and Andrzej Trautman for many friendly discussions and suggestions over the past several years; Louis Boutet de Monvel and Ivan Kupka for urging me to study hyperfunction theory; and David Park for helping with the plots. I am especially grateful to Arje Nachman for his sustained support of my work, most recently through AFOSR Grant F49620-01-1-0271, and to Bill Miceli for support through ONR in the past.

Appendix. Proofs of the source theorems

We begin with some preliminaries concerning the oblate spheroidal (OS) coordinates associated with the complex distance in $\mathbb{C}^3$ (for $\mathbb{C}^n$, see [K00])

$$\tilde{r}(\boldsymbol{x}-\mathrm{i}\boldsymbol{y}) = \sqrt{(\boldsymbol{x}-\mathrm{i}\boldsymbol{y})^2} = p - \mathrm{i}q \qquad p \geqslant 0 \quad |q| \leqslant |\boldsymbol{y}|.$$

Let ∇ be the gradient and Δ the Laplacian with respect to $\boldsymbol{x}$, for given $\boldsymbol{y} \neq 0$. Then

$$\tilde{r}^2 = \boldsymbol{z}^2 \Rightarrow \tilde{r}\nabla\tilde{r} = \boldsymbol{z} \qquad (\nabla\tilde{r})^2 = 1.$$

The unnormalized OS basis ∇p, ∇q is given by

$$\nabla\tilde{r} = \frac{\boldsymbol{z}}{\tilde{r}} = \frac{\tilde{r}^*\boldsymbol{z}}{\tilde{r}^*\tilde{r}} \Rightarrow \nabla p = \frac{p\boldsymbol{x}+q\boldsymbol{y}}{\tilde{r}^*\tilde{r}} \qquad \nabla q = \frac{p\boldsymbol{y}-q\boldsymbol{x}}{\tilde{r}^*\tilde{r}}.$$

Its normalization and orthogonality follow from

$$\nabla\tilde{r}\cdot\nabla\tilde{r} = 1 \Rightarrow (\nabla p)^2 - (\nabla q)^2 = 1 \qquad \nabla p\cdot\nabla q = 0$$

$$\nabla\tilde{r}^*\cdot\nabla\tilde{r} = \frac{|\boldsymbol{z}|^2}{\tilde{r}^*\tilde{r}} \Rightarrow (\nabla p)^2 + (\nabla q)^2 = \frac{r^2+a^2}{\tilde{r}^*\tilde{r}}$$

which give

$$(\nabla p)^2 = \frac{a^2+p^2}{\tilde{r}^*\tilde{r}} \qquad (\nabla q)^2 = \frac{a^2-q^2}{\tilde{r}^*\tilde{r}}.$$

Taking the divergence of $\tilde{r}\nabla\tilde{r} = \boldsymbol{z}$ gives

$$\Delta\tilde{r} = \frac{2}{\tilde{r}} \qquad \text{hence} \quad \Delta p = \frac{2p}{\tilde{r}^*\tilde{r}} \quad \Delta q = -\frac{2q}{\tilde{r}^*\tilde{r}}. \tag{A.1}$$

To compute volume integrals in the OS coordinates, recall (59) that

$$a\xi = pq \qquad a^2\rho^2 = (p^2+a^2)(a^2-q^2). \tag{A.2}$$

Thus

$$\rho\,\mathrm{d}\rho\wedge\mathrm{d}\xi = \frac{1}{2}\,\mathrm{d}(\rho^2)\wedge\mathrm{d}\xi = \frac{1}{2a^3}\,\mathrm{d}[(p^2+a^2)(a^2-q^2)]\wedge\mathrm{d}(pq) \tag{A.3}$$

$$= a^{-1}(p\,\mathrm{d}p - q\,\mathrm{d}q)\wedge(p\,\mathrm{d}q + q\,\mathrm{d}p) = a^{-1}|\tilde{r}|^2\,\mathrm{d}p\wedge\mathrm{d}q \tag{A.4}$$

where $\mathrm{d}p\wedge\mathrm{d}q$ denotes the antisymmetric exterior product of differential forms (see [AMT88], for example). Therefore the volume measure in OS coordinates is

$$\mathrm{d}\boldsymbol{x} = a^{-1}|\tilde{r}|^2\,\mathrm{d}p\,\mathrm{d}q\,\mathrm{d}\phi. \tag{A.5}$$

Proof of theorem 1. Using the shorthand

$$W_\varepsilon(z) = \Theta(p-\varepsilon a)\frac{g(\tau-\tilde{r})}{4\pi\tilde{r}} \equiv \Theta\frac{g}{4\pi\tilde{r}} \qquad \delta \equiv \delta(p-\varepsilon a) \qquad (\nabla p)^2 = N$$

we have, taking into account the above relations,

$$-2\pi\nabla W_\varepsilon = -\delta\frac{g}{2\tilde r}\nabla p + \Theta\frac{g'}{2\tilde r}\nabla\tilde r + \Theta\frac{g}{2\tilde r^2}\nabla\tilde r$$
$$-2\pi\Delta W_\varepsilon = -\delta'\frac{g}{2\tilde r}N + \delta\frac{g'}{\tilde r}N + \delta\frac{g}{\tilde r^2}N - \delta\frac{g}{2\tilde r}\Delta p - \Theta\frac{g''}{2\tilde r}$$

therefore

$$2\pi S_\varepsilon = -2\pi\,\square\, W_\varepsilon = -\delta'\frac{g}{2\tilde r}N + \delta\frac{g'}{\tilde r}N + \delta\frac{g}{\tilde r^2}N - \delta\frac{g}{2\tilde r}\Delta p.$$

Multiplying through by $|\tilde r|^2$ and letting $\sigma = p^2 + a^2$,

$$2\pi|\tilde r|^2 S_\varepsilon = -\delta'\frac{\sigma g}{2\tilde r} + \delta\frac{\sigma g'}{\tilde r} + \delta\frac{\sigma g}{\tilde r^2} - \delta\frac{\varepsilon g}{\tilde r}.$$

Since the only singularities are in $\boldsymbol{x}$, no smearing is needed in t and S_ε acts on a test function $f(\boldsymbol{x})$ by

$$\langle S_\varepsilon, f\rangle \equiv \int \mathrm{d}\boldsymbol{x}\, S_\varepsilon(\boldsymbol{x} - \mathrm{i}\boldsymbol{y}, \tau) f(\boldsymbol{x})$$
$$= \frac{1}{a}\int_0^\infty \mathrm{d}p \int_{-a}^{a}\mathrm{d}q\left[-\delta'\frac{\sigma g\mathring{f}}{2\tilde r} + \delta\frac{\sigma g'\mathring{f}}{\tilde r} + \delta\frac{\sigma g\mathring{f}}{\tilde r^2} - \delta\frac{\varepsilon g\mathring{f}}{\tilde r}\right]$$

where $\mathring{f}(p,q)$ is the mean (94) of $f(p,q,\phi)$ over ϕ. Integrating the first term by parts in p and simplifying gives

$$\langle S_\varepsilon, f\rangle = \frac{\varepsilon^2 a^2 + a^2}{2a}\int_{-a}^{a}\mathrm{d}q\left\{\frac{g\mathring{f}_p}{\tilde r} + \frac{g'\mathring{f}}{\tilde r} + \frac{g\mathring{f}}{\tilde r^2}\right\} \tag{A.6}$$

which is (96). But $g(\tau - \tilde r) = g(\tau - \varepsilon a + \mathrm{i}q)$ is analytic off the real axis, hence

$$g'(\tau - \tilde r) = -\mathrm{i}g_q. \tag{A.7}$$

Integrating the second term in (A.6) by parts in q gives

$$\langle S_\varepsilon, f\rangle = \frac{\alpha^*\alpha}{2a}\int_{-a}^{a}\mathrm{d}q\, g\left\{\frac{\mathring{f}_p + \mathrm{i}\mathring{f}_q}{\tilde r}\right\} + \frac{\alpha^*\alpha}{2a}\left[\frac{g\mathring{f}}{\mathrm{i}\tilde r}\right]_{\tilde r=\alpha^*}^{\tilde r=\alpha} \tag{A.8}$$

which is (97).

The last two terms in (A.6) will diverge as $\varepsilon \to 0$. To pre-empt this, we use the regularization method introduced in [K00, section 4]. As shown there,

$$\int_{-a}^{a}\frac{\mathrm{d}q}{\varepsilon a - \mathrm{i}q} = \pi - 2\tan^{-1}\varepsilon$$
$$\int_{-a}^{a}\frac{\mathrm{d}q}{(\varepsilon a - \mathrm{i}q)^2} = \frac{2a}{\alpha^*\alpha}$$
$$\int_{-a}^{a}\frac{\mathrm{i}q\,\mathrm{d}q}{(\varepsilon a - \mathrm{i}q)^2} = \frac{2\varepsilon a^2}{\alpha^*\alpha} + 2\tan^{-1}\varepsilon - \pi.$$

Hence we can rewrite the second term in (A.6) as

$$\int_{-a}^{a}\mathrm{d}q\frac{g'\mathring{f}}{\tilde r} = \int_{-a}^{a}\mathrm{d}q\frac{g'\mathring{f} - g'(\tau)\mathring{f}(0) + g'(\tau)\mathring{f}(0)}{\tilde r}$$
$$= \int_{-a}^{a}\mathrm{d}q\frac{g'\mathring{f} - g'(\tau)\mathring{f}(0)}{\tilde r} + (2\tan^{-1}\varepsilon - \pi)g'(\tau)\mathring{f}(0).$$

The subtracted integral regularizes the original, remaining finite as $\varepsilon \to 0$. For the last term in (A.6), note that when $\varepsilon = 0$ we have

$$g(\tau + \mathrm{i}q)\mathring{f}(-\mathrm{i}q) = g(\tau)\mathring{f}(0) + \mathrm{i}qg'(\tau)\mathring{f}(0) + \mathcal{O}(q^2)$$

since $\mathring{f}_q(0) = 0$ (A.9). The correct regularization is therefore

$$\begin{aligned}
\int_{-a}^{a} \mathrm{d}q\, \frac{g\mathring{f}}{\tilde{r}^2} &= \int_{-a}^{a} \mathrm{d}q\, \frac{g\mathring{f} - g(\tau)\mathring{f}(0) - \mathrm{i}qg'(\tau)\mathring{f}(0)}{\tilde{r}^2} + \int_{-a}^{a} \mathrm{d}q\, \frac{g(\tau)\mathring{f}(0) + \mathrm{i}qg'(\tau)\mathring{f}(0)}{\tilde{r}^2} \\
&= \int_{-a}^{a} \mathrm{d}q\, \frac{g\mathring{f} - g(\tau)\mathring{f}(0) - \mathrm{i}qg'(\tau)\mathring{f}(0)}{\tilde{r}^2} \\
&\quad + \frac{2a}{\alpha^*\alpha} g(\tau)\mathring{f}(0) + (2\tan^{-1}\varepsilon - \pi)g'(\tau)\mathring{f}(0).
\end{aligned}$$

When these regularizations are substituted into (A.6), they give (98).

Finally, to prove (99) and (100), simply apply the given expressions for $S_\varepsilon(z)$ to a test function and integrate using the volume form (A.5). □

Proof of theorem 2. Since the test function f is continuous and $\tilde{r} = \pm \mathrm{i}q$ denote the same point on $\mathcal{D}$ (regarded as being in the upper and lower layer), we have

$$\mathring{f}(-\mathrm{i}q) = \mathring{f}(\mathrm{i}q).$$

Furthermore, (59) gives

$$\begin{aligned}
&\partial_p = \frac{p\rho}{p^2 + a^2}\partial_\rho + \frac{q}{a}\partial_\xi \qquad \partial_q = -\frac{p^2 + a^2}{a^2\rho} q\,\partial_\rho + \frac{p}{a}\partial_\xi \\
&\Rightarrow \frac{a}{\tilde{r}}(\partial_p + \mathrm{i}\partial_q) = \frac{2a}{\tilde{r}}\partial_{\tilde{r}} = \frac{a - \mathrm{i}\xi}{\rho}\partial_\rho + \mathrm{i}\partial_\xi .
\end{aligned} \tag{A.9}$$

This shows that both partials are antisymmetric in q on $\mathcal{D}$, with

$$\begin{aligned}
&\mathring{f}_p(\mathrm{i}q) = -\mathring{f}_p(-\mathrm{i}q) = \frac{q}{a}\mathring{f}_\xi \\
&\mathring{f}_q(\mathrm{i}q) = -\mathring{f}_q(-\mathrm{i}q) = -\frac{q}{\rho}\mathring{f}_\rho \\
&\frac{2a}{\tilde{r}}\mathring{f}_{\tilde{r}}(\mathrm{i}q) = \frac{a}{\rho}\mathring{f}_\rho + \mathrm{i}\mathring{f}_\xi .
\end{aligned} \tag{A.10}$$

Inserting this into (A.8), taking the limit $\varepsilon \to 0$, and observing that

$$\tilde{r}(\boldsymbol{z}) = \pm \mathrm{i}a \Rightarrow \boldsymbol{x} = \mathbf{0} \Rightarrow \mathring{f}(\pm \mathrm{i}a) = f(\mathbf{0})$$

gives

$$\begin{aligned}
\langle S, f\rangle &= a\int_{-a}^{a} \mathrm{d}q\, g(\tau + \mathrm{i}q)\left\{\frac{\mathring{f}_{\tilde{r}}}{\tilde{r}}\right\} + \frac{a}{2}\left\{\frac{g(\tau + \mathrm{i}a)}{a} - \frac{g(\tau - \mathrm{i}a)}{-a}\right\} f(\mathbf{0}) \\
&= \int_0^a \mathrm{d}q\, \tilde{g}(\tau, q)\left\{\frac{2a}{\tilde{r}}\mathring{f}_{\tilde{r}}\right\} + \tilde{g}(\tau, a) f(\mathbf{0})
\end{aligned}$$

which is (102). Using (A.10) and changing the integration variable to $\rho = \sqrt{a^2 - q^2}$ gives

$$\begin{aligned}
\langle S, f\rangle &= \int_0^a \mathrm{d}q\, \tilde{g}(\tau, q)\left\{\frac{a\mathring{f}_\rho + \mathrm{i}\rho\mathring{f}_\xi}{\rho}\right\} + \tilde{g}(\tau, a) f(\mathbf{0}) \\
&= \int_0^a \mathrm{d}\rho\, \tilde{g}\left\{\frac{a\mathring{f}_\rho + \mathrm{i}\rho\mathring{f}_\xi}{\sqrt{a^2 - \rho^2}}\right\} + \tilde{g}(\tau, a) f(\mathbf{0})
\end{aligned}$$

which is (105). To prove (103), take the limit of (98) as $\varepsilon \to 0$:

$$\langle S, f\rangle = \frac{a}{2}\int_{-a}^{a} \mathrm{d}q \left\{ \frac{\mathrm{i}g\mathring{f}_p}{q} + \frac{\mathrm{i}g'\mathring{f} - \mathrm{i}g_0'\mathring{f}_0}{q} - \frac{g\mathring{f} - g_0\mathring{f}_0 - \mathrm{i}qg_0'\mathring{f}_0}{q^2} \right\} + g_0\mathring{f}_0.$$

Cancelling two of the counterterms, using

$$g'(\tau + \mathrm{i}q) - g'(\tau - \mathrm{i}q) = -2\mathrm{i}\partial_q\tilde{g}(\tau, q) \equiv -2\mathrm{i}\tilde{g}_q(\tau, q)$$

and noting that $g_0 = g(\tau)$ and $\mathring{f}_0 = \mathring{f}(0)$ gives

$$\langle S, f\rangle = a\int_0^a \mathrm{d}q \left\{ \frac{\mathrm{i}\tilde{g}\mathring{f}_p + \tilde{g}_q\mathring{f}}{q} - \frac{\tilde{g}\mathring{f} - g(\tau)\mathring{f}(0)}{q^2} \right\} + g(\tau)\mathring{f}(0)$$

which is (103). Note that because we have cancelled the two counterterms, the two integrals above no longer converge individually.

Again, (106) is proved by applying the expression for $S(z)$ to a test function and integrating. □

Proof of corollary 1. For $g_0(t) = \delta(t)$, $g(\tau) = 1/2\pi\mathrm{i}\tau$ and

$$\tilde{g}(\tau, q) = \frac{1}{4\pi\mathrm{i}}\left[\frac{1}{\tau + \mathrm{i}q} + \frac{1}{\tau - \mathrm{i}q}\right] = -\frac{\mathrm{i}\tau}{2\pi(\tau^2 + q^2)} = \frac{\mathrm{i}\tau}{2\pi z^2} \qquad z \in \tilde{\mathcal{D}}.$$

Since $W(z) = \tilde{D}^{+}(z)$, this proves (107). For $g_0(t) \equiv 2$, $g(\tau) = \hat{u} = \tilde{g}(\tau, q)$ by (91) and

$$W(z) = \frac{\hat{u}}{4\pi\tilde{r}} = \hat{u}G_3(z) \Rightarrow S(z) = \hat{u}\tilde{\delta}_3(\boldsymbol{z})$$

proving (108). Finally, for $g_0(t) = \mathrm{e}^{-\mathrm{i}\omega t}$, $g(\tau) = \hat{u}\Theta(\omega u)\,\mathrm{e}^{-\mathrm{i}\omega\tau}$ and

$$\begin{aligned}\tilde{g}(\tau, q) &= \frac{\hat{u}}{2}\Theta(\omega u)\,\mathrm{e}^{-\mathrm{i}\omega\tau}(\mathrm{e}^{\omega q} + \mathrm{e}^{-\omega q}) \\ &= \hat{u}\Theta(\omega u)\,\mathrm{e}^{-\mathrm{i}\omega\tau}\cosh(\omega q).\end{aligned}$$

□

Proof of theorem 3. On $E_{\varepsilon a}$ we have

$$\xi(q) = \varepsilon q \qquad \rho(q) = |\eta|\sqrt{a^2 - q^2} \equiv |\eta|\rho_0(q).$$

We will need the temporal Fourier transform of $g(\tau - \tilde{r})$,

$$\int_{-\infty}^{\infty} \mathrm{d}t\,\mathrm{e}^{\mathrm{i}\omega t}g(t - \mathrm{i}u - \tilde{r}) = \hat{g}(\omega, u)\,\mathrm{e}^{\mathrm{i}\omega\tilde{r}} = \hat{g}(\omega, u)\,\mathrm{e}^{\mathrm{i}\varepsilon\omega a}\,\mathrm{e}^{\omega q} = A\,\mathrm{e}^{\omega q}$$

since the integration contour can be moved by $t \to t + \tilde{r}$ without crossing the discontinuity of $g(\tau - \tilde{r})$ across the real axis. (Note that $\mathbb{R} + \tilde{r} = \mathbb{R} - \mathrm{i}q$, so the deformation is bounded uniformly by $|q| \leqslant a$.) For the test function in (97) choose the plane wave

$$f(\rho, \phi, \xi) = \mathrm{e}^{-\mathrm{i}\boldsymbol{k}\cdot\boldsymbol{x}} = \mathrm{e}^{-\mathrm{i}h\rho\cos\phi - \mathrm{i}l\xi}.$$

Thus, using (A.9),

$$\mathring{f}(\tilde{r}) \equiv \int_0^{2\pi} \mathrm{d}\!\!\!{}^-\phi\, f(\rho, \phi, \xi) = \mathrm{e}^{-\mathrm{i}l\xi}J_0(h\rho) = \mathrm{e}^{-\mathrm{i}\varepsilon lq}J_0(h\rho)$$

$$\frac{2a}{\tilde{r}}\mathring{f}_{\tilde{r}} = \mathrm{e}^{-\mathrm{i}\varepsilon lq}\left\{-\frac{ha - \mathrm{i}\varepsilon hq}{\rho}J_1(h\rho) + lJ_0(h\rho)\right\}.$$

Inserting this into (97) and taking the temporal transform gives

$$\hat{S}_\varepsilon(k, y) = A(\omega, u)\Omega_\varepsilon(k, \boldsymbol{y})$$

$$\Omega_\varepsilon(k, \boldsymbol{y}) = \frac{|\eta|^2 a}{2\mathrm{i}}\left\{\frac{\mathrm{e}^{\omega_\varepsilon a}}{\eta a} - \frac{\mathrm{e}^{-\omega_\varepsilon a}}{\eta^* a}\right\} + \frac{|\eta|^2}{2}\int_{-a}^{a}\mathrm{d}q\,\mathrm{e}^{\omega_\varepsilon q}\left\{-\frac{ha - \mathrm{i}\varepsilon hq}{\rho}J_1(h\rho) + lJ_0(h\rho)\right\}.$$

Recalling that $h_\varepsilon = |\eta|h$ and thus $h\rho = h_\varepsilon\rho_0$, this simplifies to

$$\Omega_\varepsilon(k, \boldsymbol{y}) = \cosh(\omega_\varepsilon a) - \mathrm{i}\varepsilon\sinh(\omega_\varepsilon a) - I_1 + \mathrm{i}\varepsilon I_2 + \eta^*\eta I_3 \tag{A.11}$$

where

$$\begin{aligned}
I_1 &= \frac{h_\varepsilon a}{2}\int_{-a}^{a}\frac{\mathrm{d}q}{\rho_0}\,\mathrm{e}^{\omega_\varepsilon q}J_1(h_\varepsilon\rho_0) = h_\varepsilon a\int_0^a\frac{\mathrm{d}q}{\rho_0}\cos(\mathrm{i}\omega_\varepsilon q)J_1(h_\varepsilon\rho_0)\\
I_2 &= \frac{h_\varepsilon}{2}\int_{-a}^{a}\frac{\mathrm{d}q}{\rho_0}q\,\mathrm{e}^{\omega_\varepsilon q}J_1(h_\varepsilon\rho_0) = a^{-1}\partial_{\omega_\varepsilon}I_1\\
I_3 &= \frac{l}{2}\int_{-a}^{a}\mathrm{d}q\,\mathrm{e}^{\omega_\varepsilon q}J_0(h_\varepsilon\rho_0) = l\int_0^a\mathrm{d}q\cos(\mathrm{i}\omega_\varepsilon q)J_0(h_\varepsilon\rho_0).
\end{aligned}$$

The first two integrals can be evaluated by letting

$$q = a\cos\gamma \qquad 2\psi = \mu_\varepsilon a = a\sqrt{h_\varepsilon^2 - \omega_\varepsilon^2} \qquad 2\chi = \mathrm{i}\omega_\varepsilon a \qquad \psi^2 - \chi^2 = h_\varepsilon^2 a^2/4.$$

Then, by [GR65, p 742 (6.688-1)],

$$\begin{aligned}
I_1 &= h_\varepsilon a\int_0^{\pi/2}\mathrm{d}\gamma\cos(\mathrm{i}\omega_\varepsilon\cos\gamma)J_1(h_\varepsilon a\sin\gamma)\\
&= (h_\varepsilon a\pi/2)J_{1/2}(\psi+\chi)J_{1/2}(\psi-\chi)\\
&= h_\varepsilon a\sqrt{\psi^2-\chi^2}\,j_0(\psi+\chi)j_0(\psi-\chi)\\
&= \frac{h_\varepsilon a}{\sqrt{\psi^2-\chi^2}}\sin(\psi+\chi)\sin(\psi-\chi)\\
&= 2\sin^2\psi\cos^2\chi - 2\cos^2\psi\sin^2\chi\\
&= 2\cos^2\chi - 2\cos^2\psi\\
&= \cos 2\chi - \cos 2\psi.
\end{aligned}$$

Thus

$$\begin{aligned}
I_1 &= \cosh(\omega_\varepsilon a) - \cos(\mu_\varepsilon a)\\
I_2 &= \frac{1}{a}\frac{\partial I_1}{\partial\omega_\varepsilon} = \sinh(\omega_\varepsilon a) - (\omega_\varepsilon/\mu_\varepsilon)\sin(\mu_\varepsilon a)
\end{aligned} \tag{A.12}$$

where we have used

$$\frac{\partial\mu_\varepsilon}{\partial\omega_\varepsilon} = -\frac{\omega_\varepsilon}{\mu_\varepsilon}.$$

The third integral is obtained from [GR65, p 737 (6.677-6)]:

$$I_3 = (l/\mu_\varepsilon)\sin(\mu_\varepsilon a). \tag{A.13}$$

Inserting these into (A.11) gives some 'miraculous' cancellations resulting in (114). The final details are given section 7. □

References

[AMT88] Abraham R, Marsden J E and Ratiu T 1988 *Manifolds, Tensor Analysis, and Applications* 2nd edn (Berlin: Springer)

[B96] Bialynicki-Birula I 1996 Photon wave function *Progress in Optics* vol 36 ed E Wolf (Amsterdam: Elsevier)

[B99] Baylis W E 1999 *Electrodynamics: A Modern Geometric Approach* (Boston, MA: Birkhäuser)

[BC87] Baker B B and Copson E T 1987 *The Mathematical Theory of Huygens' Principle* 3rd edn (New York: Chelsea)

[BFP80] Boyer C P, Finley J D III and Plebański J F 1980 Complex general relativity, H and HH spaces: a survey of one approach *General Relativity and Gravitation: One Hundred Years After the Birth of Albert Einstein* vol 2 ed A Held (New York: Plenum) pp 241–81

[BW75] Born M and Wolf E 1975 *Principles of Optics* 5th edn (Oxford: Pergamon)

[C68] Carter B 1968 *Phys. Rev.* **174** 1559

[D92] Daubechies I 1992 *Ten Lectures on Wavelets* (Philadelphia, PA: SIAM)

[E54] Erdélyi A (ed) 1954 *Tables of Integral Transforms* vol 2 (New York: McGraw-Hill)

[F97] Fink M 1997 Time reversed acoustics *Phys. Today* **50** (March) 34–40

[G46] Gabor D 1946 Theory of communication *J. IEE* **93** 429–57

[G01] Gibbons G W 2001 Holography and the future tube *Class. Quantum Grav.* **17** 1071–9 (*Preprint* hep-th/911027)

[GJ87] Glimm J and Jaffe A 1987 *Quantum Physics: A Functional Integral Point of View* 2nd edn (New York: Springer)

[Gr64] Gross L 1964 Norm-invariance of mass-zero equations under the conformal group *J. Math. Phys.* **5** 687–95

[GR65] Gradshteyn I S and Ryzhik I M 1965 *Tables of Integrals, Series, and Products* (New York: Academic)

[GS64] Gel'fand I M and Shilov G E 1964 *Generalized Functions, Volume 1: Properties and Operations* (New York: Academic)

[HF01] Heyman E and Felsen L B 2001 Gaussian beam and pulsed beam dynamics: complex source and spectrum formulations within and beyond paraxial asymptotics *J. Opt. Soc. Am.* **18** 1588–611

[HI79] Hawking S W 1979 The path-integral approach to quantum gravity *General Relativity: An Einstein Centenary Survey* ed S W Hawking and W Israel (Cambridge: Cambridge University Press)

[HLK00] Hayman E, Lomakin V and Kaiser G 2000 Physical source realization of complex-source pulsed beams *J. Acoust. Soc. Am.* **107** 1880–91

[HNPT78] Hansen R O, Newman E T, Penrose R and Tod K P 1978 The metric and curvature properties of H-space *Proc. R. Soc.* A **363** 445–68

[I92] Imai I 1992 *Applied Hyperfunction Theory* (Dordrecht: Kluwer)

[IZ80] Itzykson C and Zuber J-B 1980 *Quantum Field Theory* (New York: McGraw-Hill)

[K76] Kaiser G 1977 Phase-space approach to relativistic quantum mechanics *Doctoral Thesis* Mathematics Department, University of Toronto

Kaiser G 1976 Relativistic coherent-state representations *Group Theoretical Methods in Physics (Montreal)* ed R T Sharp and B Kolman (New York: Academic) pp 313–9

[K77] Kaiser G 1977 Phase-space approach to relativistic quantum mechanics: I. Coherent-state representation for massive scalar particles *J. Math. Phys.* **18** 952–9; webpage www.wavelets.com/77JMP.pdf

[K78] Kaiser G 1978 Phase-space approach to relativistic quantum mechanics: II. Geometrical aspects *J. Math. Phys.* **19** 502–7; webpage www.wavelets.com/78JMP.pdf

[K87] Kaiser G 1987 Quantized fields in complex spacetime *Ann. Phys., NY* **173** 338–54; webpage www.wavelets.com/87AP.pdf

[K88] Kaneko A 1988 *Introduction to Hyperfunctions* (Dordrecht: Kluwer)

[K90] Kaiser G 1990 *Quantum Physics, Relativity, and Complex Spacetime* (Amsterdam: North-Holland) out of print, available at www.wavelets.com/NH90.pdf

[K92] Kaiser G 1992 Wavelet electrodynamics *Phys. Lett.* A **168** 28–34 (*Preprint* math-ph/0108009)

[K94] Kaiser G 1994 *A Friendly Guide to Wavelets* (Boston, MA: Birkhäuser)

[K94a] Kaiser G 1994 Wavelet electrodynamics: II. Atomic composition of electromagnetic waves *Appl. Comput. Harmon. Anal.* **1** 246–60 (*Preprint* math-ph/0108014)

[K96] Kaiser G 1996 Physical wavelets and radar *IEEE Antennas Propag. Mag.* **38** (February) 15–24; webpage www.wavelets.com/96AP.pdf

[K97] Kaiser G 1997 Short-pulse radar via electromagnetic wavelets *Ultra-Wideband, Short-Pulse Electromagnetics 3* ed C E Baum, L Carin and A P Stone (New York: Plenum)

[K00] Kaiser G 2000 Complex-distance potential theory and hyperbolic equations *Clifford Analysis* ed J Ryan and W Sprössig (Boston, MA: Birkhäuser) (*Preprint* math-ph/9908031)

[K01] Kaiser G 2001 Communications via holomorphic Green functions *Clifford Analysis and Its Applications* ed F Brackx, J S R Chisholm and V Souček (New York: Plenum) (*Preprint* math-ph/0108006)

[K01a] Kaiser G 2001 Distributional sources for Newman's holomorphic field (*Preprint* gr-qc/0108041)

[K02] Kaiser G 2002 Electromagnetic wavelets as Hertzian pulsed beams in complex spacetime (*Preprint* gr-qc/0209031)

[K02a] Kaiser G 2002 Complex-distance potential theory, wave equations, and physical wavelets *Math. Methods Appl. Sci.* **25** 1577–88; webpage www3.interscience.wiley.com/cgi-bin/issuetoc?ID=100519959

[K03] Kaiser G 2003 Making pulsed-beam wavelets *Workshop on Multiscale Geometric Analysis, IPAM (13–17 Jan.)* (*Preprint* math-ph/0301002)

[K0x] Kaiser G *Physical Wavelets and Wave Equations* (Basle: Birkhäuser) in preparation

[Kan87] Kannenberg L 1987 A note on Hertz potentials in electromagnetism *Am. J. Phys.* **55** 370–2

[KM80] Kaiser G 1980 Holomorphic gauge theory *Geometric Methods in Mathematical Physics (Lecture Notes in Mathematics vol 775)* ed G Kaiser and J E Marsden (New York: Springer)

[KS92] Kaiser G and Streater R F 1992 Windowed Radon transforms, analytic signals, and the wave equation *Wavelets: A Tutorial in Theory and Applications* ed C K Chui (New York: Academic) pp 399–441 (*Preprint* math-ph/0108010)

[Kr03] Krasnov K 2003 Black hole thermodynamics and Riemann surfaces *Preprint* gr-qc/0302073

[M57] McCrea W H 1957 Hertzian electromagnetic potentials *Proc. R. Soc.* A **240** 447–57

[MW95] Mandel L and Wolf E 1995 *Optical Coherence and Quantum Optics* (Cambridge: Cambridge University Press)

[MTW73] Misner C W, Thorne K S and Wheeler J A 1973 *Gravitation* (San Francisco, CA: Freeman)

[N55] Nisbet A 1955 Hertzian electromagnetic potentials and associated gauge transformations *Proc. R. Soc.* A **231** 250–63

[N57] Nisbet A 1957 Electromagnetic potentials in a heterogeneous nonconducting medium *Proc. R. Soc.* A **240** 375–81

[N65] Newman E T, Couch E C, Chinnapared K, Exton A, Prakash A and Torrence R 1965 Metric of a rotating, charged mass *J. Math. Phys.* **6** 918–9

[N65a] Newman E T and Janis A I 1965 A note on the Kerr spinning-particle metric *J. Math. Phys.* **6** 915–7

[N73] Newman E T 1973 Maxwell's equations and complex Minkowski space *J. Math. Phys.* **14** 102–3

[N02] Newman E T 2002 On a classical, geometric origin of magnetic moments, spin-angular momentum and the Dirac gyromagnetic ratio *Phys. Rev.* D **65** 104005 (*Preprint* gr-qc/0201055)

[NPT78] Newman E T, Porter J R and Tod K P 1978 Twistor surfaces and right-flat spaces *Gen. Rel. Grav.* **8** 1129–42

[NW74] Newman E T and Winicour J 1974 A curiousity concerning angular momentum *J. Math. Phys.* **15** 1113–5

[P75] Plebański J 1975 Some solutions of complex Einstein equations *J. Math. Phys.* **16** 2395–402

[P76] Penrose R 1976 Nonlinear gravitons and curved twistor theory *Gen. Rel. Grav.* **7** 31–52

[P87] Penrose R 1987 On the origins of twistor theory *Gravitation and Geometry, a Volume in Honour of I Robinson* ed W Rindler and A Trautman (Naples: Bibliopolis)

[PR84] Penrose R and Rindler W 1984 *Spinors and Space-Time* vol 1 (Cambridge: Cambridge University Press)

[S65] Synge J L 1965 *Relativity: The Special Theory* 2nd edn (Amsterdam: North-Holland)

[SW64] Streater R F and Wightman A S 1964 *PCT, Spin and Statistics, and All That* (Reading, MA: Addison-Wesley)

[T62] Trautman A 1962 Analytic solutions of Lorentz-invariant linear equations *Proc. R. Soc.* A **270** 326–8

[T02] Trautman A 2002 Robinson manifolds and Cauchy–Riemann spaces *Class. Quantum Grav.* **19** R1–R10

[T96] Taylor M 1996 *Partial Differential Equations* vol 1 (Berlin: Springer)